Universidade de Aveiro Secção Autónoma de Ciências da Saúde
2012

Ana Regina Silva Cerqueira

PPA e a sua fosforilação na sinalização STAT3 induzida por $G\alpha_o$

APP and APP phosphorylation in $G\alpha_o$-induced STAT3 signaling

Universidade de Aveiro Secção Autónoma de Ciências da Saúde
2012

Ana Regina Silva Cerqueira

PPA e a sua fosforilação na sinalização STAT3 induzida por $G\alpha_o$

APP and APP phosphorylation in $G\alpha_o$-induced STAT3 signaling

Dissertação apresentada à Universidade de Aveiro para cumprimento dos requisitos necessários à obtenção do grau de Mestre em Biomedicina Molecular, realizada sob a orientação científica da Professora Doutora Sandra Vieira, Professora Auxiliar Convidada da Secção Autónoma de Ciências da Saúde da Universidade de Aveiro.

Este trabalho contou com o apoio do Centro de Biologia Celular (CBC) da Universidade de Aveiro, e é financiado por fundos FEDER através do Programa Operacional Factores de Competitividade – COMPETE e por Fundos nacionais da FCT – Fundação para a Ciência e a Tecnologia no âmbito dos projectos PTDC/QUI-BIQ/101317/2008, PTDC/SAL-NMC/111980/2009 e PEst-OE/SAU/UI0482/2011.

Dedicada ao meu avô, Rui Silva.

Dedicada aos meus pais e irmã, a quem devo tudo o que tenho na vida.

o júri

presidente

Odete Abreu Beirão da Cruz e Silva
Prof. Auxiliar Com Agregação, Secção Autónoma de Ciências da Saúde, Universidade de Aveiro

Sandra Isabel Moreira Pinto Vieira
Prof. Auxiliar Convidada, Secção Autónoma de Ciências da Saúde, Universidade de Aveiro

Ana Sofia Duarte
Prof. Auxiliar Convidada, Departamento de Ciências da Saúde, Universidade Católica Portuguesa

agradecimentos

À minha orientadora, Sandra Vieira, agradeço a motivação, sabedoria, inspiração e dedicação que contribuíram para uma melhor aprendizagem.

À professora Odete da Cruz e Silva por me ter dado a oportunidade de realizar esta etapa no laboratório de neurociências do Centro de Biologia Celular.

Aos meus pais e à minha irmã pelo apoio incondicional, confiança, afecto, compreensão, dedicação e incentivo, que tornaram a concretização desta etapa possível.

À linda família que tenho a sorte de ter e por, apesar das adversidades face ao trabalho, me proporcionarem o melhor ambiente familiar.

Ao Bruno, à Pati, à Lili e à Ana Cristina por me darem o prazer de desfrutar diariamente de uma boa e verdadeira amizade.

Ao João, à Carina, Daniela, Juliana, Ana Silva e Catarina por demonstrarem que a distância é um mero pormenor, quando o sentimento é verdadeiro.

À Ana, Vanessa, Liliana, ao Tiago e Diogo por serem a prova que o tempo voa, mas que a amizade se pode manter.

Ao Ivo, Marcelo e Rafael pela boa disposição e momentos de descontração, que tornam não só os jantares como, principalmente, a companhia insubstituíveis.

A todos os meus colegas do CBC, particularmente aos meus colegas do laboratório de Neurociências. Ao Roberto e à Joana Rocha, pelo companheirismo, altruísmo e respeito que foram fundamentais para a realização deste trabalho.

À FCT pelo financiamento dos projetos PTDC/QUI-BIQ/101317/2008 e PTDC/SAL-NMC/111980/2009.

palavras-chave

Proteína precursora de amilóide de Alzheimer (PPA); fosforilação da PPA na S655; sinalização da STAT3; proteína $G\alpha_o$; células SH-SY5Y

resumo

A proteína precursora de amilóide de Alzheimer (PPA) é uma proteína cerebral fundamental, envolvida em mecanismos celulares como a adesão e migração celular e neuritogénese. Como fosfoproteína, a PPA apresenta oito resíduos fosforiláveis no seu domínio citoplasmático. Um desses resíduos, Serina 655 (S655), localiza-se no motivo funcional ^{653}YTSI^{656}, e a sua fosforilação altera o tráfego e o processamento da PPA, podendo ainda mediar a ligação desta a outras proteínas através de um *hydrophobic pocket* localizado imediatamente a jusante ao motivo YTSI (^{657}His-Lys^{676}). Nomeadamente, a proteína $G\alpha_o$, uma subunidade α de proteínas G heterotrimérica, liga-se à PPA neste local. A $G\alpha_o$ está envolvida em várias cascatas de sinalização e é o membro da família $G_{i/o}$ mais abundante no cérebro. Quando ativada, a $G\alpha_o$ consegue induzir fatores de crescimento relacionados com a via JAK2/STAT3 via Rap, provavelmente através da interação e sequestro de proteínas RapGAP. Adicionalmente, a $G\alpha_o$ foi sugerida como um transdutor da PPA, funcionando esta como um *guanidine exchange factor* (GEF) para a $G\alpha_o$. No entanto, ainda não foi atribuído nenhum papel funcional a esta interação.

O presente trabalho teve como principal objetivo determinar o papel da PPA na cascata de sinalização da STAT3 induzida por $G\alpha_o$, pela análise dos efeitos da co-transfecção de PPA-$G\alpha_o$ nos níveis de STAT3 e STAT3 fosforilada através de Western blot. Para isto, células humanas de neuroblastoma SH-SY5Y são co-transfectadas por 6h e 24h com PPA-GFP cDNAs (Wt ou fosfomutantes S655: S655A, SA, e S655E, SE) e $G\alpha_o$ ou $G\alpha_o$CA (um mutante Q205L que mimetiza um estado constitutivamente activo da $G\alpha_o$). Adicionalmente, foi estudado como é que os metabolismo da PPA e da $G\alpha_o$ afetam-se um ao outro, através da quantificação dos níveis de $G\alpha_o$, PPA e PPAs secretada por Western blot.

Em geral, os resultados obtidos mostram que as co-expressões de PPA-GFPs com $G\alpha_o$/$G\alpha_o$CA levam a um decréscimo da fosforilação da STAT3 induzida por $G\alpha_o$. Isto parece ocorrer através da indução de um efeito retro-inibitório nas vias $G\alpha_o$-STAT3 após a ativação inicial da $G\alpha_o$ e, enquanto este efeito é mais pronunciado para o mutante que reproduz desfosforilação do resíduo S655 da PPA, a fosforilação neste mesmo resíduo parece retardar este efeito. Em concordância, a PPA invariavelmente diminui os níveis de $G\alpha_o$ e a $G\alpha_o$ também diminui os níveis de PPA, potencialmente envolvendo um mecanismo de inibição da ativação da STAT3 induzida pela $G\alpha_o$ através da PPA por degradação lisossomal PPA/$G\alpha_o$.

keywords

Alzheimer's Amyloid Precursor Protein (APP); APP phosphorylation at S655; STAT3 signalling; $G\alpha_o$ protein; SH-SY5Y cells

abstract

The transmembranar Alzheimer's Amyloid Precursor Protein (APP), an important brain protein, is potentially involved in cellular mechanisms such as cell adhesion, migration and neuritogenesis. As a phosphoprotein, APP has eigth phosphorylatable residues in its cytoplasmic domain. One of these residues, S655, lies within the APP ^{653}YTSI^{656} sorting motif, and its phosphorylation alters APP trafficking and processing, and may potentially mediate its binding to other proteins by means of a hydrophobic pocket localized immediately downstream the YTSI motif (^{657}His-Lys^{676}). This is the pocket to which $G\alpha_o$, an alpha subunit of heterotrimeric G proteins, binds to. $G\alpha_o$ mediates various signaling pathways and is the most brain-enriched member of the $G\alpha_{i/o}$ family. When activated, $G\alpha_o$ can induce the growth factors-related JAK2/STAT3 pathway via Rap, probably through interaction and sequestration of RapGAP proteins. $G\alpha_o$ has been suggested to be a transducer of APP, with APP acting as a guanidine exchange factor (GEF) for $G\alpha_o$. Nonetheless, no functional role has been attributed to this interaction.

In the work here described, the role of APP in $G\alpha_o$-induced STAT3 signaling was assayed, by analysing the effects of APP-$G\alpha_o$ co-transfection in STAT3 and phospho-STAT3 levels by Western blot means. For this, human SH-SY5Y neuroblastoma cells were co-transfected for 6h and 24h, with APP-GFP fusion cDNAs (Wt or S655 phosphomutants: dephosphomimicking S655A and phosphomimicking S655E) and $G\alpha_o$ or $G\alpha_o$CA (a Q205L mutant mimicking constitutively active $G\alpha_o$). Additionally, the effects of APP and $G\alpha_o$ in each other metabolism were also evaluated, by quantifying the levels of $G\alpha_o$, APP and medium secreted sAPP by Western blot analysis.

In general, the results obtained show that APP-GFPs co-expression with $G\alpha_o$/$G\alpha_o$CA leads to a decrease in $G\alpha_o$-induced STAT3 phosphorylation. This appears to occur via a retro-inhibition effect on the $G\alpha_o$-STAT3 pathways following an initial $G\alpha_o$ activation and, while is more pronounced for the S655 dephosphomimicking mutant, phosphorylation at S655 appears to delay this effect. Accordingly, APP invariably decreases $G\alpha_o$ half-life, and $G\alpha_o$ also decreases APP levels, with APP/$G\alpha_o$ lysosomal co-degradation being a potential mechanism by which APP inhibits $G\alpha_o$-induced STAT3 activation.

Index

Abbreviations

AD	Alzheimer's disease
ADP	Adenosine diphosphate
AGS	Activator of protein signaling
AICD	APP intracellular C-terminal domain
AMP	Adenosine monophosphate
APLP	Amyloid precursor-like proteins
APLP	Amyloid precursor-like protein
APOE	Apolipoprotein E gene
ApoE	Apolipoprotein E protein
APP	β-amyloid precursor protein
APPL	Amyloid precursor protein-like
APs	Amyloid plaques
Aβ	Amyloid β-peptide
BACE1	β-site APP-cleaving enzyme
BSA	Bovine serum albumin
Ca^{2+}	Calcium
CaMKII	Calmodulin-dependent protein kinase II
cAMP	Cyclic adenosine monophosphate
CB1	Cannabinoid 1 receptor
Cdc2	Cyclin-dependent protein kinase 2
Cdk5	Cyclin-dependent kinase 5
cDNA	Complementary deoxyribonucleic acid
CNS	Central nervous system
CNTF	Ciliary neurotrophic factor
CTF	Carboxy-terminal fragment
CuBD	Copper-binding domain
DAPI	4',6-diamidino-2-phenylindole
ECL	Enhanced chemiluminescence
ER	Endoplasmic reticulum
FAD	Familial Alzheimer's disease
G protein	GTP-bindign protein
$G\alpha_i$	inhibitory G-protein alpha
GAIP	Gα-interating protein
GAP-43	Growth cone-associated protein
GAPs	GTPase-activating proteins
Gβγ	G-protein beta-gamma subunits
GDP	Guanosine diphosphate
GEFs	Guanine nucleotide exchanger factors
GFD	Growth factor domain

GFP	Green fluorescent protein
G_i	inhibitory G-protein
G_o	Heterotrimeric 'other' G protein
gp130	Glycoprotein 130
GPCRs	G protein-coupled receptors
GPR	G protein regulatory
G_q	G protein q
GRIN	G protein-regulated inducer of neurite outgrowth
GSK-3β	Glycogen synthase kinase 3β
GTP	Guanosine triphosphate
G_z	G-protein z
$G\alpha_o$	G-protein alpha-subunit o
$G\alpha_oCA$	constitutively active G-protein alpha o
JAK	Janus Kinase
JNK	c-Jun N-terminal kinase
K^+	Potassium
KPI	Kunitz-type protease inhibitor
LD	Linker domain
LIF	Leukemia inhibitory factor
MAPK	Mitogen-activated protein kinase
ND	N-domain
NFTs	Neurofibrillary tangles
NT	non-transfected cells
PARP	poly ADP ribose polymerase
PI3K	Phosphadylinositol-3-kinase
PKC	Protein kinase C
PM	Plasma membrane
PPCs	Proprotein convertases
PS1 and PS2	Presenilin 1 and 2 protein
pSTAT3	STAT3 phosphorylated
PTX	Pertussis toxin
Rac	Rho family of GTPase subfamily
Rap	Ras-related protein or a small GTPase protein
Rap-GAP	Rap GTPase activating protein
Ras	Small G protein superfamily
RGS	Regulators of G protein signaling
S/SerXXX	Serine amino acid residue at position XXX
S655A	APP Serine 655 mutated at alanine
S655E	APP Serine 655 mutated at glutamate
SA APP/SA	Dephosphorylated S655 APP mutant
sAPP	Secreted APP
SDS	Sodium dodecylsulfate

SE APP/SE	Phosphorylated S655 APP mutant
SEM	Standard Error of he mean
SH2	Src homology 2 domain
Src	Non-receptor protein tyrosine kinase
STAT	Signal transducer and activator of transcription
STAT3	Signal transducer and activator of transcription 3
TACE	Tumor necrosis factor-α converting enzyme
TGN	Trans-Golgi network
Thr	Threonine amino acid residue at position XXX
Tip60	Tat interactive protein, 60kDa
TK	Tyrosine-Kinase
Tyr	Tyrosine amino acid residue at position XXX
VPS	Vacuolar protein sorting
WB	Western Blot
Wt APP	Wild-type APP

1. Introduction

1.1. Alzheimer's Disease

1.1.1. Alzheimer's Disease pathology

Alzheimer's disease (AD), a disorder of unknown etiology, is the most common form of dementia in the elderly. AD is a chronic disorder, apparently preceded by a clinically silent period of several years or even decades, which slowly and irreversibly destroys neurons and causes serious cognitive disability (Arendt, 2001; Bojarski, Herms et al., 2008).

Since it was presented for the first time in 1906 by Alois Alzheimer, this neurodegenerative disease is affecting an increasing number of individuals. In 2006, approximately 26.6 million people worldwide suffered from AD, and because of the growing life expectancy, the global prevalence of Alzheimer's can be predicted to be more than 100 million in 2050 (Selkoe, 2004; Brookmeyer, Johnson et al., 2007).

AD cases have been described according to lesions type, the type of onset, the cause (genetic or sporadic) and associated lesions (e.g. vascular lesions). Clinically, in the beginning, AD is characterized by a mild cognitive impairment and deficits in short-term and spatial memory, which can be confused with the normal changes of aging. The symptoms become more severe with disease progression and not only destroy a person's memory, but the patient also presents disturbances in language use, perception, ability to learn necessary skills, reason, solve problems, think abstractly, make judgment, communicate and carry out daily activities. In some patients, AD can even lead to personality and behavioural changes (Marotta, Majocha et al., 1992; Arakawa, Kita et al., 2008; Hooijmans and Kiliaan, 2008). In Figure 1 is depicted a comparison between a normal and an AD brain, through a brain cross-section, highlighting some of the neuropathological alterations in AD brains, including brain shrinkage.

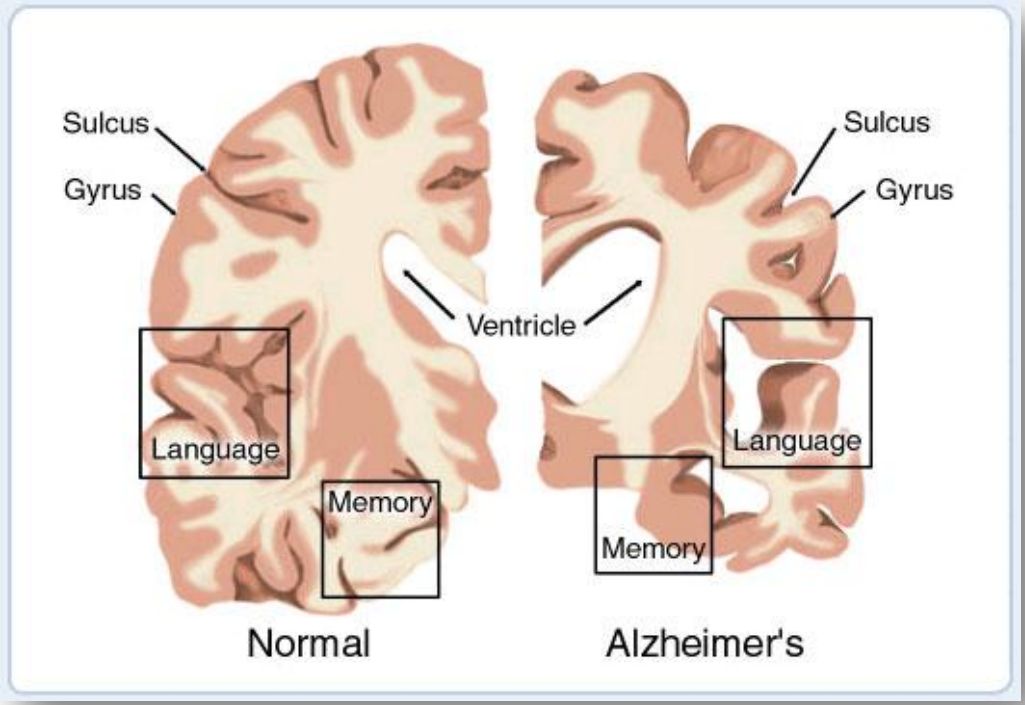

Fig. 1: This image represents a cross-section of the brain as seen from the front. On the left the cross-section represents a normal brain and the one on the right represents a brain with Alzheimer's disease. Reproduced from American health assistance foundation (January 2012), http://www.ahaf.org/alzheimers/about/understanding/brain-with-alzheimers.html

The clinical symptoms of AD result from neuropathological lesions, including deposition of amyloid plaques (APs) and neurofibrillary tangles (NFTs), in characteristic brain regions, together with downstream reactive processes such as inflammation and oxidative stress, leading to loss of effective neural network connectivity, synaptic degeneration and progressive neuronal cell death (Bojarski, Herms et al., 2008; Duyckaerts, Delatour et al., 2009; Hampel, Shen et al., 2010; Lin and Luo, 2011). Of note, some reports indicate that AD could be a disease where not only neurons are affected, but also peripheral cells such as fibroblasts, lymphocytes and platelets (Bojarski, Herms et al., 2008).

The neuropathological and biochemical features of AD develop the disorder and delay the diagnosis, since the symptoms appear later on (Lemere and Masliah, 2010). Although there are currently accepted clinical guidelines for the probable diagnosis of AD, the definitive diagnosis of AD happens at autopsy with the postmortem examination of the brain, which reveals large quantities of NFTs and APs within the parenchyma (Marotta,

Majocha et al., 1992). In Figure 2, we can observe AP and NFT in a microscopic analysis of the AD brain.

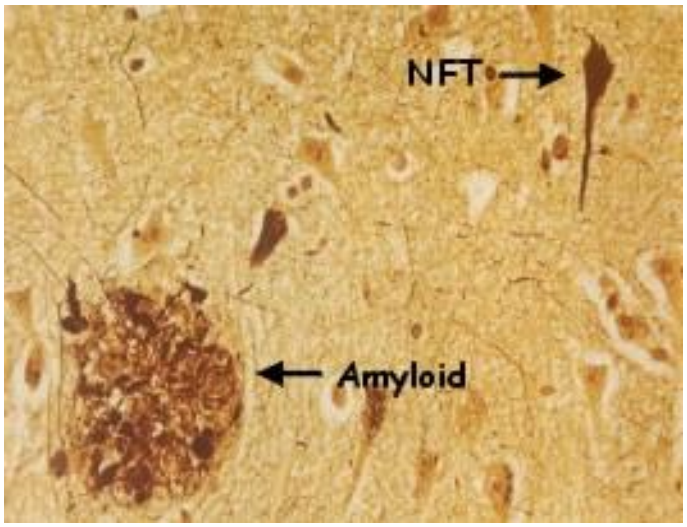

Fig. 2: Histopathological analysis of an AD brain tissue, post-mortem. In this tissue cut we can observe the neurofibrillary tangles and amyloid plaques. Reproduced from Experimental genetics group (January 2012), http://med.kuleuven.be/legtegg/AD.html

Several symptomatic treatments are in use for AD, but they are incapable of reversing the pathology of disease, namely, the widely used acetylcholinesterase inhibitors, which reduce inflammation and alleviate the symptoms. Recently, new therapeutic drugs are being developed, including vaccines aiming to destroy AP plaques before or after being aggregated.

1.1.2. Hallmarks of AD

The two major pathological hallmarks of AD that appear to be more correlated with the clinical symptoms are the extracellular amyloid plaques (also called senile plaques), and the intracellular neurofibrillary tangles.

The APs are aggregated, insoluble, dense cores of 5-10 nm amyloid fibrils with surrounding reactive cells, dystrophic neurites, lysosomes, abnormal mitochondria, astrocytic processes and activated microglia (Fig. 3). The main proteinaceous component of APs is the neurotoxic β-amyloid (Aβ) peptide, produced by proteolytic cleavages of a type I transmembranar glycoprotein named β-amyloid precursor protein, APP (Selkoe, 1999; Duyckaerts, Delatour et al., 2009; Hampel, Shen et al., 2010; Lemere and Masliah, 2010). Amyloid-containing senile plaques are a prominent feature of specific AD brain

regions, affect limbic and cortical structures, like cerebral cortex, amygdaloid nucleus, corpus striatum, diencephalon and hippocampus, but they also have been described in the cerebellum (Marotta, Majocha et al., 1992; Lukiw and Bazan, 2000; Merlo, Spampinato et al., 2010). The mechanisms responsible for the excessive accumulation of β-amyloid in the AD brain are unknown, but a few genetic, molecular biology and protein chemistry hypotheses have been proposed to explain the disease process (Marotta, Majocha et al., 1992).

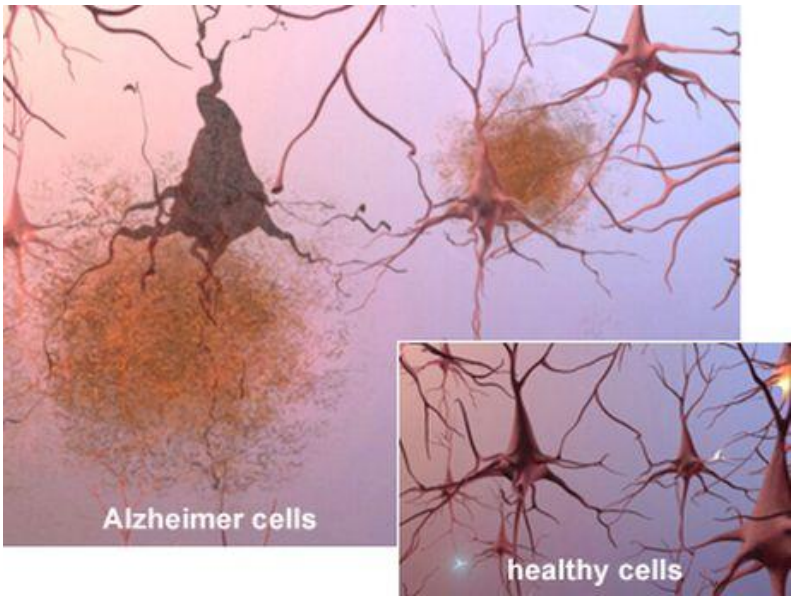

Fig. 3: Representation of nerve cells within AD brains. The tissue with AD presents a much smaller number of nerve cells and synapses than a healthy brain; APs are abnormal deposits of protein fragments between nerve cells; the dead and dying nerve cells contains neurofibrillary tangles. Reproduced from health news (January 2012), http://www.healthinformer.net/alzheimer-disease-plaques-seen-with-conventional-mri-in-animal-model-for-the-first-time.html

The neurofibrillary tangles (Fig. 3) derive from the intracellular accumulation of paired helical filaments resulted from hyperphosphorylation of a microtubule-associated protein known as Tau, causing it to aggregate into an insoluble form. In AD, this abnormal Tau protein induces the microtubule structures to collapse inside neuronal cell bodies, axons and dendrites (Hooijmans and Kiliaan, 2008; Duyckaerts, Delatour et al., 2009; Merlo, Spampinato et al., 2010). The progression of Tau pathology is stepwise and stereotyped from the entorhinal cortex, through the hippocampus, to the neocortex (Marotta, Majocha et al., 1992).

Although controversies still exist on the real causes of AD and on the precise relationship between Aβ, Tau and AD pathogenesis, the ability to determine both proteins levels in living people could markedly improve AD diagnosis and treatment, and these proteins still considered the most possible targets for new therapies (Merlo, Spampinato et al., 2010).

The synaptic loss in AD is difficult to evaluate, however it is an early pathological hallmark of AD that is age dependent and largely independent of Aβ. More than Aβ deposits, this hallmark could be the neuropathological alteration that is more correlated with neuronal damage, cognitive decline and memory impairment (Hooijmans and Kiliaan, 2008; Duyckaerts, Delatour et al., 2009). Furthermore, synaptic dysfunction and failure of brain connectivity appears to predate neuronal loss (Coleman, Federoff et al., 2004; Hooijmans and Kiliaan, 2008). Studies indicate that the neurodegenerative process initiates in the temporal lobe structures, like entorhinal cortex, followed by synapse disfunction and loss in the hippocampus (Coleman, Federoff et al., 2004; Duyckaerts, Delatour et al., 2009).

The plaques and tangles formation accompany this process, however research demonstrate that synaptic loss and memory impairment precede APs in the limbic system (Mucke, Masliah et al., 2000), and AD has been associated with synaptic disruption also in specific cortical areas (Duyckaerts, Delatour et al., 2009).

These evidences demonstrate that synaptic failures of AD begin prior to neuronal loss, plaques and tangles development, and also prior to clinical detection of disease. The explicit recognition that AD starts long before the appearance of the traditional ways of detecting the illness will highlight the need of the development of early diagnosis (Coleman, Federoff et al., 2004).

1.1.3. Risk factors

As mentioned above, the cause or causes of AD are not yet identified and there is no cure, so efforts are needed for preventing the development of the dementia. Many theories have been proposed, like the "amyloid cascade hypothesis". The amyloid deposition is seen as the primary pathway leading to neurodegeneration and AD. Although this hypothesis is one of the most persistent, there are yet controversy in some results, such as: the conflicting results about the neurotoxicity of deposited Aβ in vivo (Bishop and

Robinson, 2002); the fact that Aβ accumulation is not the earliest hallmark and is not always correlated to neuronal loss (Mucke, Masliah et al., 2000); the fact that many non-demented persons show large amounts of AD neuropathologicals events (Hooijmans and Kiliaan, 2008).

So, it becomes necessary to study the AD risk factors and underlying theories to explain the etiology of this illness. Some researchers suggest various theories and risk factors that play an important role in AD pathogenesis, like deregulation of calcium homeostasis (Bojarski, Herms et al., 2008), cardiovascular disorders (Hooijmans and Kiliaan, 2008), abnormal activation of lipid signaling (Lukiw and Bazan, 2000), induction of oxidative stress, and others.

AD risk factors can be subdivided in sporadic and familial AD. About 95% of all AD cases appear to be of random, idiopathic or sporadic origin (Hooijmans and Kiliaan, 2008). These sporadic cases involve the most significant risk factor – age – in concert with genetic and environmental risk factors. Some researchers suggest that a combination of lifestyle, genetic, and amyloid related factors, which enhance each other contribution in the onset and course of AD, will probably be at the etiology of the disease instead of being only one mechanism (Hooijmans and Kiliaan, 2008). In the group of risk factors for sporadic AD, the environmental factors are associated with a combination of life events, such as early-life childhood and adolescent environment, psychosocial and mental inactivity, loss of motivation and mental stress, a lower level of education and occupation, improper diet, higher age, exposure to neurotoxic factors, brain injury, and vascular disease (Arendt, 2001). The best-known genetic risk factor in late-onset sporadic AD is the apolipoprotein E (APOE) gene. This gene is located on chromosome 19 that encode the apolipoprotein E (ApoE) protein (Ling, Morgan et al., 2003). ApoE is polymorphic with three isoforms, ApoE2, ApoE3 and ApoE4, which translate into three alleles of the gene and differ from each other at two amino acids. ApoE plays an important role in cholesterol transport in the central nervous system and in AD development, which relates to its ability to interact with Aβ (Ling, Morgan et al., 2003; Hooijmans and Kiliaan, 2008; O'Brien and Wong, 2011). The mechanism by which ApoE4 predisposes individuals to AD is not clear. However, pathologically the evidence is that ApoE4 accelerates brain Aβ deposition, APs formation and loss of neuronal function by stimulating APP processing and reducing Aβ clearance (Ling, Morgan et al., 2003; Hooijmans and Kiliaan, 2008).

Familial AD is the second most important risk factor group. About 1% of AD cases occur due to this group of risk factors (Chiba, Nishimoto et al., 2007). This early onset AD develops because of missense mutations in the genes coding for the amyloid precursor protein (APP) on chromosome 21, presenilin 1 (PSEN1) on chromosome 14, and presenilin 2 (PSEN2) on chromosome 1, all causing abnormal processing of APP to Aβ and production of Aβ-related neurotoxic peptides (Lukiw and Bazan, 2000; Hooijmans and Kiliaan, 2008).

As mentioned before, APP is the precursor of Aβ and these proteins are implicated in the pathogenesis of both sporadic and familial AD. The APP gene localizes in the same chromosome that causes Down's syndrome (trisomy 21), chromosome 21. The patients with this syndrome reveal the classical neuropathological features of AD, like APP overexpression, which results in brain Aβ accumulation, and formation of neurofibrillary tangles (Hooijmans and Kiliaan, 2008; O'Brien and Wong, 2011). This finding led to a specific search for families with early-onset AD with genetic linkage to chromosome 21 and resulted in the identification of several missense mutations in APP, associated to familial AD (Hooijmans and Kiliaan, 2008). In familial AD, mutations of APP gene cause a change in amino acids adjacent to the BACE1 (enzyme essential for the generation of Aβ) cleavage site, or occur around the γ-secretase cleavage site, and result in alteration of APP proteolytic processing to Aβ, leading to increased production of total Aβ or to production of a more toxic Aβ peptide (Chiba, Nishimoto et al., 2007; Cole and Vassar, 2007; O'Brien and Wong, 2011).

Presenilins proteins (PS1 and PS2) are integral components of a multiprotein protease complex, called γ-secretase, which is responsible for the cleavage of APP and other important proteins such as Notch, an essential cell development protein, similar to APP in size and intracellular localization (Ling, Morgan et al., 2003; Bojarski, Herms et al., 2008). Presenilins are involved in a range of physiological and biological processes (Ling, Morgan et al., 2003). The familial AD mutations in PSEN1 and PSEN2 show that the efficiency of presenilin-mediated Notch cleavage is reduced, in contrast to the effects on APP processing (Ling, Morgan et al., 2003). Indeed, mutations in presenilins genes lead to an increased production of the more toxic Aβ42, a form of Aβ peptide that is particularly prone to precipitate and aggregate, relative to Aβ40 (Ling, Morgan et al., 2003; O'Brien and Wong, 2011).

The Figure 4 summarizes the various AD risk factors above mentioned.

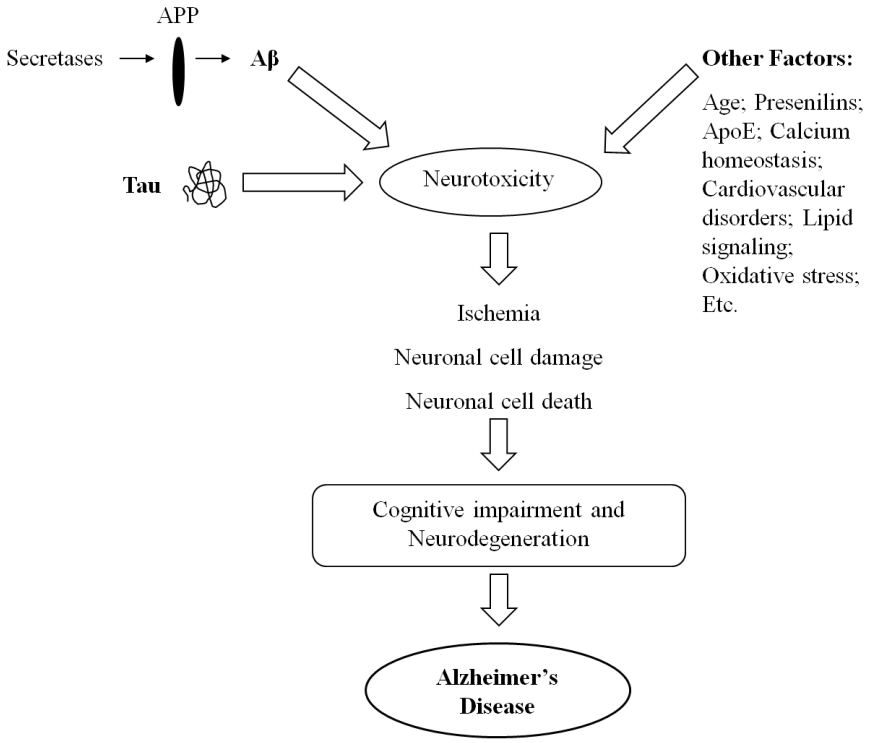

Fig. 4: Various risk factors involved in neurotoxicity and AD onset. Proposed sequence of events in the development of AD, with a possible influence of Aβ, Tau and other risk factors. Adapted from Arakawa, Kita et al. (2008)

1.2. The β-Amyloid Precursor Protein (APP)

As mentioned previously, Amyloid Precursor Protein (APP) is the precursor of the major protein component of senile plaques in Alzheimer's disease, Aβ. APP is an integral type-I transmembranar glycoprotein that suffers cleavages, by protease activity, in different fragments including the Aβ.

APP is ubiquitously expressed, as e.g. in endothelial cells, smooth muscle cells and all peripheral cells; in the central nervous system (CNS) it is abundantly expressed in neurons. Other brain cells that also express APP and release variable amounts of Aβ are glial cells, such as astrocytes (Perez, Zheng et al., 1997; King and Scott Turner, 2004).

Despite years of intense investigation, the biological functions of normal APP are still far from clear. It is known that APP is important for normal CNS function. APP resembles a cell surface signaling receptor, and has been involved in memory regulation,

cell-cell interaction, cell adhesion, cell survival, cell growth, neurite outgrowth, and protease inhibition (King and Scott Turner, 2004). APP has also been implied in pro- and anti-apoptotic functions. (De Strooper and Annaert, 2000).

1.2.1. APP gene family, isoforms and domains

In humans, the APP gene is located on the chromosome 21q21, and contains 19 exons, of which exons 7, 8 and 15 can be alternatively spliced (De Strooper and Annaert, 2000; da Cruz e Silva and da Cruz e Silva, 2003; Ling, Morgan et al., 2003). APP belongs to a family of related proteins that includes the amyloid precursor-like proteins (APLP1 and APLP2) in mammals and amyloid precursor protein-like (APPL) in *Drosophila*, *Caenorhabditis elegans*, and *Xenopus* (De Strooper and Annaert, 2000; O'Brien and Wong, 2011). All these are homologous type I transmembranar proteins with overlapping expression in brain, similarly metabolism, and that exhibit some functional redundancy (King and Scott Turner, 2004). Nonetheless, only APP cleavage gives rise to the Aβ peptide, which is derived from the domain encoded by parts of exons 16 and 17 (da Cruz e Silva and da Cruz e Silva, 2003; Ling, Morgan et al., 2003).

Alternative splicing of the APP transcript generates at least 8 isoforms, ranging from 365 to 770 amino acids (da Cruz e Silva and da Cruz e Silva, 2003; King and Scott Turner, 2004; O'Brien and Wong, 2011). The three most common isoforms, however, predominate in a cell-type specific manner, and differ only in the size of their extracellular sequence: APP_{695}, APP_{751} and APP_{770} (Fig. 5). APP_{695} is expressed predominantly in the CNS neurons, and the APP_{751} and APP_{770} are more expressed in non-neuronal cells, but are also found in brain glial cells (Selkoe, 2001; King and Scott Turner, 2004; O'Brien and Wong, 2011). All of these transcripts encode multidomain proteins with a single membrane-spanning region. The APP_{751} and APP_{770} differ from the APP_{695} in the expression of exon 7, which encodes a Kunitz serine protease inhibitor (KPI) domain (Selkoe, 2001).

Studies revealed that the different APP isoforms respond differently under various experimental conditions, like Aβ addition. All these three isoforms contain exons 16 and 17, but APP_{695} responds more readily than the other isoforms to the accumulation of Aβ (da Cruz e Silva and da Cruz e Silva, 2003).

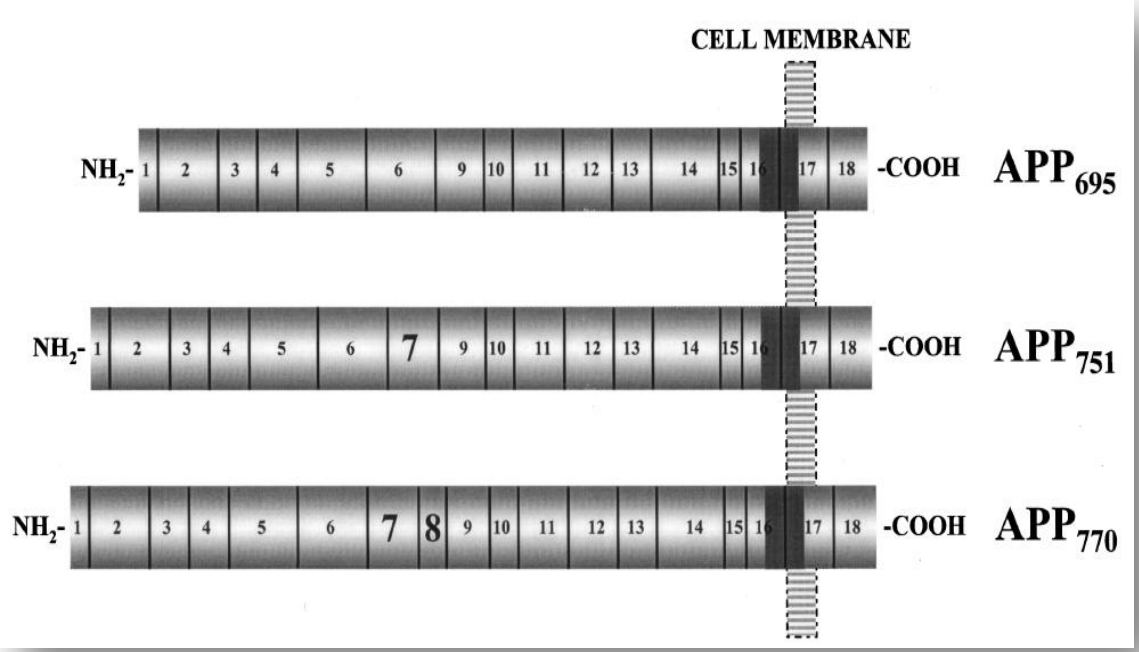

Fig. 5: Schematic representation of the three major APP isoforms found in mammalian tissues. The number and vertical lines delineate the corresponding exons. The most abundant neuronal isoform is APP_{695} (exons 1-6, 9-18) that comprises 695 amino acids. As illustrated, APP_{751} (exons 1-7, 9-18) and APP_{770} (exons 1-18) are alternatively spliced isoforms that differ from APP_{695} in the expression of exons 7 and 8. The sequences encoded by the APP gene exons are indicated approximately to scale. The Aβ domain it's represented in this figure as the solid gray region, whose sequence is divided between exons 16 and 17. Reproduced from da Cruz e Silva and da Cruz e Silva (2003)

The complete crystal structure of APP and the ligands or receptors that interact with the large APP ectodomain are not yet much understood (De Strooper and Annaert, 2000). However, a number of distinct, large independently-folding structural domains have been identified in the APP sequence. APP possesses three general domains: a large glycosylated extracellular component, a single membrane-spanning region and a short intracellular cytoplasmic domain (Hampel, Shen et al., 2010) (Fig. 6).

Fig. 6: Schematic representation of functional domains arrangement of APP, highlighting some important regions. The N-terminal growth factor domain (GFD) is followed by copper-binding domain (CuBD), an acidic-rich region, Kunitz-type protease inhibitor (KPI) and OX2 domains that occur in some APP isoforms, a couple of glycosylated domains (D6a, sometimes called the E2 domain, followed by an unstructured domain, D6b), a transmembrane region (TM) and a cytoplasmic tail. The location of the Aβ region, a major component of Alzheimer's disease plaques, is shown in red. Reproduced from Kong, Miles et al. (2008)

The large extracellular region can be subdivided into several functional domains (Fig. 6). At the N-terminal is a cysteine-rich region consisting in a growth factor domain (GFD) and a copper-binding domain (CuBD) that interact tightly together. The GFD binds heparin and can stimulate neurite outgrowth (Kong, Miles et al., 2008). The CuBD of APP may regulate proteolytic processing or act as a metallotransporter. The copper binding to this domain affects the dimerization state of APP leading to reduction in Aβ production, whereas copper binding to the Aβ generates toxic species (Bossy-Wetzel, Schwarzenbacher et al., 2004; Kong, Miles et al., 2008). Studies revealed that the cysteine-rich region also contains a zinc-binding domain. This APP metal-binding site was assumed to play mainly a structural role, modifying its conformation and interfering with APP binding to constituents of the extracellular matrix (De Strooper and Annaert, 2000).

The copper-binding domain is followed by an acidic domain, which links the cystein-rich region to a Kunitz-type protease inhibitor (KPI) domain and an OX2 domain. The KPI and OX2 domains can be spliced out, to produce three main isoforms: APP_{770}, APP_{751} and APP_{695}. The longer isoforms APP_{751} and APP_{770} contain a 56-amino acid KPI domain, located in the middle of the APP ectodomain, which inhibits serine proteases. The OX2 domain is only present in APP_{770} (King and Scott Turner, 2004). Following these domains there is a glycosylated domain referred to as E2 (sometimes called the D6a, like in Figure 6) and an unstructured region, D6b, which precedes the transmembranar domain. The E2 domain possesses the RERMS motif that appears to have putative growth-promoting properties and also has a heparin binding site (De Strooper and Annaert, 2000; Kong, Miles et al., 2008).

Another specific domain that implicates a role for APP as a cell surface receptor is the C-terminal cytoplasmic tail. This region contains several consensus motifs that regulate

its trafficking and suggest a role in signal transduction, through interaction with several proteins (De Strooper and Annaert, 2000; Evin and Weidemann, 2002). The APP cytoplasmic domain has been shown to bind to the Fe65 protein and G proteins, for example. Some APP hereditary mutations that are linked with AD can cause constitutive activation of G_o, a member of the heteromeric G protein family that serve as signal transducers of various cell surface receptors (Kong, Miles et al., 2008).

1.2.2. APP metabolism: trafficking and processing

As described above, APP is produced in large quantities in neurons and is metabolized very rapidly. APP traffic (Fig. 7) is tightly regulated and along it APP can be cleaved by specific proteases. APP follows the constitutive secretory pathway, being N-glycosylated in the endoplasmic reticulum (ER) (immature APP) and further O-glycosylated (APP maturation) in the Golgi, where it is highly abundant (Thinakaran and Koo, 2008; Vieira, Rebelo et al., 2010). After sorting in the ER and Golgi, APP is delivered to the axon, where it is transported by fast axonal transport to presynaptic terminals (O'Brien and Wong, 2011). APP can be packaged into secretory vesicles in the Trans-Golgi network (TGN) and delivered to the plasma membrane (PM). On the cell surface, APP may be proteolytically processed or suffer internalization, via its YENPTY motif, being delivered into the endocytic pathway (endosomes). Then, APP is either transport to lysosomes, where it suffers lysosomal degradation, or recycled by transport vesicles to the TGN or to the cell surface (Vieira, Rebelo et al., 2010).

Crucial steps in APP metabolism occur at the cell surface and in the TGN. From the TGN, APP is transported via a clathrin coat complex, which mediate two steps: the transport directly to an endosomal compartment, and its reinternalization from the cell surface into the endocytic pathway, connecting the cell surface to the endosome (O'Brien and Wong, 2011). APP contains the NPXY (asparagiNe-Proline-any-tYrosine) amino acid motif (YENPTY domain), a conserved sorting signal that regulates the targeting of proteins for clathrin pit localization and their transport via clathrin-associated vesicles from the cell surface to the endosome (Evin and Weidemann, 2002; Small and Gandy, 2006; O'Brien and Wong, 2011).

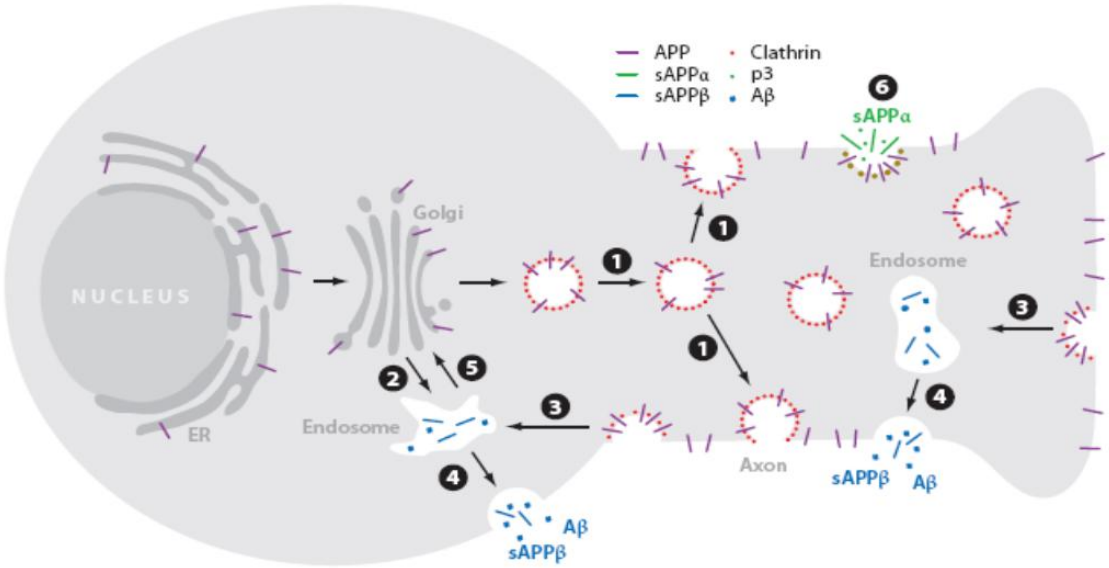

Fig. 7: Schematic representation of APP trafficking in neurons. Newly synthesized APP (purple) is transported from the Golgi down the axon to the cell surface (1) or into a cell body endosomal compartment (2), with clathrin-associated vesicles (red) mediating both steps. In the cell surface, some APP is cleaved by α-secretase (6), generating the sAPPα fragment (green), and some is re-internalized into endosomes (3), where Aβ and sAPPβ are generated (blue). Following proteolysis, the endosome recycles to the cell surface (4), releasing Aβ and sAPPβ. Transport from the endosomes to the Golgi prior to APP can also occur, mediated by the retromer (5). Reproduced from O'Brien and Wong (2011)

Another complex that is implicated in APP transport is the retromer complex. The retromer is a multi-subunit complex that mediates the retrograde transport of several transmembranar proteins from endosomes to the TGN (Vieira, Rebelo et al., 2010). This complex consists of two sorting nexin subunits and a cargo-recognition trimer, vacuolar protein sorting (VPS) 26, VPS29, VPS35 (Small and Gandy, 2006). Several findings indicate that a dysfunctional retromer complex and/or one of its sorting receptor components, sorLA (a type-1 transmembrane molecule), can be related to late onset AD pathology (Vieira, Rebelo et al., 2010). Indeed, the TGN retrieval pathway, involving sorLA and the retromer, has been inversely correlated with Aβ production. Further studies revealed that phosphorylation of APP in the Ser655 residue enhances APP binding affinity for sorting proteins, such as the retromer-related VPS35 protein (at the core of the retromer) (Vieira, Rebelo et al., 2010). Ser655 phosphorylation was found to enhance both the protein exit from the Golgi, and its recycling back to the TGN from endosomes, increasing its cleavage to sAPPα during this trafficking cycle.

In what concerns cleavage, there are mainly two pathways for APP proteolytic processing: the amyloidogenic and non-amyloidogenic, distinguished by the mutually exclusive action of two different enzymes in the first cleavage event (Fig. 8).

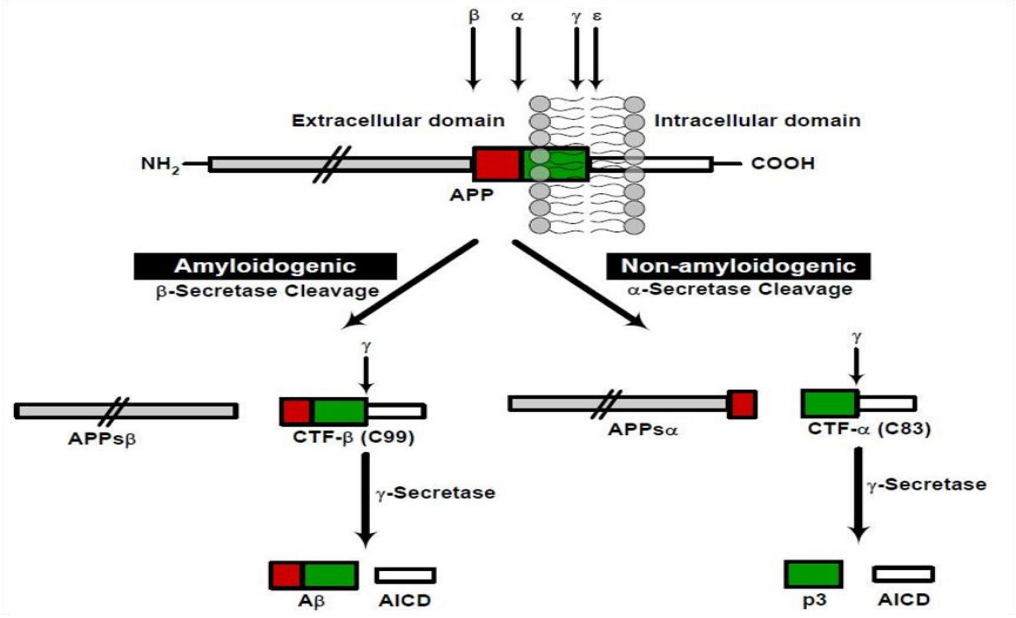

Fig. 8: Schematic diagram of APP proteolytic processing. APP can undergo proteolytic processing via two pathways: amyloidogenic and non-amyloidogenic. Cleavage of APP by β-secretase occurs at the beginning of the Aβ domain and generates a shorter soluble N-terminus, APPsβ, as well as an amyloidogenic C-terminal fragment (CTF-β, C99). Alternatively, α-secretase cleavage, within the Aβ domain, generates the large soluble N-terminal, APPsα, and a non-amyloidogenic C-terminal fragment (CTF-α, C83). Further proteolysis of these fragments by γ-secretase results in generation of either the Aβ (amyloidogenic pathway) or p3-fragment (non-amyloidogenic pathway) and a cytoplasmic APP intracellular C-terminal domain (AICD). Reproduced from Kumar and Walter (2011)

In the non-amyloidogenic pathway, cleavage of APP by α-secretase produces a large soluble extracellular N-terminal fragment, sAPPα, which has neuroprotective properties, and a C83 membrane-bound C-terminal fragment. This cleavage divides the Aβ domain and precludes the formation of intact Aβ. So, stimulating α-cleavage of APP leads to a significant decrease in Aβ generation (Evin and Weidemann, 2002; Ling, Morgan et al., 2003). This activation is a relatively major and ubiquitous pathway of APP metabolism in most cells. Membrane-bound disintegrin and metalloproteinases including ADAM17 (also called TACE), ADAM10, ADAM9 and MDC-9 are proteins that have been identified as having α-secretase-like activity (Evin and Weidemann, 2002; Ling, Morgan et al., 2003). The constitutive α-secretase activity occurs primarily at the cell surface, while the

regulated activity is predominantly located within the Golgi apparatus (Ling, Morgan et al., 2003; Small and Gandy, 2006). There are several factors that can increase this pathway, by mechanisms involving the formation and release of secretory vesicles from the TGN, and thus enhancing APP (and possibly α-secretase) trafficking to the cell surface, as for example the activation of protein kinase C by phorbol esters (Evin and Weidemann, 2002; Ling, Morgan et al., 2003; da Cruz e Silva, Rebelo et al., 2009).

The alternative, amyloidogenic pathway is characterized by the cleavage of APP by β-secretase at its β-cleavage site, producing the large soluble sAPPβ peptide and the carboxy-terminal fragment (CTF) C99. This pathway constitutes the first step in the formation of Aβ and is particularly enriched in neurons (Evin and Weidemann, 2002). Two novel transmembrane aspartyl proteases homologues, β-site APP-cleavage enzymes BACE1 and BACE2, were identified to cleave APP at the β-secretase sites. The major neuronal β-secretase that governs the first enzymatic step in this APP processing is BACE1. This protease appears to be produced as a pro-enzyme predominantly within the nuclear envelope and the ER (Ling, Morgan et al., 2003). The prodomain in BACE1 does not support activity but appears to facilitate correct folding of the active protease domain. This domain is cleaved by proprotein convertases (PPCs) immediately before trafficking through the Golgi (Ling, Morgan et al., 2003). Although the interaction of APP with BACE1 can occur in the ER and on the cell surface, evidence suggests that active BACE1 predominantly localizes in the TGN and endosomes, consistent with the amyloidogenic cleavage of wild-type APP during endocytic/recycling steps (Evin and Weidemann, 2002; Ling, Morgan et al., 2003; Small and Gandy, 2006). The precise role of BACE2 in APP processing remains unclear. BACE2 shows similar substrate specificity, cleaving APP at the β-secretase site, but it also shows a distinct cellular localization pattern and intracellular protease specificity in the cleavage of APP that differentially affects the generation of Aβ (Ling, Morgan et al., 2003). Indeed, BACE2 can also have an α-secretase activity, cleaving APP in the middle of the Aβ domain, between Phe19 and Phe20 (Ling, Morgan et al., 2003).

The second enzymatic step is determined by cleavage of the membrane-bound C-terminal APP fragments (CTFs) of each pathway by γ-secretase. The C83 and C99, fragments resulting from α-secretase and β-secretase cleavage, respectively, remain anchored in the membrane and may become degraded or can be further cleaved by γ-

secretase, leading to the release and secretion of non-pathogenic p3 peptide and Aβ (Evin and Weidemann, 2002). In addition, in both pathways, γ-secretase cleavage generates a cytoplasmic APP intracellular C-terminal domain (AICD). γ-secretase is a multimeric complex composed of four essential transmembrane proteins: presenilin 1 or 2 (PS1 or PS2, respectively), nicastrin, APH-1 and PEN-2 (Small and Gandy, 2006; Thinakaran and Koo, 2008; O'Brien and Wong, 2011). This complex is essential for the sequential intramembranous proteolysis of a variety of transmembrane proteins, like APP, Notch and Cadherin. APH-1 aids the formation of a precomplex, which interacts with PS1 or PS2 while Pen-2 enters the complex to facilitate the proteolytic cleavage of PS1 or PS2, which are critical to the γ-secretase complex (O'Brien and Wong, 2011). The ectodomain of nicastrin recognizes and binds to the previously cleaved transmembrane proteins (O'Brien and Wong, 2011).

Several data indicates the presence of γ-secretase complex and its enzymatic activity in multiple compartments, including the ER, Golgi, TGN, endosomes and plasma membrane, but studies in cell lines have showed that APP cleavages occur mainly in the TGN and endosomes (Thinakaran and Koo, 2008). The γ-secretase complex cleaves at multiple sites within the APP transmembrane domain. The cleavage of C83, CTF resulting of α-secretase, leads to AICD and p3 fragments production. The processing of C99, consequent CTF of the amyloidogenic via, results in different Aβ forms and AICD. The AICD, free from the membrane, has been suggested to function as a transcription factor, but genes regulated by AICD have not been unambiguously identified (Hampel, Shen et al., 2010). The release of the cytoplasmic tail of APP by γ-cleavage may function in gene expression, with AICD being targeted to the nucleus, where it forms a multimeric complex with the nuclear adaptor protein Fe65 and the histone acetyltransferase Tip60, potentially stimulating the transcription of various genes, including APP itself (Ling, Morgan et al., 2003).

Noteworthy, APP metabolism may be regulated by direct APP phosphorylation, and the aberrant production of Aβ associated with AD may result from deregulated, abnormal APP phosphorylation (da Cruz e Silva and da Cruz e Silva, 2003).

1.2.3. Phosphorylation of APP

The direct phosphorylation of APP might be important in APP-mediated roles such as neuronal differentiation, possible by altering APP traffic, by regulating APP proteolytic cleavage to its physiological fragments and/or the binding of APP to specific signal transducers. APP is a phosphoprotein with several well defined phosphorylated residues at its extracellular and intracellular portions (Fig. 9).

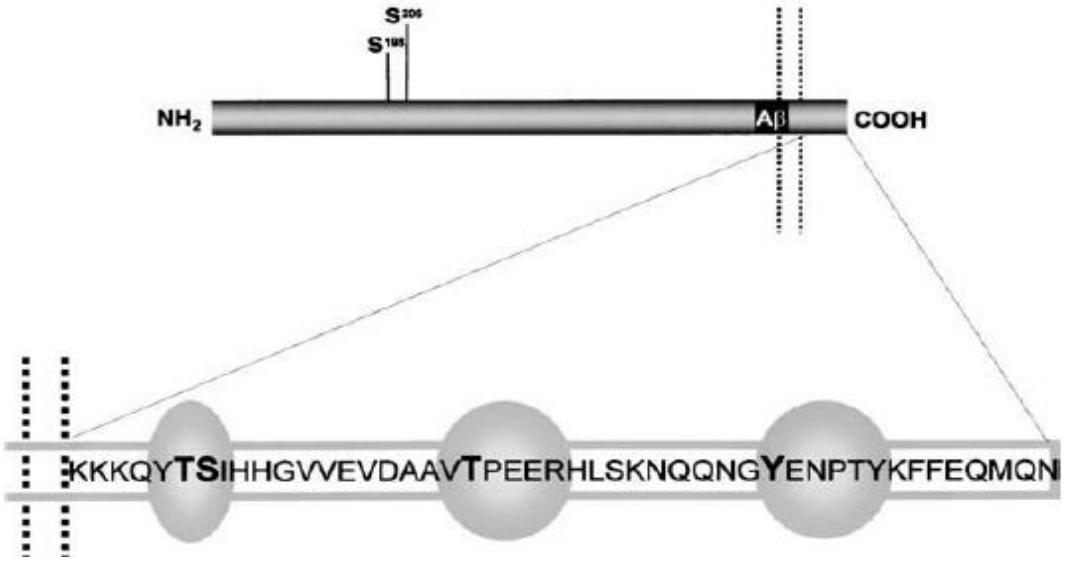

Fig. 9: Schematic representation of the APP phosphorylatable residues. The top diagram represents APP and indicates the two phosphorylated Serine residues present in its ectodomain. The bottom diagram shows the complete amino acid sequence of the cytoplasmic tail, and the three phosphorylatable functional domains. Serine, threonine and tyrosine putative phosphorylation sites are shown enlarged (numbering is relative to APP_{695}). The relative localization of the Aβ sequence is shown. Reproduced from da Cruz e Silva, Fardilha et al. (2004)

Only one phosphorylatable domain was identified in the extracellular ectodomain, and the residues shown to be phosphorylated are Ser198 and Ser206 (da Cruz e Silva, Fardilha et al., 2004). This phosphorylation appears to occur in two distinct cellular locations: in a post-Golgi secretory compartment and at the cell surface, by ectoprotein kinases (da Cruz e Silva, Fardilha et al., 2004). Particularly, phosphorylation of APP cytoplasmic tail comprises three crucial motifs, ^{653}YTSI^{656}, ^{667}VTPEER^{672}, and ^{682}YENPTY^{687}, which have been shown to regulate the interaction of APP with some of its binding proteins (da Cruz e Silva and da Cruz e Silva, 2003; Lee, Kao et al., 2003; da Cruz e Silva, Fardilha et al., 2004).

The ^{653}YTSI^{656} (amino acid numbering according human APP_{695} isoform), is a typical YXXI sorting signal, responsible for mediating APP basolateral sorting. This motif contains Thr654 and Ser655, two consensus residues for phosphorylation known to be phosphorylated in vitro and in vivo. The possible putative kinases involved in their phosphorylation are protein kinase C (PKC) and calmodulin-dependent protein kinase II (CaMKII) (Isohara, Horiuchi et al., 1999; da Cruz e Silva and da Cruz e Silva, 2003; Schettini, Govoni et al., 2010). Ser655 was also reported to be phosphorylated by APP kinase I (da Cruz e Silva and da Cruz e Silva, 2003). Phosphorylation of Ser655 was observed to occur predominantly in mature rather than immature APP isoforms (da Cruz e Silva, Fardilha et al., 2004). As described above, various studies revealed that phosphorylation within this sorting motif modulates APP trafficking. Mimicking phosphorylation at the Ser655 residue was reported to enhance APP secretory traffic, e.g. by increasing APP binding to the retromer complex and the subsequent retromer-mediated APP retrieval to the TGN (Vieira, Rebelo et al., 2010). S655 phosphorylation, potentially via PKC, also increases sAPPα production by the alpha-secretase pathway (da Cruz e Silva, Rebelo et al., 2009; Vieira, Rebelo et al., 2009).

The ^{667}VTPEER^{672} motif contains Thr668. This residue can be phosphorylated by neuronal cyclin-dependent kinase 5 (Cdk5), cyclin-dependent protein kinase 2 (Cdc2), glycogen synthase kinase 3β (GSK-3β), c-Jun-N-terminal kinase 3 and stress-activated protein kinase 1b (da Cruz e Silva and da Cruz e Silva, 2003; da Cruz e Silva, Fardilha et al., 2004; Schettini, Govoni et al., 2010). Phosphorylation at Thr668 might be involved in a neuron-specific aspect of APP metabolism and/or function, because this phosphorylation in mature APP occurs only in the brain, being detected in neurites (da Cruz e Silva, Fardilha et al., 2004). Phosphorylation of this domain appears to be an important factor in the control of interactions of APP with other proteins. However, there are contradictory results for the role of APP phosphorylation at Thr668 in Aβ production, in Fe65 binding and in nuclear translocation of AICD or AICD/Fe65 complex (Schettini, Govoni et al., 2010).

Tyrosine phosphorylation of APP may functionally link APP processing and neurotrophic signaling to intracellular pathways associated with cellular differentiation and survival. This phosphorylation occurs in residues of the amino acid sequence ^{682}YENPTY^{687}, encompassing an NPXY signaling motif, which is a typical internalization signal for membrane-associated receptor proteins (da Cruz e Silva and da Cruz e Silva,

2003). This motif is present in many Tyrosine-Kinase (TK) receptors and non-receptors TKs; it is generally phosphorylated and represents the docking site for several interacting APP-binding proteins, involved in cell signaling and gene transcription (Russo, Venezia et al., 2005; Schettini, Govoni et al., 2010). The phosphorylation of APP occurs in Tyr682 and Tyr687, although phosphorylation at this last residue is still somehow controverse (da Cruz e Silva and da Cruz e Silva, 2003; da Cruz e Silva, Fardilha et al., 2004; Rebelo, Vieira et al., 2007). In cell-culture studies, Tyr682 can be phosphorylated by the overexpression of the nerve growth factor receptor TrkA, by a constitutively active form of the tyrosine kinase Abl or by the Src kinase (da Cruz e Silva, Fardilha et al., 2004; Russo, Venezia et al., 2005; Schettini, Govoni et al., 2010). In some studies using HEK293 cells, it was reported that the phosphorylation of APP at Tyr687 is important for its processing by α- and γ- secretases, increasing CTF-α and AICD generation (Takahashi, Niidome et al., 2008). Of note, it is possible that APP may only become Tyr682 phosphorylated after full-length APP cleavage by the γ-secretase complex (da Cruz e Silva, Fardilha et al., 2004).

1.3. APP as a potential mediator of G proteins signaling

1.3.1. G proteins

G proteins, also called guanine nucleotide-binding proteins, are a family of heterotrimeric proteins that have a crucial role as molecular switches in signal transduction pathways mediated by G protein-coupled receptors (GPCRs). They are involved in transmitting extracellular messages from hormones, neurotransmitters, chemokines and other signaling factors that interact with GPCRs and G proteins to activate many intracellular signaling pathways (Hewavitharana and Wedegaertner, 2012).

The heterotrimeric G proteins are signal-transducing protein complexes composed of α, β and γ subunits, located on the cytoplasmic side of the plasma membrane (Knust, 2001). The Gα subunit contains the nucleotide binding site and GTPase activity, along with sites for binding receptors, effectors and Gβγ, and a helical domain whose function is not clear (Neer, 1995). This subunit determines G protein diversity. The β and γ subunits form a dimer, a single complex that only dissociates when it is denatured and is, therefore, a functional monomer (Neer, 1995). Today it is known that both α and βγ subunits positively

regulate effectors, acting as signaling molecules by activating other second messengers or by gating ion channels directly (Neer, 1995).

Different types of G proteins share a common mechanism. They are activated in response to a conformation change in the GPCR receptor. The GPCRs constitute a large and the most versatile protein family of transmembrane receptors in the mammalian genome (Gudermann, Schoneberg et al., 1997; Wettschureck and Offermanns, 2005). The diversity of this superfamily is a result of the large number of members, their ability to form different dimer combinations and their ability to respond to several stimuli, as well as by the large amount of intracellular signaling pathways they activate. Signaling by GPCRs is not just limited to second messenger molecules but also includes transcription factors and molecules that affect the cytoskeleton. Despite their structural and functional diversity, all GPCRs share a similar molecular architecture (Knust, 2001). They consist of an extracellular N-terminus, an intracellular C-terminus, and seven transmembrane domains in between, linked by alternating intracellular and extracellular loops (Gudermann, Schoneberg et al., 1997).

In the inactive state, the Gα subunit has GDP in its binding site. When a chemical or physical signal stimulates the receptor, the receptor becomes activated and changes its conformation. The Gα subunit responds with a conformational change that decreases GDP affinity, so that GDP comes off the binding site (Fig. 10). Once GTP is bound, the Gα assumes its activated conformation and dissociates both from the receptor and from Gβγ (Knust, 2001). Then, both free Gα-GTP and Gβγ can interact with downstream effectors proteins and diverse downstream signaling cascades, while the receptor is able to interact with other G proteins and amplify signal transduction (Knust, 2001). In addition to activation of second messenger molecules, Gα subunits can also modulate the activity of transcription factors, thereby regulating gene expression (Ram and Iyengar, 2001). The activated state lasts until the GTP is hydrolyzed to GDP by the inherent GTPase activity of Gα, allowing re-association with Gβγ. G protein becomes inactive and returns to the receptor, starting a new cycle (Wettschureck and Offermanns, 2005).

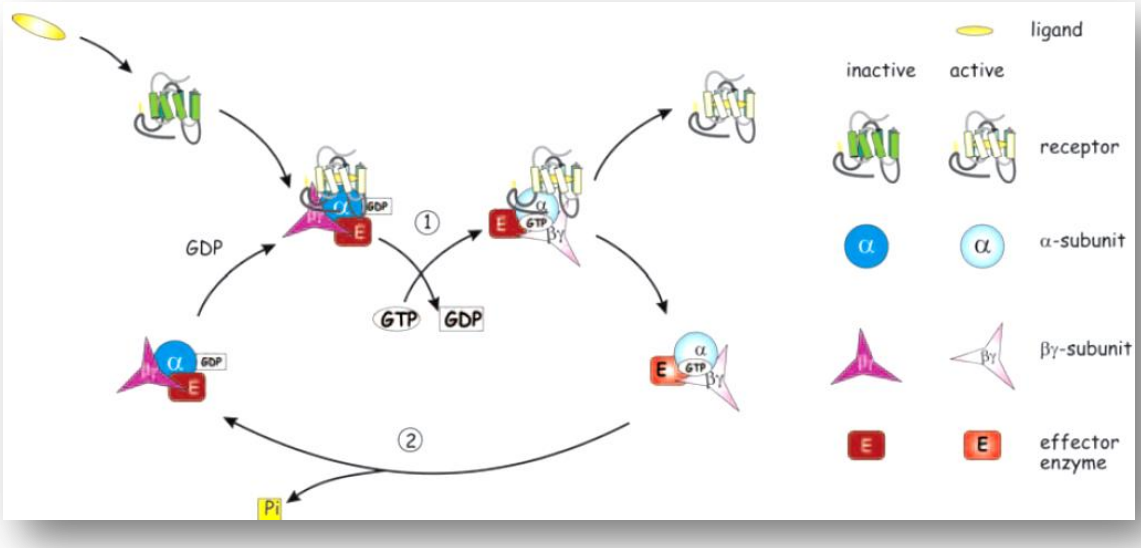

Fig. 10: Activation and deactivation of G proteins by guanine nucleotide exchange and GTP hydrolysis. A ligand binds to the receptor and is activated to become a catalyzer, enhancing the rate of detachment of bound GDP from the α-subunit of the G protein. The rapidly exchange of GDP to GTP in the α-subunit site is rapidly processed (1) and causes activation of both α- and βγ-subunits, enabling them in turn to activate specific effector enzymes. The interaction between receptor and G protein is transient, allowing the receptor to catalyze guanine nucleotide exchange on a succession of G protein molecules. The system returns to the resting state following hydrolysis of the bound GTP, and promotes deactivation of G protein (2). Reproduced from Gomperts, Kramer et al. (2009)

The GTPase cycle of G protein activation and deactivation is subject to regulation by many protein factors that either influences the rate of guanine nucleotide exchange or the rate of hydrolysis of bound GTP.

The family of regulators of G protein signaling (RGS), for example, has been found to play a role in desensitization. These proteins are GTPase-activating proteins (GAPs) that are involved in mechanisms that accelerate the rate of GTP hydrolysis and thereby negatively regulate G protein signaling (Diverse-Pierluissi, Fischer et al., 1999; Hewavitharana and Wedegaertner, 2012). RGS proteins block G protein function by accelerating α subunit GTPase activity, physically blocking the binding to G protein effectors and/or altering the level of free βγ subunits available to their downstream effectors, therefore allowing for rapid modulation of G protein-mediated signaling (Wettschureck and Offermanns, 2005; Blazer, Roman et al., 2010).

By contrast, guanine nucleotide exchanger factors (GEFs) promote the activation of G proteins by increasing the rate of GDP dissociation and GTP association (Hewavitharana and Wedegaertner, 2012). The ligand-bound GPCRs are widely recognized as guanine exchange factors for heterotrimeric G proteins.

The functional versatility of the G protein mediated signaling pathways is based on its modular architecture and on the fact that there are numerous subtypes of G proteins. In

humans, there are genes encoding 16 Gα, 5 Gβ and 12 Gγ subunits (Hewavitharana and Wedegaertner, 2012). The α-subunits increase the diversity, define the basic properties of a heterotrimeric G protein, and can be divided into four families: $G_{i/o}$; G_s; G_q and $G_{12/13}$ (Wettschureck and Offermanns, 2005; Shan, Chen et al., 2006; Hewavitharana and Wedegaertner, 2012). Each family consists of various members that often show very specific expression patterns. Members within each family have structural and functional homologies (Wettschureck and Offermanns, 2005; Hewavitharana and Wedegaertner, 2012).

The G proteins of the $G_{i/o}$ family are widely expressed. The main members of these types of G proteins are G_i proteins (G_{i1}, G_{i2} and $_{Gi3}$) that inhibit various types of adenylyl cyclases and thus lower the levels of the second messenger cyclic AMP (cAMP). The function of members of the $G_{i/o}$ family is affected by pertussis toxin (PTX), which is able to ADP-ribosylate the $G_{i/o}$ α-subunit, and, subsequently, uncouples G_o and G_i from their receptors, leading to the disruption of their signaling. A less widely distributed member of this family is G_z, which is not affected by PTX, is expressed in various tissues (nervous system and platelets) and was recently shown to interact specifically with various other proteins including Rap1GAP and certain RGS proteins. Other α-subunits that belong to the $G_{i/o}$ family, like gustducin and transducin are involved in specific sensory functions, taste and visual, respectively. The G_o member is particularly abundant in the nervous system and will be discussed later on, with its action being greatly mediated by its βγ-complex. Indeed, activation of $G_{i/o}$ is believed to be the major coupling mechanism that results in the activation of βγ-mediated signaling processes.

The ubiquitously expressed G protein G_s stimulates adenylyl cyclase, resulting in increases intracellular levels of cAMP (Wettschureck and Offermanns, 2005).

The G_q/G_{11} family of G proteins binds to and activates members of phospholipase C β-isoform family (Wettschureck and Offermanns, 2005). Interestingly, there is no obvious difference between the abilities of both G protein α-subunits to regulate β-isoforms of phospholipase C. The α-subunits of G_q and G_{11} are almost ubiquitously expressed and are involved in various biological signaling pathways (Wettschureck and Offermanns, 2005).

In the $G_{12/13}$ family, the two members G_{12} and G_{13} appear to be expressed ubiquitously. Studies have showed that $G_{12/13}$ can induce a variety of signaling pathways

leading to the activation of various downstream effectors including other G proteins (Hewavitharana and Wedegaertner, 2012). Of note, the analysis of cellular signaling processes regulated by these G proteins has been difficult since there are no specific inhibitors available. The G_{12} and G_{13} Gα subunits were described to bind to and regulate cell adhesion proteins, and interact directly with the cytoplasmic domain of some members of the Cadherin family of cell surface adhesion molecules (Wettschureck and Offermanns, 2005; Hewavitharana and Wedegaertner, 2012).

The much less understood G protein β and γ subunits, but with a very important role in the regulation of various effectors, are tightly associated and can be regarded as one functional unit. The different subunits could produce several different combinations, but not all possible pairs are formed (Neer, 1995). The β subunits show very high sequence identity and exhibit a more or less ubiquitous expression pattern, whereas γ subunits are considerably more diverse in sequence and tissue expression (Gudermann, Schoneberg et al., 1997; Hurowitz, Melnyk et al., 2000). This suggests that through their diversity these specific subunits couple selectively to effectors, although the molecular determinants of Gβγ-effector coupling are not well known.

1.3.1.1. $G\alpha_o$ Protein: genetics, expression pattern and function

The $G\alpha_o$ protein was accidently discovered during the purification of $G\alpha_i$ from bovine brain. $G\alpha_o$ was designed as the 'other' GTP-binding protein to differentiate from $G\alpha_s$, $G\alpha_i$ and transducin. PTX-mediated ADP ribosylation and electrophoresis samples detected an additional Gα subunit with molecular weight of 39 kDa and revealed a highly $G\alpha_o$ expression in brain tissue (Jiang and Bajpayee, 2009; Bromberg, Lyengar et al., 2011). In contrast to the well characterized pathways transduced by other G-proteins, only recently some mechanism details of $G\alpha_o$ signaling were elucidated. Nonetheless, the identification of direct effectors of $G\alpha_o$ and the determination of $G\alpha_o$-induced cellular responses are still far from known.

The cDNAs encoding $G\alpha_o$ have been cloned and identified in several species, such as human, rat, mouse, bovine, *Drosophila*. $G\alpha_o$ has a highly degree of similarity among the species, suggesting that $G\alpha_o$-mediated signaling are important to receive, integrate and execute the transduction of extracellular stimuli (Jiang and Bajpayee, 2009).

Analysis of genomic cDNA clones encoding $G\alpha_o$ revealed that the human $G\alpha_o$ gene localizes on chromosome 16q13 and contains 11 exons. Both $G\alpha_o$ isoforms, $G\alpha_o1$ ($G_oA\alpha$) and $G\alpha_o2$ ($G_oB\alpha$), are generated via alternative splicing and are identical in the first two-thirds of the amino acid sequence. The two forms differ by only 20 amino acids in human cells. $G\alpha_o1$ and $G\alpha_o2$ share the first 6 exons that encode 241 N-terminal amino acids, and each isoform has unique exons 7, 8 and 9. Different sets of exons suggest that each isoform may contribute to distinctive biological functions in the body and, especially, in the human brain (Jiang and Bajpayee, 2009).

The $G\alpha_o$ protein has a less ubiquitous expression pattern than $G\alpha_i$ or $G\alpha_s$. The protein is expressed widely in the CNS and was estimated to compose 0.5%-1% of membrane proteins in brain (Jiang and Bajpayee, 2009; Bromberg, Lyengar et al., 2011). However, the regional distribution of $G\alpha_o$ protein in all brain is not homogeneous. At the anatomic level, high concentrations of $G\alpha_o$ have been detected in the frontal cortex, cerebellum, hypothalamus, hippocampus and substantia nigra, being principally found on the cytoplasmic face of the plasma membrane coating the cell body and the neurites, particularly at 'cell-to-cell' contacts. It was also determined that $G\alpha_o$ is one of the most abundant proteins in the neuronal growth cones, structure at the tip of the growing neurite that is generated during neuronal differentiation. In addition, $G\alpha_o$ expression has also been observed in heart tissue, pituitary gland and pancreatic islets (Jiang and Bajpayee, 2009).

The $G\alpha_o$ protein has been received considerable attention aiming to determine its physiological role in the body, mainly due to its high expression in CNS. $G\alpha_o$ has been associated to cell survival, neuronal development, neuronal adhesion, migration and some diseases as Alzheimer's and Parkinson's. Studies with $G\alpha_o$ knockout mice have reported several neurological deficiencies, including poor motor coordination, hyperactive and abnormal behaviour, as well as hyperalgesia, when subjected to the lack of this protein (Jiang and Bajpayee, 2009). Another study has revealed that $G\alpha_o$ activation can induce neurite outgrowth in PC12 cells through inhibition of PKC and modulation of intracellular calcium levels (Strittmatter, Fishman et al., 1994).

1.3.1.2. Modulation of $G\alpha_o$ activity

Many protein factors are involved in signal transduction through G proteins to regulate the strength, duration, efficiency and specificity of signaling. $G\alpha_o$ is a highly

effective molecular signaling transducer and many GPCRs have been identified to couple to $G\alpha_o$ protein, such as the cannabinoid 1 (CB1) receptor, muscarinic cholinergic receptors, α_2-adrenergic receptors, and as previously mentioned, these are widely recognized as GEFs for heterotrimeric G proteins. However, several non-receptor proteins have also shown to affect the $G\alpha_o$ subunit G protein activity, including the growth cone-associated protein with molecular weight of 43 kDa (GAP-43), APP, Presenilin 1 and the activator of protein signaling (AGS) (Jiang and Bajpayee, 2009).

GAP-43, a protein highly expressed in the growth cones of developing and regenerating neurons, has the ability to enhance $G\alpha_o$ binding to GTP in the distal tips of growth cones (acting as a GEF), suggesting that $G\alpha_o$ protein can have a neurite outgrowth role. Interestingly, PTX does not alter the $G\alpha_o$ activation by GAP-43 like in the others GEFs. AGS is another GEF involved in regulating $G\alpha_o$-mediated signaling, enhancing GTPγS binding to both G_i and G_o proteins. APP and Presenilin 1 have also been hypothesized to act as a GEF for $G\alpha_o$ protein (Jiang and Bajpayee, 2009).

Other protein factors have also been identified, but these act as decreasers of the guanine nucleotide exchange rate. A RGS protein identified was the Gα-interacting protein (GAIP) that is responsible to selectively accelerate the deactivation of $G\alpha_o$ protein. This RGS protein is not only responsible for deactivation of $G\alpha_o$ protein signaling, but also regulates the duration and specificity of receptor-stimulated $G\alpha_o$ protein signaling (Jiang and Bajpayee, 2009). Other studies revealed the existence of G protein regulatory (GPR) or GoLoco motifs, which bind to $G\alpha_o$ and stabilize it in the GDP-bound conformation while simultaneously competing with Gβγ for Gα binding (Siderovski, Diverse-Pierluissi et al., 1999; Jiang and Bajpayee, 2009).

1.3.1.3. $G\alpha_o$-mediated signaling transduction

The signaling transduction mechanism of $G\alpha_o$ protein and its intracellular effectors has received widely attention, in an attempt to identify the ligands that might stimulate the signal, the downstream signaling pathways subsequently activated, and the cellular functional output of the signaling cascades.

Several studies have shown that $G\alpha_o$ is required to activate phospholipase C (PLC)-β, adenylyl cyclases 2 and 4, and phosphoinositol-3-kinase (PI3K)-β and -γ; also, $G\alpha_o$ has

inhibitory effects on adenylyl cyclase 1 and several voltage-gated calcium (Ca^{2+}) channels. Besides that, $G\alpha_o$ knockout mice have indicated that $G\alpha_o$ has a critical role in the muscarinic inhibition of L-type Ca^{2+} channels in the heart and in the regulation of Ca^{2+} and potassium (K^+) channels in hippocampal neurons. In addition to the regulation of Ca^{2+} and K^+ channels, $G\alpha_o$ proteins may also regulate sodium (Na^+) channels in cells (Jiang and Bajpayee, 2009; Bromberg, Lyengar et al., 2011).

The role of $G\alpha_o$ in the mediation of the MAPK signaling is still elusive, but in Chinese hamster ovary cells it was demonstrated that the expression of an active $G\alpha_o$ mutant is not sufficient to directly induce MAPK activation, but greatly potentiates the activation of PKC, a PI3K-dependent mechanism, that leads to B-Raf kinase and MAPK pathway stimulation (Jiang and Bajpayee, 2009; Bromberg, Lyengar et al., 2011).

As previously described, $G\alpha_o$ signaling induces neurite outgrowth, by several ligands that activate $G_{i/o}$ coupled receptors, but only recently two pathways have begun to elucidate some mechanistic details of how $G\alpha_o$ mediates neurite outgrowth. In Neuro2A cells it was demonstrated that de CB1 receptor stimulates $G\alpha_o$ and activates downstream signaling converging on signal transducer and activator of transcription 3 (STAT3) that finally leads to neurite outgrowth (He, Gomes et al., 2005). The interaction of STAT3 signaling and $G\alpha_o$ will be discussed in more detail below. The other signaling involved in neurite outgrowth, but not as well detailed, is the GRIN pathway. G protein-regulated inducer of neurite outgrowth 1 and 2 (GRIN1 and GRIN2) bind specifically to $G\alpha_o$ and are also enriched in neuronal growth cones. Studies demonstrated that co-expression of GRIN with an activated mutant of $G\alpha_o$ leads to activation of Cdc42 and enhances neurite outgrowth in Neuro2A cells (Nakata and Kozasa, 2005; Bromberg, Lyengar et al., 2011).

1.3.1.4. APP-$G\alpha_o$ binding and Alzheimer's disease

A physical interaction between APP and $G\alpha_o$ protein was demonstrated in synthetic vesicle preparations (Okamoto, Takeda et al., 1995). A completely conserved cytoplasmic APP_{695} sequence, ^{657}His-Lys^{676}, was reported to form a complex with and to activate the $G\alpha_o$ protein (Nishimoto, Okamoto et al., 1993). In further studies using phospholipid vesicles containing APP_{695} and $G\alpha_o$, 22C11, a monoclonal antibody against the extracellular domain of APP, was used to evaluate the interaction between APP and $G\alpha_o$. The authors have found that 22C11 acts on APP_{695} to stimulate $G\alpha_o$ in APP_{695}/G_o vesicles,

increasing GDP/GTP exchange rate of $G\alpha_o$. This effect of 22C11 was specific among various antibodies and was observed neither in $G\alpha_o$ vesicles alone nor in APP_{695}/G_{i2} vesicles. These data demonstrated that APP behaves like a $G\alpha_o$-linker receptor whereby it specifically activates $G\alpha_o$ in a ligand-dependent and ligand-specific manner (Okamoto, Takeda et al., 1995).

Presenilin 1 was also shown to directly interact with $G\alpha_o$. These in vitro studies suggest that $G\alpha_o$ may be involved in neuronal loss in AD through apoptotic signaling mediating by either Aβ, mutant APP or mutant PS1 (Jiang and Bajpayee, 2009). G protein inhibitors (like PTX) have been demonstrated to block Aβ toxicity (Sola Vigo, Kedikian et al., 2009). In neuronal cultures, data has shown that interaction of APP with toxic Aβ species promotes toxicity by a mechanism that involves APP-mediated $G\alpha_o$ protein activation (Sola Vigo, Kedikian et al., 2009). A mechanism proposed is that under pathological loads of Aβ, the interaction of APP and $G\alpha_o$ is reduced, liberating $G\alpha_o$ and subsequently increasing G-protein activity, which may in turn results in downstream effects including calcium deregulation and subsequent cell death (Shaked, Chauv et al., 2009). The $G\alpha_o$ protein may be involved in the pathogenesis of AD by other mechanism(s). In familial Alzheimer's disease (FAD), three missense mutation into isoleucine, phenylalanine and glycine at 642 position of valine (V642) have been identified in the APP_{695} isoform (Okamoto, Takeda et al., 1995; Giambarella, Yamatsuji et al., 1997). These mutations co-segregate with the disease phenotype. All three mutants have been shown to specifically activate the $G\alpha_o$ protein and induce PTX-sensitive apoptosis in COS-NK1 cells. Studies of $G\alpha_o$ knockout, and expression of V642-APPs mutant lacking the His^{657}-Lys^{676} in COS-NK1 cells, provided strong evidence for a mediating function of $G\alpha_o$ in APP-induced apoptosis. Data further demonstrated that the $G\beta\gamma$ subunit was responsible for triggering apoptosis in COS-NK1 cells and the expression of mutationally activated $G\alpha_o$ only induced little apoptosis (Giambarella, Yamatsuji et al., 1997).

1.3.2. STAT3 signaling

1.3.2.1. STAT proteins

Signal transducer and activator of transcription (STAT) transcription factors have been reported to play a variety of roles in biological processes, such as cellular

proliferation, differentiation, migration and apoptosis, regulation of target genes transcription and cell mediation of cytokine receptor signaling (Horvath, 2000; Lee, Park et al., 2007; Chiba, Yamada et al., 2009; Chiba, Yamada et al., 2009).

Seven mammalian STAT family members have so far been identified: STAT1, 2, 3, 4, 5a, 5b and 6, which are structurally conserved and essential for carrying out multiple cellular functions in response to cytokine stimulation, hormones and growth factors signals in a wide range of cell types and tissues (Horvath, 2000; Chiba, Yamada et al., 2009; Chiba, Yamada et al., 2009). The domain structure of STAT proteins is critical for STAT functions and several structural and functional regions have been defined, including a N-domain (ND) responsible for dimer-dimer interactions, a Coiled-Coil domain responsible for protein interactions, a src homology 2 (SH2) domain for receptor recognition and dimerization, which is connected to the DNA binding domain via a linker domain (LD) implicated in transcription. A tyrosine phosphorylation site required for activation and dimerization, and a serine phosphorylation site in a C-terminal transcriptional activation domain were also described (Fig. 11) (Horvath, 2000).

Fig. 11: The structural domains and functional regions of the STAT proteins. ND, N-domain responsible for dimer-dimer interactions (yellow box); Coiled-Coil, coiled-coil domain responsible for protein interactions (green box); DNA-binding, a sequence-specific DNA-binding domain (red box); LD, linker-domain implicated in transcription (orange box); SH2, src homology 2 domain for receptor recognition and dimerization (blue box). All STATs include a tyrosine (Y) phosphorylation (P, red circles) site required for activation and dimerization. Several of the STATs also have a serine (S) phosphorylation (P, red circles) site in their C-terminal transcriptional activation domain (TAD, purple box). Adapted from Horvath (2000)

Ligand-activated cytokine or growth factor receptors initiate STAT signal transduction by the activation of cytoplasmatic tyrosine kinases of the Janus Kinase (JAK) family, or receptors with intrinsic tyrosine kinase activity, which results in the recognition of specific receptor phosphotyrosine residues by a latent cytoplasmatic STAT protein SH2 domain. Phosphorylation of tyrosine residues of STATs allows STAT dimerization and nuclear translocation, where they transcriptionally regulate the expression of target genes. The phosphorylation of STATs serine residues are required to regulate their transcriptional functions (Horvath, 2000; Lee, Park et al., 2007; Chiba, Yamada et al., 2009). A general model for receptor-mediated activation of STAT signaling is represented in Fig. 12.

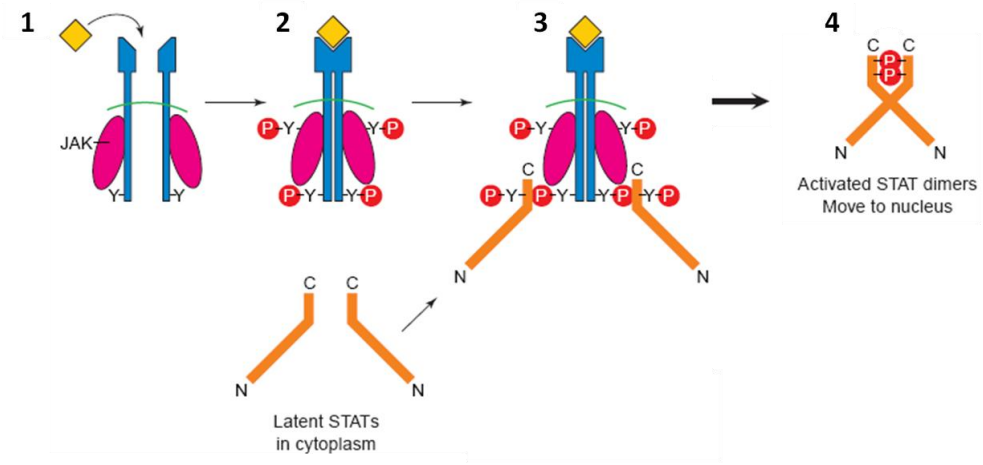

Fig. 12: Classical example of STAT activation mechanism by transmembrane receptors. 1- The binding of the ligand (yellow triangle) induces receptor oligomerization and activation of JAKs. 2- JAKs phosphorylate (P) each other and phosphorylate the receptor cytoplasmic domain on tyrosine residues (Y), creating sites for interaction with proteins. 3- SH2 domains of latent cytoplasmic STAT protein recognize specific receptor phosphotyrosine residues, and the receptor-bound STATs become tyrosine phosphorylated by JAKs. 4- The phosphorylation of STATs allows STAT dimerization (homodimers are illustrated, but heterodimers can also form), and recruitment of them to the nucleus where they bind to promoter response elements and activate transcription of their target genes. Receptors with intrinsic tyrosine kinases and oncogenic tyrosine kinases can apparently activate STATs without the participation of JAK kinases. Adapted from Horvath (2000)

1.3.2.2. STAT3 function

The STAT proteins are structurally similar, but they diverged functionally and coevolved with specific enhancers, and cannot substitute for one another in the regulation of target genes. Several studies on the functional roles of STAT3 revealed that this protein is essential for growth regulation, organogenesis, early embryonic development, neural stem cell differentiation, survival and inflammatory response of neurons, being implicated in the regulation of several genes linked to cell division downstream of growth signals (Horvath, 2000; Ng, Cheung et al., 2006; Chiba, Yamada et al., 2009). Of note, the STAT3 transcript can be alternatively spliced to generate STAT3b, which lacks the 55-aa C-terminal domain of STAT3a and, instead, has a 7-aa C-terminal domain (Horvath, 2000).

In diverse cell types, activation of STAT3 has been reported downstream of receptors for cytokines such as interleukin-6 (IL-6), leukemia inhibitory factor (LIF) and ciliary neurotrophic factor (CNTF) that utilize a common receptor subunit gp130, as well as a number of receptors with intrinsic tyrosine kinase activity (Horvath, 2000; Lee, Park et al., 2007). The recruitment of proteins containing SH2 domains, including STAT3, subsequently leads to the phosphorylation of STAT3 by receptor-associated Janus kinases at tyrosine 705 (Tyr705). The activate STATs causes homo- or heterodimerization of

STAT1/3 transcription factors and subsequent translocation to the nucleus, activating multiple target gene transcription via interaction with specific DNA-response elements (Ng, Cheung et al., 2006).

1.3.2.3. APP and $G\alpha_o$ in STAT3 signaling

The STAT3 signaling pathway has been extensively spotlighted due to its involvement and regulatory role in various biological processes, such as neuronal development. Studies demonstrated that CNTF is an instructive signal for astroglial type 2 cell fate, specifically mediated via activation of STAT3 (Aberg, Ryttsen et al., 2001; Xu, Chen et al., 2009). In AD patients, studies showed controversies regarding the involvement of STAT3 signaling. Some experiences have detected an elevation of STAT3 phosphorylation at Tyr705 in the postmortem samples of AD brains (Wan, Fu et al., 2010), while others have concluded that STAT3 inactivation is involved in the pathogenesis of AD (Chiba, Yamada et al., 2009; Chiba, Yamada et al., 2009). It has also been reported that APP relies on the activation of the JAK/STAT3 signaling pathway to induce cell death, increasing the expression of a chemokine with neuroinflammatory properties (Vrotsos, Kolattukudy et al., 2009). These results indicated that APP expression increased phosphorylation of STAT3 at Tyr705. Other studies indicate that the STAT3 signaling is crucial for sAPPα-induced glial differentiation. Results have demonstrated that sAPPα is able to enhance phosphorylation of STAT3 at Tyr705 in a time-dependent manner, by directly and indirectly activation of JAK/STAT signaling through gp130 (Kwak, Dantuma et al., 2010).

The ability of Gα subunits to stimulate STAT3 is especially intriguing because STAT3 plays an important role in differentiation, proliferation, transformation, apoptosis, and development of cells. In a previous study, results have showed that overexpression of a constitutively active $G\alpha_o$ mutant, $G\alpha_o$ Q205L, in NIH-3T3 fibroblast cells leads to the activation of the STAT3 pathway, resulting in increased proliferation and in the transformation of the cells (Ram, Horvath et al., 2000). $G\alpha_o$ was shown to increase both Tyr705 STAT3 phosphorylation and STAT3 transcriptional activity. In Neuro-2A cells, where endogenous $G\alpha_o$ proteins are expressed, previous data indicated that activation of cannabinoid receptor 1-coupled $G\alpha_{i/o}$ (CB1), a GPCR that regulates neurite outgrowth, leads to the activation of STAT3 and changes in gene expression and, subsequently, in the

normal cell physiology (He, Gomes et al., 2005). STAT3 phosphorylation by $G\alpha_o$ subunits (Fig. 13) appears to be mediated via Src, a member of a family of cytoplasmic tyrosine kinases, and to involve activation of a cascade of signaling intermediates, like small GTPases (Rap1-GAP, Rac 1, Rap 1 and Ral 1) (Ram and Iyengar, 2001; He, Gomes et al., 2005). This may be an important pathway in neurons, where $G\alpha_o$ activation can lead to neurite outgrowth and neuronal plasticity. Activation of many GPCRs has also been reported to phosphorylate and activate STAT3 via others Gα subunits, like $G\alpha_{16}$, leading to changes in gene transcription (Wu, Lo et al., 2003).

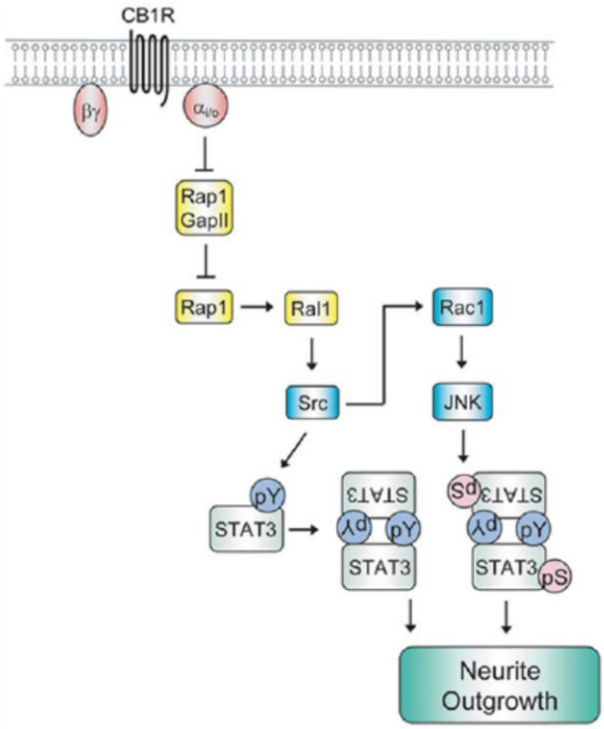

Fig. 13: G_o signaling to the nucleus during the induction of neurite outgrowth. In Neuro2A cells, activation of CB1 cannabinoid receptor mediates neurite outgrowth. Overexpression of $G\alpha_o$ reduces the stability of Rap1GapII, which results in the activation of Rap1. Activation of Rap1 leads to the activation of Src and STAT3 that mediate gene expression that promotes neurite outgrowth. The CB1 activation also stimulates the small GTPase Rac1 and subsequently c-Jun N-terminal kinase (JNK). Both of these proteins are activated downstream Src, and JNK also enhances STAT3 phosphorylation. Reproduced from Bromberg, Lyengar et al. (2011)

The work here described is thus aimed to prove the interaction of APP and $G\alpha_o$ in STAT3 signaling and the cellular/molecular role of this interaction, elucidating the sequence of events/signaling pathways after activation.

2. Aims of this thesis

In the work here described we mainly intended to test if APP and APP phosphorylated at S655 could modulate $G\alpha_o$-induced STAT3 signaling. For this, the SH-SY5Y neuroblastoma cell line was used, along with specific cDNAs for APP and $G\alpha_o$ and several molecular and cellular biology procedures.

2.1. General Aims

- To study if APP-$G\alpha_o$ co-transfection modulates $G\alpha_o$-induced STAT3 signaling by western blot analysis;
- To study if APP phosphorylation at S655 modulates $G\alpha_o$-induced STAT3 signaling;
- To evaluate the effect of $G\alpha_o$ activation and APP S655 phosphorylation in APP-$G\alpha_o$ binding.

2.2. Specific Aims

- To purchase and amplify $G\alpha_o$ and $G\alpha_o$CA (a Q205L mutant mimicking constitutively active $G\alpha_o$) cDNAs.
- To optimize SH-SY5Y cells transfection with $G\alpha_o$ and $G\alpha_o$CA cDNAs, and test anti-$G\alpha_o$ antibodies.
- To optimize time conditions of SH-SY5Y cells transfection with $G\alpha_o$ and $G\alpha_o$CA in terms of their effects on STAT3 signaling.
- To test if APP overexpression affected $G\alpha_o$ and $G\alpha_o$CA-induced STAT3 signaling.
- To test if APP phosphorylation at S655 influences $G\alpha_o$- and $G\alpha_o$CA-induced STAT3 signaling, by co-transfecting cells with APP-GFP fusion cDNAs (Wt or S655 phosphomutants: S655A and S655E) and $G\alpha_o$ or $G\alpha_o$CA CDNAs.
- To analyse if $G\alpha_o$ and $G\alpha_o$CA have an effect on APP turnover and/or cleavage.
- To evaluate if APP-GFP proteins differentially interact with $G\alpha_o$ or $G\alpha_o$CA proteins using the GFP-trap® pull-down technique.

3. Materials and Methods

3.1. Culture and maintenance of the SH-SY5Y cell line

The human neuroblastoma SH-SY5Y cell line is derived from the original cell line SK-N-SH, isolated from a bone marrow biopsy of a neuroblastoma patient. The SH-SY5Y cell line was maintained in a 5% CO_2 humidified incubator at 37°C with a recommended culture medium: 10% fetal bovine serum (FBS) minimal essential medium (MEM):F12 (1:1), with 2mM L-glutamine and 100U/mL penicillin and 100mg/mL streptomycin [10mL Streptomycin/Penicilin/Amphotericin solution, Gibco]. Cells were split at 70-80% confluence.

3.2. Wt and S655 Phosphomutants APP-GFP cDNAs

APP-GFP cDNAs were already available at the lab. Namely, APP isoform 695 (APP_{695}) cDNA was used as template to generate S655 cDNA point mutations, namely Serine 655 to Alanine (S655A) or to Glutamate (S655E), using site directed mutagenesis (da Cruz e Silva, Iverfeldt et al., 1993; Vieira, Rebelo et al., 2010). These two amino acids, due to their size and charge, mimic a constitutively dephosphorylated (S655A) and phosphorylated (S655E) S655 residue, respectively. Further, PCR was performed to remove the stop codons of Wt and S655 phosphomutants APP_{695} cDNAs and engineer the APP_{695}-GFP cDNA constructs (APP-GFP) by subcloning the amplified APP cDNA fragments into the EGFP-N1 plasmid, encoding for the Green Fluorescent Protein (GFP) (Vieira, Rebelo et al., 2009).

3.3. Wild-type and constitutively active G-protein alpha o – $G\alpha_o$ and $G\alpha_oCA$ (Q205L) cDNAs

The G-protein alpha o cDNA was obtained at the Missouri S&T cDNA Resource Center. The human wild type G-protein alpha o subunit has been cloned into pcDNA3.1+ (Invitrogen) at KpnI (5') and Xba I (3'). The open reading frame was amplified by PCR from human whole brain cDNA (Clontech). The Q205L mutation was introduced into the

wild-type human G-protein alpha o by Quickchange mutagenesis kit (Stratagene). The constitutively activated $G\alpha_o$ is characterized by a change in Glutamine 205 to Leucine (Q205L), resulting in a $G\alpha_o$ subunit mutation that lacks guanosine triphosphatase (GTPase) activity, remaining in a constitutively active form. Both these clones are distributed in Invitrogen's pcDNA3.1+ vector, which can be used for mammalian expression and production of stably transfected cell lines. Upon purchase, these cDNAs, together with the empty pcDNA3.1 plasmid vector, were transformed in competent *E. coli* strains, and plasmid DNA amplified by megaprep technique using the Promega Wizard® Plus Megapreps DNA Purification System, following the manufacturer instructions.

3.4. SH-SY5Y cells transfection with APP-GFP and $G\alpha_o$ or $G\alpha_o$CA cDNAs

In order to study the effect of APP and APP phosphorylation on $G\alpha_o$-induced STAT3 signaling, SH-SY5Y neuroblastoma cells were transiently transfected or co-transfected with Wt, S655A (SA), or S655E (SE) APP-GFP fusion cDNAs contructs, and $G\alpha_o$ or $G\alpha_o$CA (a Q205L mutant)cDNAs. To optimize SH-SY5Y cells transfection with these constructs, three different transfection methods were initially tested, the Polyplus, the TurboFect™ lipid-mediated, and TurboFect™ combined with CombiMag methods. In these preliminary experiment cells were left to transfect for 24h. In further experiment the transfection method of choice was the TurboFect™ and cells were transfected for specific time periods (2h, 4h, 6h, 8h or 24h). Cells were then harvested in 1% SDS for Western blotting (WB).

3.4.1. Transfection by the Polyplus method

To proceed the transfection with the polyplus method, cells were seeded per well in 2 mL of cell growth medium 24h prior transfection and, at the time of transfection, cells were 60-80% confluent. First, the transfection mix was prepared, where 1 µg of DNA was diluted in 100 µL of jetPRIME™ buffer (this must be diluted 1:5). After being mix by vortexing and a briefly spin down, 2 µL of jetPRIME™ reagent were added to the diluted DNA (1:2 DNA to jetPRIME™ reagent ratio). The mixture was vortexed, subjected to spin down and incubated for 10 min at room temperature. Then, 100 µL of transfection mix was added, per well, dropwise onto the cells in regular cell growth medium, and distributed

evenly. The six-well plates were gentle agitated and incubated at 37ºC in a humidified incubator in an atmosphere of 5% CO_2. After 4h of incubation, this transfection medium had to be replaced by 2 ml of growth medium and the plates returned to the incubator, in order to complete 24h of transfection.

3.4.2. Transfection using the TurboFect™ reagent

Transfections were carried out according to the manufacter's instructions (Fermentas Life Sciences). Before transfection the appropriate medium was replaced. Briefly, for each monolayer of cells grown in six-well plates, 2 μg of the respective DNA were diluted in 100 μL of serum-free growth medium. After being quickly vortexed, 4 μL of TurboFect™ were added to the diluted DNA. The mixture was vortexed, incubated for 15-20 min at room temperature, and then transferred dropwise to each well, with gentle agitation of the plate to achieve even distribution. The cells were incubated at 37ºC in a CO_2 incubator. After 6h, cell medium was replaced and transfection was left to occur until the selected transfection time. In the main experiments the transfection levels were decreased by down-scaling the protocol to 1 μg of cDNA to 2 μL of TurboFect™.

3.4.3. Transfection using the TurboFect™ reagent plus CombiMag

In this transfection method, TurboFect™ lipid-mediated transfection is improved, by incorporating a CombiMag reagent. This last component increases transfection efficiency, due to the use of magnetism by a magnetic plate (also called 'magnetofection'). Cells were seeded in order to accomplish 60-90% confluency at the time of transfection. Before magnetofection the appropriate medium was replaced, and for each monolayer of cells to transfect, 1 μL of the CombiMag reagent, previously vortexed, was pipetted into a microtube. The DNA and TurboFect™ reagent mixture was prepared in a second microtube: first, 1 μg of DNA was diluted in 100 μL of serum-free growth medium; second, TurboFect™ is vortexed and 1 μL of this was added to the diluted DNA. This mixture was added to the first microtube with the CombiMag reagent. After being vortexed, the microtube was incubated for 15-30 min at room temperature. This was added onto the medium above each cell monolayer, with gentle mixing, and then the six-well plates were placed over a magnetic plate (OZ Biosciences), during 15 min. Transfected

cells were incubated at 37ºC in a CO_2 incubator, cell medium exchanged after 6h, according to the Turbofect^{TM} protocol, and transfection was left to occur for a total of 24h.

3.5. Cell collection and quantification of protein content (BCA)

Cells' conditioned medium (500 µl) was collected into a microtube containing 55 µl of 10% SDS, the remainder medium was sucked with a Pasteur pipette, and further cells were collected with 250 µl of 1% boiling SDS. Cellular and medium lysates were boiled for 10 min, and cell lysates were sonicated for 30 sec.

The total protein quantification method was performed by Pierce's BCA protein assay kit in an aliquot of the cell lysates, following the manufacturer's instructions. This assay is the result of two reactions. Firstly, there is the reduction of Cu^{2+} to Cu^{+} by protein in an alkaline medium to form a light blue complex. In this biuret reaction peptides containing three or more amino acid residues form a coloured chelate complex with cupric ions in an alkaline environment containing sodium potassium tartrate. The amount of Cu^{2+} reduced is proportional to the amount of protein present in the solution. The bicinchoninic acid reagent (BCA) addition leads to a sensitive colorimetric detection of the Cu^{+} cation, by chelation of two molecules of BCA with each Cu^{+} ion (a temperature dependent reaction). This gives rise to a purple-coloured reaction product that strongly absorbs light at a wavelength of 562 nm. The BCA/copper complex exhibits a high linearity in a working range of increasing BSA concentration between 20 to 2000 µg/ml. Total protein concentration of each sample was determined through a standard curve prepared by plotting BSA absorbance vs. BSA standard concentration. The standards were prepared, as in Table 1, directly into the wells of a 96-well microplate.

Table 1. Standards used in the BCA protein assay method, with standard protein concentrations. BSA, Bovine serum albumin solution (2 mg/ml).

Standard	BSA (µl)	10% SDS (µl)	H_2O (µl)	Protein mass (µg)	W.R. (µl)
P_0	-	2,5	22,5	0	200
P_1	1	2,5	21,5	2	200
P_2	2	2,5	20,5	4	200
P_3	5	2,5	17,5	10	200
P_4	10	2,5	12,5	20	200
P_5	20	2,5	2,5	40	200

The samples were prepared in each well by adding 5 µl of each sample to 20 µl of the solution in which the sample was collected (in this case 1% SDS). 200 µl/well of working reagent (W.R), was prepared by the mixture of BCA reagent A with BCA reagent B in the proportion of 50:1, respectively, and was rapidly added to each well (standards and samples). The microplate was incubated at 37ºC exactly for 30 min, and then cooled to RT. The absorbance at 562 nm was immediately measured using a microplate reader (Infinite M200, Tecan), with gentle oscillation and 25 readings for each well.

3.6. Antibodies

The primary antibodies used in this study were: the monoclonal 22C11 mouse antibody (Chemicon) directed against APP N-terminus, recognizing full-length APP and secreted APP (sAPP), and the polyclonal CT695 rabbit antibody (Invitrogen) that recognizes APP C-terminal (detection of APP full length and APP C-terminal peptides), for APP and APP-GFP detection; the polyclonal rabbit anti-$G\alpha_o$ (Upstate) and the monoclonal mouse anti-$G\alpha_o$ (Chemicon) antibody that recognizes the G_o α subunit; the monoclonal rabbit anti-phospho-STAT3 (Tyr705, Millipore) and the monoclonal mouse anti-STAT3 (Cell Signaling Technology) antibodies, directed against the STAT3 isoforms alpha (~84kDa) and beta (~76kDa), were used to evaluate the modulation of STAT3 signaling. A polyclonal rabbit anti-PARP cleavage site (214/215) antibody that can be used as a marker for detecting apoptotic cells by recognizing the 85 kDa fragment of cleaved PARP was used in the transfection optimization assay. As potential loading control for Western blot assays, the monoclonal antibody anti-β-Tubulin, that binds the two major and a minor β-tubulin isotypes, was used. A list of all the antibodies used, together with their respective dilutions and secondary antibodies is depicted in Table 2.

Table 2. Antibodies used in the Western blots, respective target proteins and specific dilutions used. All the secondary antibodies are from Amersham Pharmacia.

Target Protein/Epitope	**Primary Antibody**	**Secondary Antibody**
APP C-terminal	**CT695** (Invitrogen) Dilution: 1:500	Horseradish Peroxidase conjugated α-Rabbit IgG Dilution: 1:5000
APP N-terminal	**22C11** (Chemicon) Dilution: 1:250	Horseradish Peroxidase conjugated α-Mouse IgG Dilution: 1:5000

Target Protein/Epitope	Primary Antibody	Secondary Antibody
$G\alpha_o$	**Anti- $G\alpha_o$** (Upstate) Dilution: 1:5000	Horseradish Peroxidase conjugated α-Rabbit IgG Dilution: 1:5000
$G\alpha_o$	**Anti- $G\alpha_o$** (Chemicon) Dilution: 1:3000, 1:1000 1:500	Horseradish Peroxidase conjugated α-Mouse IgG Dilution: 1:5000
PARP cleavage site 214-215	**Anti-PARP cleavage site (214/215)** (Chemicon) Dilution: 1:1000	Horseradish Peroxidase conjugated α-Rabbit IgG Dilution: 1:5000
Phospho-STAT3	**Anti-phospho-STAT3** (Tyr 705), clone EP2147Y (Millipore) Dilution: 1:3000	Horseradish Peroxidase conjugated α-Rabbit IgG Dilution: 1:1000
STAT3	**Anti-STAT3** (124H6) (Millipore) Dilution: 1:1000	Horseradish Peroxidase conjugated α-Mouse IgG Dilution: 1:2000
β-Tubulin	**2-28-33** (Invitrogen) Dilution: 1:2000	Horseradish Peroxidase conjugated α-Mouse IgG Dilution: 1:5000

3.7. Western Blot Assays

Mass-normalized cell aliquots were subjected to a 7.5% (for the medium samples) and 5-20% gradient (optimization and experimental assays) sodium dodecylsulfate (SDS) polyacrylamide gel electrophoresis (PAGE), being subsequently electrotransferred onto nitrocellulose membranes. After proteins transfer, the membranes were hydrated in 1X TBS for 10 min. To block possible non-specific binding sites of the primary antibody, a blocking solution was used of 5% non-fat dry milk in 1X TBS-T solution. The membranes were immersed in this solution for 1h or 2h. Then, the incubation with primary antibody was achieved for a period of time according to the manufactures instructions (ranging from 2 h to overnight incubation). After this incubation, membranes were washed three times for 10 min each, with 1X TBS-T. The membrane was further incubated with the specific secondary antibody conjugated with horseradish peroxidase which binds to the respective primary antibody, for 2h with agitation. All primary and secondary antibodies used, with specific dilutions (Table 2), were diluted in 1X TBS-T/3% non-fat dry milk, 1X TBS-T/5% non-fat dry milk or 1X TBS/1% BSA. Then, the membranes were again subjected to three washes for 10 min each, with 1X TBS-T. To proceed to the detection of the secondary

antibody and consequently of the proteins, membranes were submitted to the enhanced chemiluminescence (ECL) detection method. This method is a light emitting non-radioactive method for detection of immobilised specific antigens, conjugated directly or indirectly with horseradish peroxidase-labelled antibodies. The washed membranes were incubated at RT for 1 min with home-made ECL detection solution (detailed composition in appendix) or for 2-5 min with Luminata™ Crescendo (Millipore). The excess of detection reagent was drained off the membrane. In a dark room the blot was then placed in an x-ray film cassette with a sheet of a Hyperfilm ECL (GE Healthcare) on the top of it. The cassette was closed and the blot exposed for an appropriate period of time. The film was then removed and developed with developer solution (Sigma Aldrich), washed in water, and fixed in a fixing solution (Sigma Aldrich). Then one can estimate if the membrane needs more or less time inside the x-ray cassette. The blot was further washed in 1X TBS-T and distilled water before drying, for better conservation.

3.8. GFP-trap® pull-down assays

For biochemical studies, the green fluorescent protein (GFP)-fusion proteins and their interacting factors can be isolated fast and efficiently via pull down of GFP with GFP-trap® (Chromotek). Since the interaction is mediate by a small GFP-binding protein coupled to a monovalent matrix (e.g. agarose beads) the GFP-trap® enables purification of any protein of interest fused to GFP, eGFP, YFP or Venus.

After transfection (as in section 3.4.2.), SH-SY5Y cells were washed in 1x PBS and 1 ml of cold PBS with 1x PMSF (dilute stock 1:100) was added, keeping the six-well plate on ice. The cells were collected with a scrapper to a microtube and immediately putted on ice. The sample was then centrifuged for 5 min at 4ºC at 3000 g, the supernatant was removed, and 500 µl of lysis buffer was added to the pellet. This was maintained 30 min on ice and vortexed twice, with 10 min intervals. Meanwhile, the protein sepharose G beads and the GFP-TRAP beads (Chromotek) were being prepared, by resuspending them in wash buffer, centrifuging at 13000 g for 1 min and keeping at 4ºC. After the 30 min, the sample was centrifuged for 5 min at 10000 g at 4ºC, 25 µl of supernatant were transferred to a new microtube and 12 µl of Loading Buffer/10% SDS were added, always keeping the sample on ice (‘cells lysates’). The rest of the supernatant was transferred to a new microtube and, to pre-clear the cell lysate, washed protein sepharose G beads were added

(25 µl for sample) for 1h at 4ºC with orbital agitation. After BCA protein quantification (as described before in section 3.5.), mass normalized lysates were centrifuged for 5 min at 13000 g at 4ºC, and the supernatant transferred to GFP-TRAP beads (20 µl for sample) and incubated overnight with orbital shaking at 4ºC. The mixture was then centrifuged for 5 min at 10000 g at 4ºC, 25 µl of supernatant were collected to a new microtube and 12 µl of Loading Buffer/10% SDS were added ('Supernatant'). The pellet was washed with 1 ml of wash buffer, incubated for 10 min with agitation at 4ºC and centrifuged for 1 min at 10000 g at 4ºC. The supernatant was fully discarded and these operations were repeated for eight or nine times. 50 µl of Loading Buffer/1% SDS and 2,5 µl of β-mercaptoethanol were added to the precipitates. Afterwards, all protein samples were sonicated for 30 sec, boiled for 10 min and frozen. The precipitates, lysates and supernatants were separated by WB.

3.9. Ponceau S staining of proteins bands

Ponceau S staining of proteins bands has been applied as an alternative means to actin or β-tubulin immunoblotting to assess equal gel loading, or quality control of membrane transfer in Western blots. This loading control practice has been described as a fast, inexpensive, and nontoxic method, and binding is fully reversible in a few minutes (Romero-Calvo, Ocon et al., 2010). The nitrocellulose membranes were incubated in Ponceau S solution (Sigma Aldrich, 0.1 % [w/v] in 5% acetic acid) for seven minutes, followed by a brief rinse in distilled water so that the bands were clearly visible. The membranes were then inserted into transparency sheets and scanned (Fig. 14) in a GS-800 calibrated imaging densitometer (Bio-Rad). After that, membranes were washed in 1x TBS-T for 2–3 min with gentle agitation and 1x in distilled water until the staining was completely eliminated. The stain solution can be re-used and the membranes can be immunologically detected.

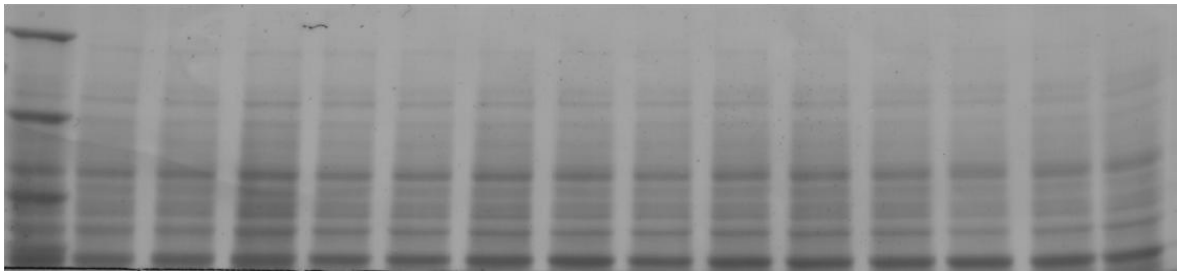

Fig. 14: Example of a Ponceau S staining to be used as a loading control in Western blots. Nitrocellulose membranes were subjected to reversible Ponceau S staining, and lanes of bands scanned in a GS-800 calibrated imaging densitometer (Bio-Rad).

3.10. Fluorescence Microscopy

Cells grown on coverslips were fixed with a 4% paraformaldehyde PBS solution for 30 min and permeabilized with a 0,2% TRITON in PBS solution for 10 min; after these procedures, coverslips were immediately washed three times with PBS solution. Afterward, the cells were blocked with 50 μL PBS-3% BSA for 30 min. In order to visualize Gαo and APP, 20 μL of both anti-Gαo and 22C11 antibodies were added in each coverslip. After two hours of incubation, the primary antibodies were removed by washing the coverslips three times with PBS, for 10 min each wash. 40 μL of secondary antibodies, Alexa Fluor 488 and Texas-Red, were diluted in PBS-3%BSA and added to the coverslips for two hours in the dark, at room temperature. Coverslips were further washed three times with PBS and one last time with distilled water, and then mounted onto microscope glass slides with a drop of DAPI-containing antifading Reagent (Bio-Rad) for further fluorescence microscopy analysis. Fluorescence microphotographs were taken using confocal microscopy, LSCM. Images were acquired in a LSM 510 META confocal microscope (Zeiss) using an Argon laser line of 488 nm (green channel), a 561 nm DPSS laser (red channel), and a Diode 405-430 laser (blue channel).

3.11. Data analysis

Autoradiography films resulting from immunoblots detection were scanned in a GS-800 calibrated imaging densitometer (Bio-Rad) and protein bands were quantified using the Quantity One densitometry software (Bio-Rad). Data from $G\alpha_o$/$G\alpha_o$CA and APP-GFP cDNAs transfected cells was compared to vector pcDNA3 (V_1) and N1-EGFP (V_2) transfected cells, respectively, and expressed as mean ± SEM (standard error of the mean) of four independent experiments. Statistical significance analysis was conducted by one way analysis of variance (ANOVA) followed by the Tukey test.

4. Results

4.1. Optimization of APP/Gα$_o$ cDNAs transfection

In order to optimize SH-SY5Y cells transfection, three transfection methods - Polyplus, Turbofect^{TM}, and Turbofect^{TM} plus CombiMag - were tested. For this, SH-SY5Y neuroblastoma cells were plated at 70-80% confluence, being transfected at the next day with Gα$_o$ and Gα$_o$CA cDNAs, using the three different transfection methods as described in sections 3.4. The levels of Gα$_o$ transfection were evaluated by Western blot analysis using an anti-Gα$_o$ antibody (Fig. 15), by comparing with non-transfected cells (NT, Fig.15 at the right).

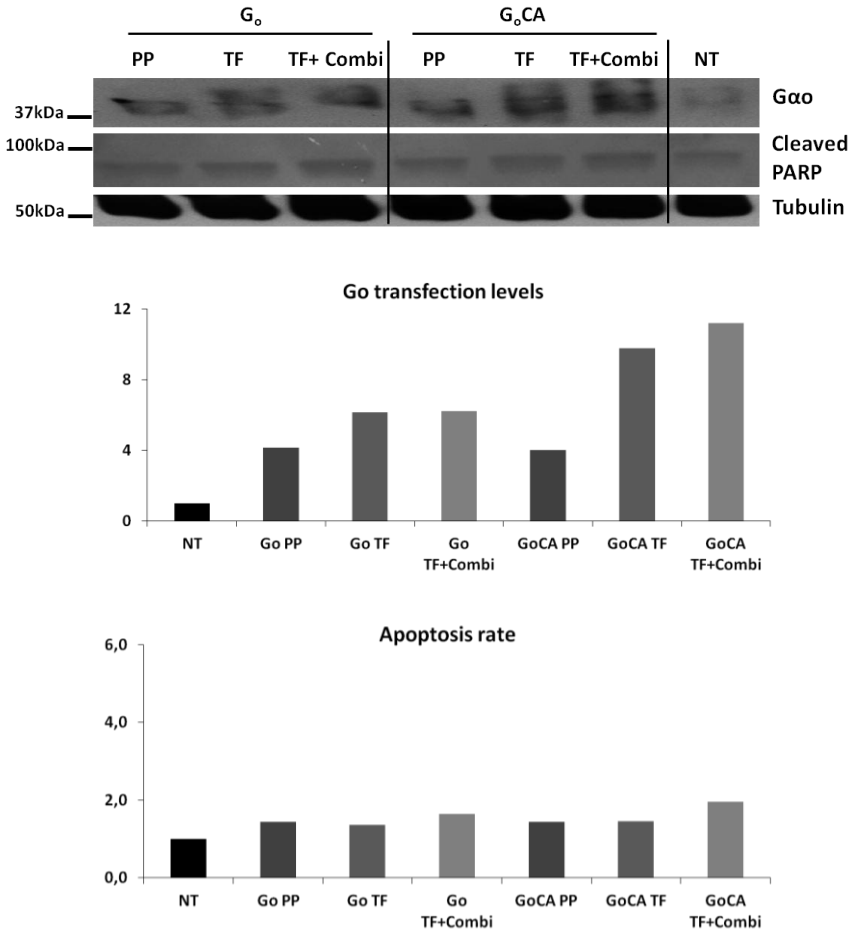

Fig. 15: Evaluation of Gα$_o$ and Gα$_o$CA cDNAs transfection in SH-SY5Y cells using different transfection methods. Upper panel: Immunoblot analysis of Gα$_o$ and Gα$_o$CA cDNAs transfection, cleaved PARP (for apoptosis analysis) and STAT3 signaling, using anti-Gα$_o$, anti-PARP cleavage site (214/215), anti-STAT3 and anti-phospho-STAT3 (Tyr705) antibodies, respectively. Lower panel and graphs: Protein expression profiles of Gα$_o$ and cleaved PARP with different transfection methods, allowed evaluate Gα$_o$ transfection and apoptosis rate. NT: non-transfected cells; Go PP, Go TF and Go TF+Combi: cells transfected with Gα$_o$ cDNA, using Polyplus, Turbofect^{TM}, and Turbofect^{TM} plus CombiMag respectively; GoCA PP, GoCA TF and GoCA TF+Combi: Gα$_o$CA cDNA transfected cells, using Polyplus, Turbofect^{TM} lipid-mediated and Turbofect^{TM} plus CombiMag respectively.

All the transfection methods tested rendered good levels of $G\alpha_o$ transfection, but both the Turbofect™ and Turbofect™ plus CombiMag methods yield higher transfections. Although the Turbofect™ plus CombiMag method yielded the best efficient transfection rate, it was associated with an increase in cell death. PARP cleavage, a classical characteristic of apoptosis, was used to evaluate the apoptosis rate, by Western blot analysis using an anti-PARP cleavage site (214/215) antibody (Fig. 15). Therefore, in all successive experimental assays, the Turbofect™ reagent method was used. Of note, the mouse anti-$G\alpha_o$ antibody (Chemicon) was first tested here and rendered no visible signal.

4.2. Pilot experiment – time periods of $G\alpha_o$ transfection

Subsequently, a pilot experiment was delineated in order to optimize the best time periods of $G\alpha_o$ transfection for the study of $G\alpha_o$–induced STAT3 signaling. For that, cells were plated at 70-80% confluence and transfected, after 24h, with pcDNA3 vector alone or the $G\alpha_o$ and $G\alpha_o$CA cDNAs, for 2h, 4h, 6h, 8h and 24h. After each transfection time period, cells were collected for Western blot analysis. Both the anti-phospho-STAT3 (pSTAT3, Tyr 705) and anti-STAT3 antibodies were used to analyse STAT3 activation, and the levels of $G\alpha_o$ were analysed using the anti-$G\alpha_o$ rabbit antibody (Fig. 16). Tubulin was detected by anti-β-Tubulin antibody. Again, the mouse anti-$G\alpha_o$ antibody was not able to detect endogenous or transfected $G\alpha_o$, and hence only the rabbit antibody (Upstate) was used in further experiments.

Increase in $G\alpha_o$ expression could be observed from 6h of transfection on, and its expression increased with time of transfection; $G\alpha_o$CA expression could be observed from 4h on, and was slightly higher than for $G\alpha_o$. $G\alpha_o$ effects on the STAT3 signaling could be observed from 6h until 24h of transfection, and only $G\alpha_o$ at 6h visibly induced STAT3 phosphorylation. Indeed, for the other periods following the 6h time point, and for all the $G\alpha_o$CA transfections, the levels of STAT3 phosphorylation were found to decrease below the vector pcDNA3 ones. Hence, a retro-inhibition mechanism of this pathway appears to exist upon longer $G\alpha_o$ overexpression times or with $G\alpha_o$ activation, mimicked by the $G\alpha_o$CA mutant. Further, at 8h and 24h, $G\alpha_o$CA overexpression induces a higher negative feedback on STAT3 phosphorylation than $G\alpha_o$.

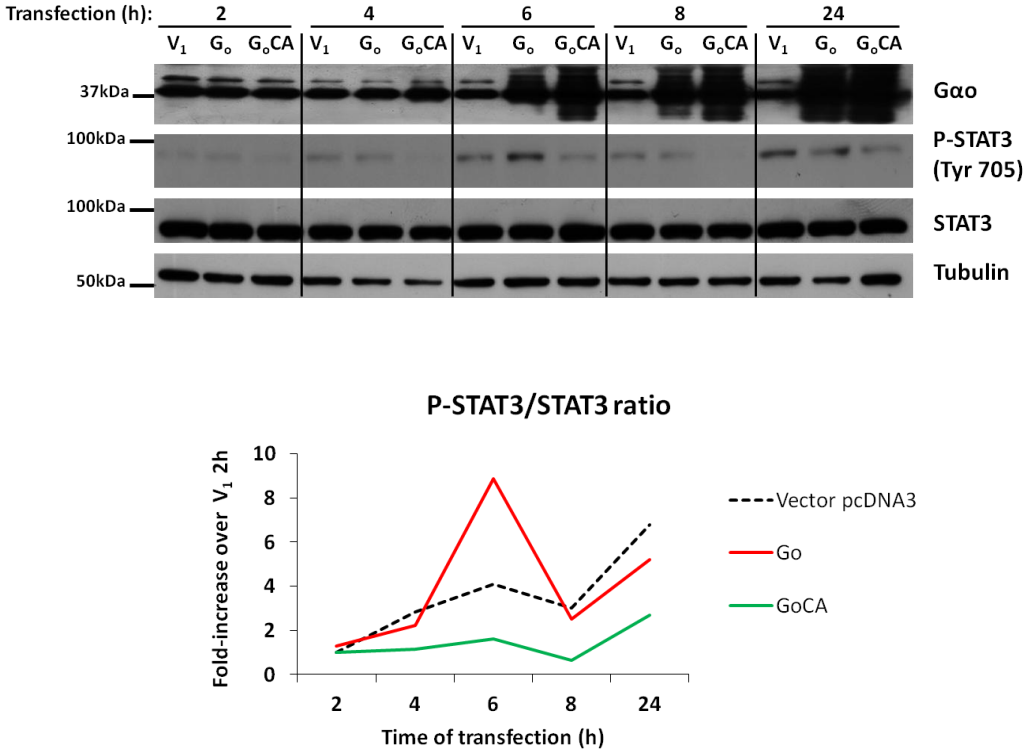

Fig. 16: Evaluation of $G\alpha_o$ transfection effects on the STAT3 signaling upon different times of transfection (2h, 4h, 6h, 8h and 24h). Upper panel: Immunoblot analysis of SH-SY5Y cells that were transfected with pcDNA3 vector, $G\alpha_o$ and $G\alpha_oCA$ cDNA. $G\alpha_o$ and $G\alpha_oCA$ cDNA transfections were confirmed by using the anti-$G\alpha_o$ antibody. STAT3 signaling was analysed by the use of anti-phospho-STAT3 (Tyr705) and total anti-STAT3 antibodies. Tubulin was also detected by using an anti-β-Tubulin antibody. Graph: The rate of STAT3 activation is presented by the ratio of Phospho-STAT3 to total STAT3 levels for the samples transfected only with the pcDNA3 vector, or with $G\alpha_o$ and $G\alpha_oCA$ cDNAs at different times of transfection. V_1: vector pcDNA3 transfected cells; Go and GoCA: cells transfected with $G\alpha_o$ and $G\alpha_oCA$ cDNA, respectively.

In synthesis, the 6h transfection period was the only one where STAT3 activation could be recorded by Western blot means, and at 24h of transfection the pSTAT3/STAT3 ratio were below vector levels for both $G\alpha_o$ and $G\alpha_oCA$. Hence, in all subsequent assays, 6h and 24h were the transfection time periods chosen, as they rendered higher and opposite effects on STAT3 signaling. Further, in the following main experiments, the transfection levels were purposely decreased in an attempt to record not only $G\alpha_o$ but also $G\alpha_oCA$-induced STAT3 phosphorylation at the 6h period.

4.3. APP effects on Gα$_o$–induced STAT3 signaling

4.3.1. APP and Gα$_o$ effects on STAT3 activation levels

In order to decipher the influence of APP and Gα$_o$ interaction on STAT3 signaling, and the underlying mechanisms, non differentiated SH-SY5Y neuroblastoma cells were transfected with pcDNA3 (V_1) and EGFP-N1 (V_2) empty vectors, APP-GFP (Wt, S655A and S655E - mimicking APP S655 dephosphorylation and phosphorylation, respectively), Gα$_o$ and Gα$_o$CA (a Q205L mutant mimicking constitutively active Gα$_o$) cDNAs, and co-transfected with APP-GFP fusion cDNAs and Gα$_o$ or Gα$_o$CA. Transfection was conducted for 6 and 24 h by the Turbofect^{TM} method, after which cells and medium were harvested for Western blot procedure. Transfection of APP-GFP constructs was confirmed for all conditions by using the 22C11 antibody against APP N-terminus (Fig. 17, bands a, b in Wt, SA or SE lanes), which also detects endogenous APP proteins (bands c-e). Transfected Gα$_o$ or Gα$_o$CA (Fig. 17, lanes Gα$_o$ and Gα$_o$CA) and endogenous Gα$_o$ were detected for all conditions, using the rabbit anti-Gα$_o$ antibody.

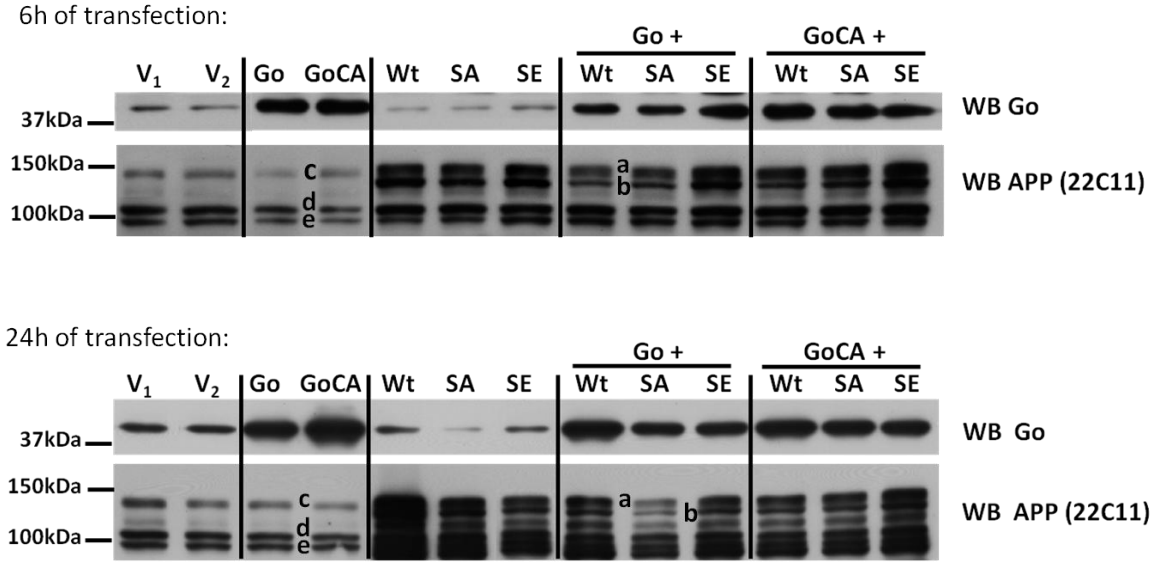

Fig. 17: Qualitative assessment of Gα$_o$ and APP-GFP levels of transfection upon 6h and 24h of transfection. Immunoblot analysis of SH-SY5Y cells transfected with pcDNA3 (**V1**) and N1-EGFP (**V2**) vectors, Gα$_o$ and Gα$_o$CA (**Go** and **GoCA**, respectively), wild-type and S655 phosphomutant APP-GFP (**Wt, SA, SE**) cDNAs, or co-transfected with APP-GFP fusion cDNAs and Gα$_o$ or Gα$_o$CA: **Go + Wt, SA or SE**: Gα$_o$ and Wt, S655A or S655E co-transfected cells; **GoCA + Wt, SA or SE**: cells co-transfected with Gα$_o$CA and Wt, S655A or S655E. Upper panel: 6h of cDNAs transfection; lower panel: 24h of cDNAs transfection. Gα$_o$ and APP expressions were detected using the anti-Gα$_o$ antibody and the 22C11 antibody, against APP N-terminus, respectively. **a)** APP-GFP 695 mature; **b)** APP-GFP 695 immature forms; **c)** endogenous APP 751/770 mature; **d)** endogenous APP 751/770 immature forms; **e)** endogenous APP 695 immature form.

Tubulin was detected by using an anti-β-Tubulin antibody. Tubulin levels showed a consistent variation pattern, indicating that it was an experimental variable and therefore not suited to be used as a loading control (Fig. 18). Thus, Ponceau S staining of total proteins bands was performed, and samples' lanes were quantified and used as loading control for further quantitative determinations.

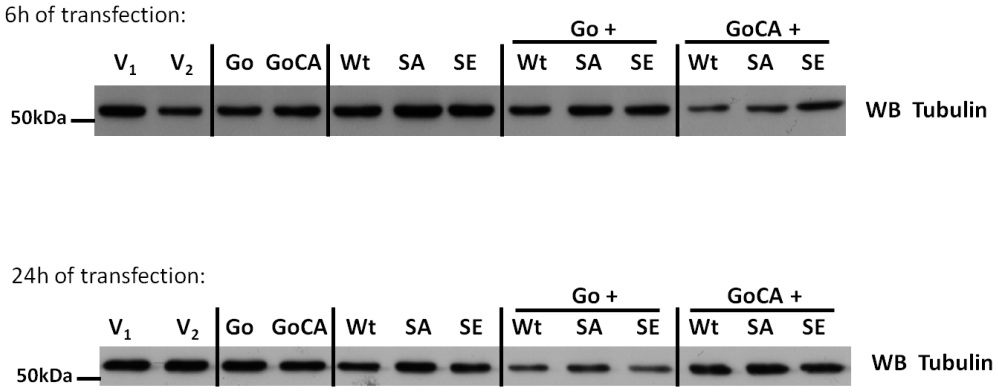

Fig. 18: Qualitative assessment of tubulin levels upon 6h and 24h of transfection. Immunoblot analysis of SH-SY5Y cells transfected with pcDNA3 (**V1**) and N1-EGFP (**V2**) vectors, $G\alpha_o$ and $G\alpha_o$CA (**Go** and **GoCA**, respectively), wild-type and S655 phosphomutant APP-GFP (**Wt, SA, SE**) cDNAs, or co-transfected with APP-GFP fusion cDNAs and $G\alpha_o$ or $G\alpha_o$CA: **Go + Wt, SA or SE**: $G\alpha_o$ and Wt, S655A or S655E co-transfected cells; **GoCA + Wt, SA or SE**: cells co-transfected with $G\alpha_o$CA and Wt, S655A or S655E. Upper panel: 6h of cDNAs transfection; lower panel: 24h of cDNAs transfection. Tubulin detected by anti-β-Tubulin antibody.

Following, the activation of STAT3 signaling was analyzed using both an anti-phosphoSTAT3 (Tyr 705) and anti-STAT3 antibodies, in the 6h and 24h Western blots.

APP effects on $G\alpha_o$-induced STAT3 signaling (6h of transfection)

The levels of STAT3 and P-STAT3 for each condition were quantified by densitometry and plotted upon their correction to the loading control (Ponceau S). At 6h of transfection, no significant variation on total STAT3 levels was observed for all conditions tested. On the other hand, significant alterations in STAT3 phosphorylation levels (P-STAT3) could be observed for some conditions. Protein quantification data were used to determine the P-STAT3/STAT3 ratio for each condition, a measure of STAT3 activation (Fig. 19).

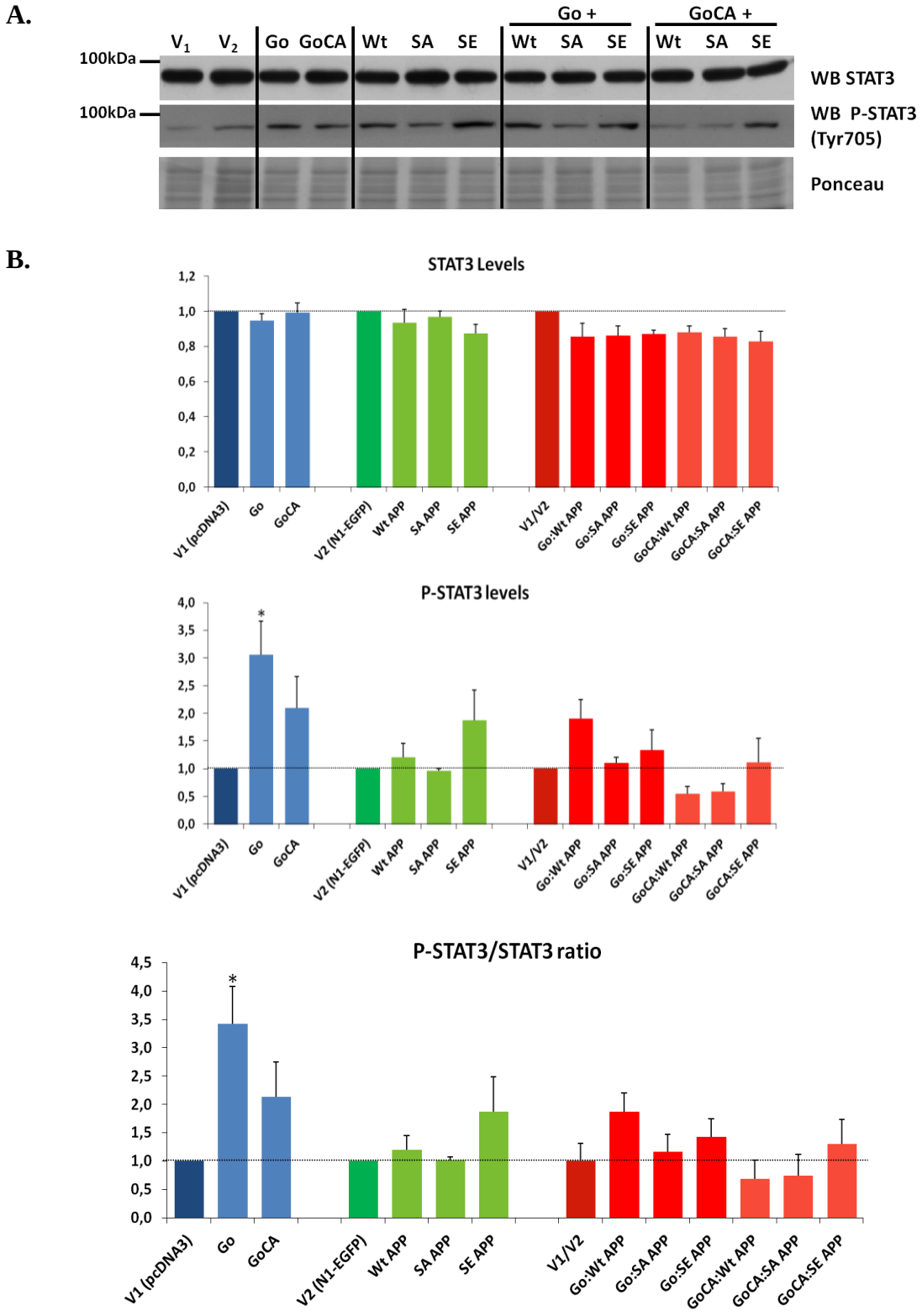

Fig. 19: Evaluation of the influence of APP and APP phosphorylation in Gα$_o$-induced STAT3 signaling in SH-SY5Y cells, upon 6h of transfection. A. Western blot analysis of cells transfected with pcDNA3 (**V1**) and N1-EGFP (**V2**) vectors, Gα$_o$ and Gα$_o$CA (**Go** and **GoCA**, respectively), wild-type and S655 phosphomutant APP-GFP (**Wt, SA, SE**) cDNAs, or co-transfected with APP-GFP fusion cDNAs and Gα$_o$ (**Go+ Wt, SA or SE)** or or Gα$_o$CA (**GoCA+ Wt, SA or SE**). STAT3 signaling was analysed using anti-phospho-STAT3 (Tyr 705) and anti-STAT3 antibodies. **B.** Graphic analysis of STAT3, phospho-STAT3 (P-STAT3) and P-STAT3/STAT3 ratio variations for all conditions tested. Data are presented as mean ± SEM, upon correction to Ponceau. *p<0.05 (experimental vs vector control data). n=4.

As expected, we observe that both $G\alpha_o$ and $G\alpha_oCA$ induce STAT3 phosphorylation, although $G\alpha_oCA$ leads to lower increases (not statistically significant), possibly due to the induction of a retro-inhibitory mechanism. Transfected alone, APP-GFP proteins do not change the phosphorylation state of STAT3, when compared to N1-EGFP values, except for the S655 phosphorylated mutant form (SE APP) that appears to be prone to increase this signaling pathway. All APP-GFPs/$G\alpha_o$ co-transfections lead to a decrease in $G\alpha_o$-induced STAT3 phosphorylation, potentially by enhancing a retro-inhibition effect following $G\alpha_o$ and/or STAT3 activation. This effect appears to be enhanced by APP S655 dephosphorylation (SA APP), and by $G\alpha_o$ activation, as it is higher when APP-GFPs are co-transfected with activated $G\alpha_o$ ($G\alpha_oCA$).

APP effects on $G\alpha_o$-induced STAT3 signaling (24h of transfection)

SH-SY5Y 24h transfected cells lysates were also probed for phosphoSTAT3 (Tyr 705) and total STAT3 (Fig. 20A). At 24h of transfection, a greater variability on the STAT3 protein levels could be observed, in comparison with the 6h time point (Fig. 19B and 20B). Indeed, slight increases could be observed upon transfection with the APP-GFP or $G\alpha_o$ cDNAs.

On the other hand, the profiles of variation of STAT3 phosphorylation were similar to the ones observed at 6h but with much lesser amplitude, which lead to no significant variations (Fig. 20B).

The P-STAT3/STAT3 ratio (Fig. 20B) generally decreases for all constructs. This was previously seen for $G\alpha_o$ and $G\alpha_oCA$ 24h transfections in the pilot experiment (Fig. 16), corroborating the existence of a retro-inhibition mechanism that, besides activation-dependent (as seen in the 6h condition), appears to be time dependent (compare P-STAT3/STAT3 ratio at 6h and 24h, Fig. 19B and 20B). Again, this downregulation is more pronounced for $G\alpha_oCA$ transfection and for its co-transfections with APP-GFP cDNAs, in particular with the S655A dephosphomimicking mutant.

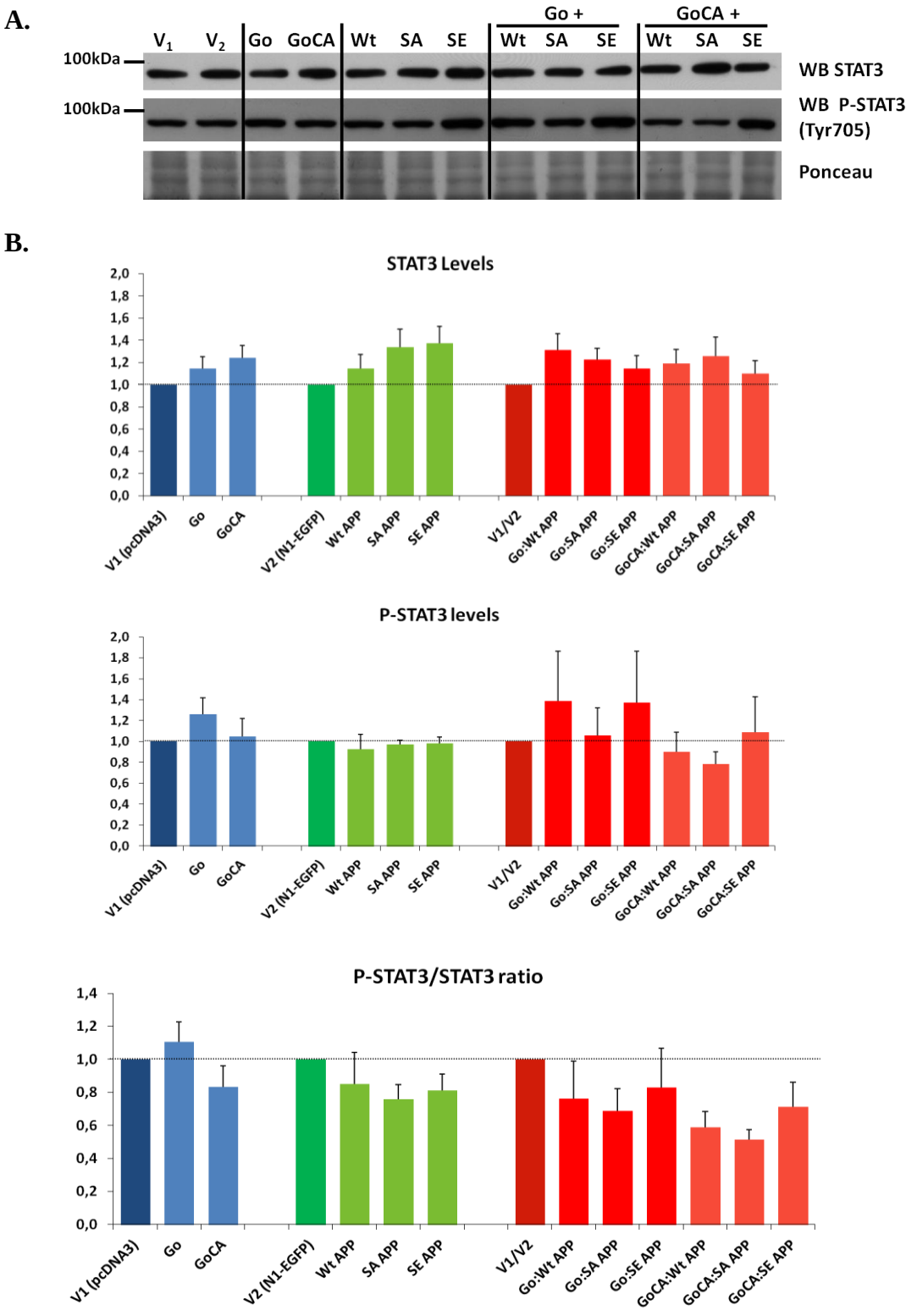

Fig. 20: Evaluation of the influence of APP and APP phosphorylation in $G\alpha_o$-induced STAT3 signaling in SH-SY5Y cells, upon 24h of transfection. A. Western blot analysis of cells transfected with pcDNA3 (**V1**) and N1-EGFP (**V2**) vectors, $G\alpha_o$ and $G\alpha_oCA$ (**Go** and **GoCA**, respectively), wild-type and S655 phosphomutant APP-GFP (**Wt, SA, SE**) cDNAs, or co-transfected with APP-GFP fusion cDNAs and $G\alpha_o$ (**Go+ Wt, SA or SE)** or or $G\alpha_oCA$ (**GoCA+ Wt, SA or SE**). STAT3 signaling was analysed using anti-phospho-STAT3 (Tyr 705) and anti-STAT3 antibodies. **B.** Graphic analysis of STAT3, phospho-STAT3 (P-STAT3) and P-STAT3/STAT3 ratio variations for all conditions tested. Data are presented as mean ± SEM, upon correction to Ponceau; n=4.

4.3.2. Effect of APP overexpression in $G\alpha_o$ levels

During the previous analysis of the STAT3 signaling activation, we have noticed that APP overexpression was having an effect on $G\alpha_o$ levels, what could also partially relate with a STAT3 retro-inhibition mechanism. To analyse this, first the levels of endogenous and transfect $G\alpha_o$ were quantified in all experimental conditions. The effect of APP-GFP expression on endogenous $G\alpha_o$ levels was determined by comparing $G\alpha_o$ levels in transfected APP-GFP samples versus N1-EGFP (V_2) samples. Variations in exogenous $G\alpha_o$ levels were obtained by analysing $G\alpha_o$ levels in APP-GFP/$G\alpha_o$ and APP-GFP/$G\alpha_o$CA co-transfections, in comparison with $G\alpha_o$ and $G\alpha_o$CA samples, respectively (Fig. 21).

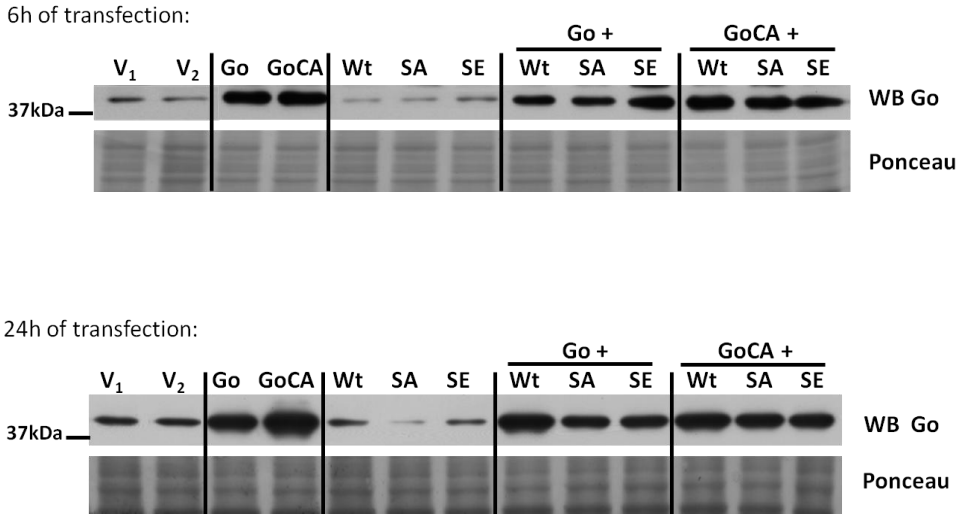

Fig. 21: Analysis of endogenous and exogenous Go levels with APP-GFPs tranfection and co-transfection, respectively, at 6h and 24h. Immunoblot analysis of SH-SY5Y cells transfected with pcDNA3 (**V_1**) and N1-EGFP (**V_2**) vectors, $G\alpha_o$ and $G\alpha_o$CA (**Go** and **GoCA**, respectively), wild-type and S655 phosphomutant APP-GFP (**Wt, SA, SE**) cDNAs, or co-transfected with APP-GFP fusion cDNAs and $G\alpha_o$ or $G\alpha_o$CA: **Go + Wt, SA or SE**: $G\alpha_o$ and Wt, S655A or S655E co-transfected cells; **GoCA + Wt, SA or SE**: cells co-transfected with $G\alpha_o$CA and Wt, S655A or S655E. $G\alpha_o$ levels were analysed by using a rabbit anti-$G\alpha_o$ antibody at 6h (upper panel) and 24h (lower panel) of transfection.

At 6h and 24h, endogenous $G\alpha_o$ levels decreased with APP-GFPs transfection in comparison to the N1-EGFP vector, except for S655E APP that only appears to have this type of effect at 24h (Fig. 21 and 22). Wt and S655A APP-GFP transfection decrease the $G\alpha_o$ levels by ~50% and ~40%, respectively, upon 6h of transfection, and S655A even decreases $G\alpha_o$ levels by ~65% at 24h.

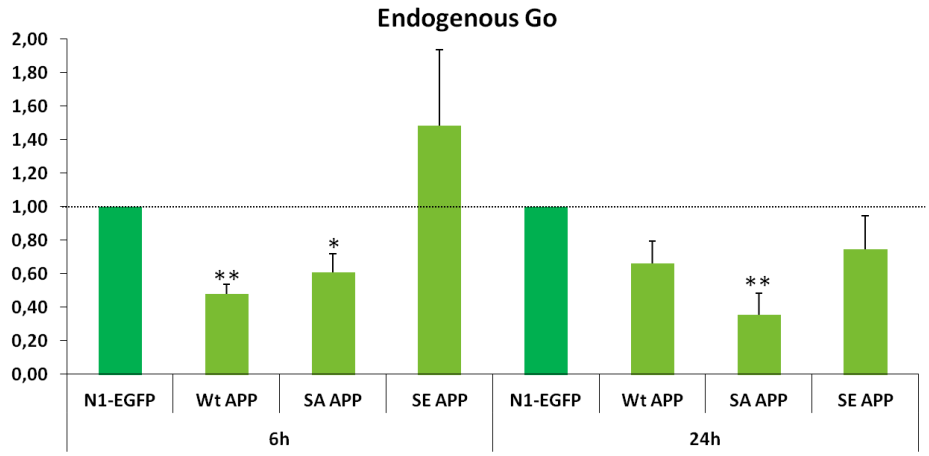

Fig. 22: Protein expression profiles of endogenous $G\alpha_o$ levels with APP-GFPs 6h and 24h of tranfection. N1-EGFP: vector N1-EGFP transfected cells; **Wt, SA, SE**: cells transfected with Wt, S655A and S655E APP-GFP cDNAs, respectively. Data are presented as mean±SEM, upon correction to Ponceau. *p<0.05, **p<0.01. n=4.

When analysing the exogenous $G\alpha_o$/$G\alpha_o$CA levels (Fig. 23), much smaller decreases could be observed, perhaps due to the strong promoter of $G\alpha_o$ plasmids and their good transfection rates. Indeed, only a small decrease in $G\alpha_o$ levels with APP co-transfection can be observed at 6h, but this effect increases with time, being more apparent upon 24h of transfection (Fig. 23). The same occurs with APP/$G\alpha_o$CA co-transfections, although more pronounced than for APP/$G\alpha_o$ co-transfections, and again slightly increasing with time, supporting that this negative effect of APP on $G\alpha_o$ levels is time and, specially, $G\alpha_o$ activation-dependent.

S655 phosphorylated APP (SE APP) decrease exogenous levels of $G\alpha_o$ again only at 24h. This downregulation effect of S655E APP on exogenous $G\alpha_o$ levels occurs already at 6h for $G\alpha_o$CA, potentially due to $G\alpha_o$ activation.

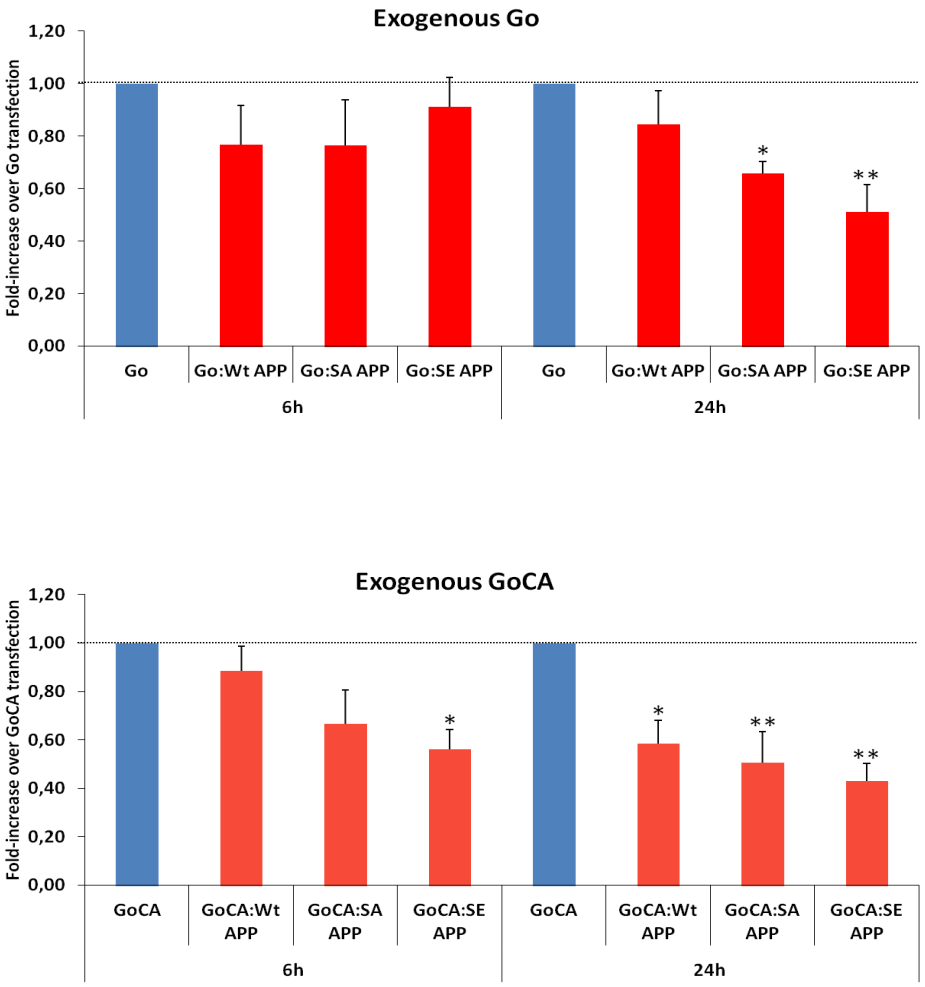

Fig. 23: Fold-increase of exogenous G_o and G_oCA protein expression levels with APP-GFPs co-tranfection at 6h and 24h. Upper panel: Exogenous $G\alpha_o$ levels at 6h and 24h of transfection. Lower panel: Exogenous $G\alpha_oCA$ levels at 6h and 24h of transfection. **Go** and **GoCA**: cells transfected with $G\alpha_o$ and $G\alpha_oCA$ cDNA, respectively; **Go:Wt, SA or SE**: $G\alpha_o$ and Wt, SA or SE co-transfected cells; **GoCA:Wt, SA or SE**: cells co-transfected with $G\alpha_oCA$ and Wt, SA or SE. Data are presented as mean±SEM, upon correction to Ponceau *p<0.05, **p<0.01. n=4.

4.3.3. Effect of $G\alpha_o$ overexpression in APP levels

To evaluate the effect of $G\alpha_o$ overexpression in APP, endogenous APP levels were quantified in $G\alpha_o$ and $G\alpha_oCA$ transfection samples and compared to pcDNA3 (V_1) samples. The analysis of exogenous APP levels was obtained by quantification of the levels of total APP, or APP-GFP alone, in APP-GFP/$G\alpha_o$ and APP-GFP/$G\alpha_oCA$ co-transfection samples, and their comparison to the corresponding APP-GFP sample (Fig. 24).

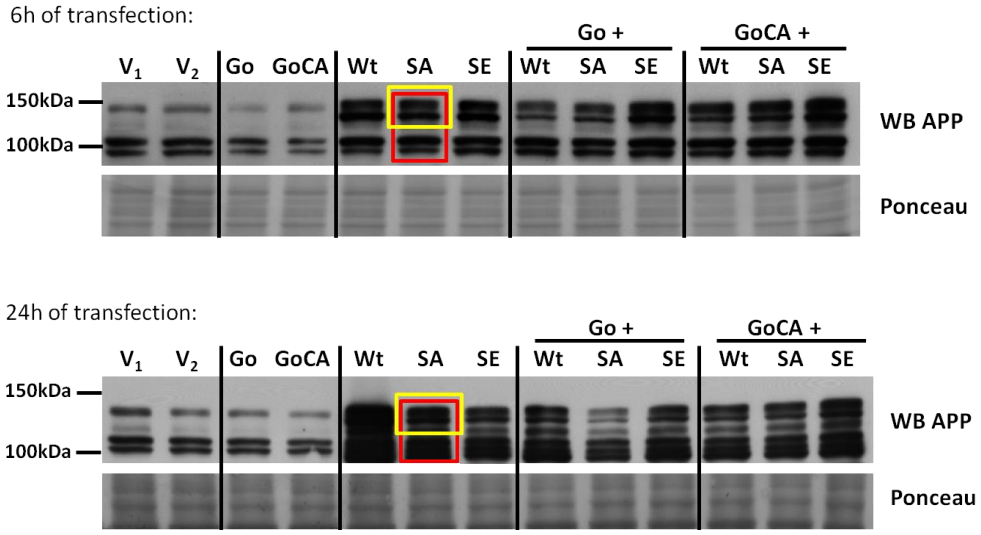

Fig. 24: Analysis of endogenous APP and transfected APP-GFP levels at 6h and 24h. Immunoblot analysis of SH-SY5Y cells transfected with pcDNA3 (**V_1**) and N1-EGFP (**V_2**) vectors, $G\alpha_o$ and $G\alpha_oCA$ (**Go** and **GoCA**, respectively), wild-type and S655 phosphomutant APP-GFP (**Wt, SA, SE**) cDNAs, or co-transfected with APP-GFP fusion cDNAs and $G\alpha_o$ or $G\alpha_oCA$: **Go + Wt, SA or SE**: $G\alpha_o$ and Wt, S655A or S655E co-transfected cells; **GoCA + Wt, SA or SE**: cells co-transfected with $G\alpha_oCA$ and Wt, S655A or S655E. Upper panel: 6h of cDNAs transfection; lower panel: 24h of cDNAs transfection. APP expressions were detected using the 22C11 antibody, against APP N-terminus, respectively. **Red box**: total APP forms; **Yellow box:** APP-GFP bands.

When observing $G\alpha_o$ and $G\alpha_oCA$ solely transfected samples, we can observe a decrease in endogenous APP levels, but this effect is more pronounced upon 24h of transfection. Contrary to what was observed for the APP-induced decrease in $G\alpha_o$ levels, this effect was similar between $G\alpha_o$ and $G\alpha_oCA$ proteins (Fig. 25).

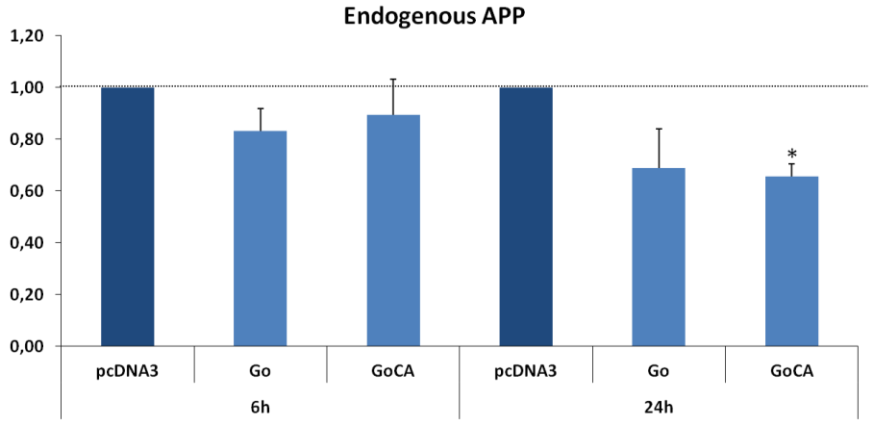

Fig. 25: Representation of protein expression profiles of endogenous APP levels with $G\alpha_o$ and $G\alpha_oCA$ tranfection at 6h and 24h. pcDNA3: vector pcDNA3 transfected cells; **Go and GoCA**: cells transfected with $G\alpha_o$ and $G\alpha_oCA$ cDNA, respectively. Data are presented as mean±SEM, upon correction to Ponceau. *$p<0.05$. n=4.

Relatively to APP-GFP and $G\alpha_o$ and $G\alpha_oCA$ co-transfections, these invariably lead to a decrease in exogenous total APP and APP-GFP levels, which in general follow the same variation profiles (Fig. 26). At 6h, either $G\alpha_o$ or $G\alpha_oCA$ decrease both Wt and SA APP-GFPs levels, an effect that is more pronounced following 24h of transfection. This time-dependent effect is also observed for the S655E mutant, but $G\alpha_o$ is less able to diminish its levels at 6h of transfection (Fig. 26).

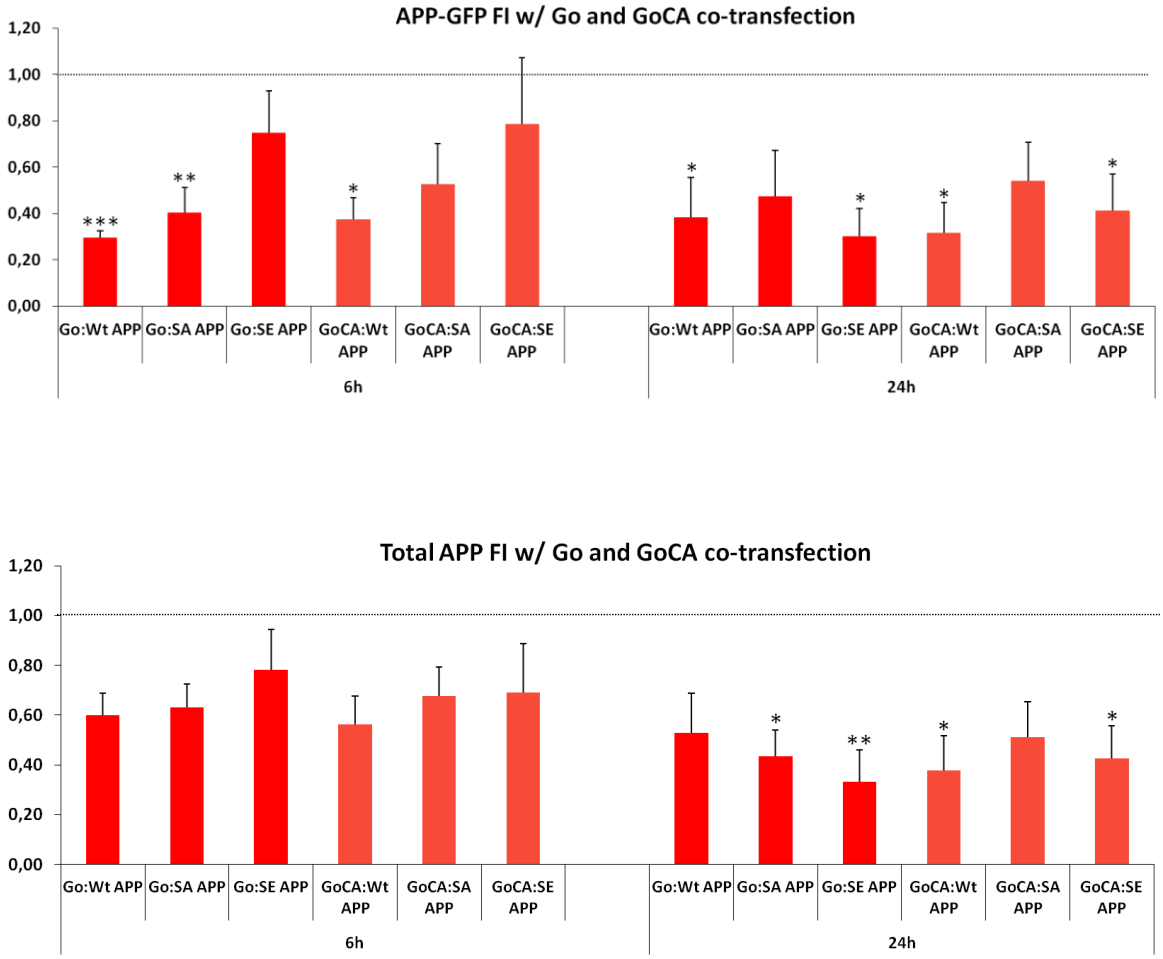

Fig. 26: Fold-increase of total APP and APP-GFP protein expression with $G\alpha_o$ and $G\alpha_oCA$ co-tranfection at 6h and 24h. Upper panel: APP-GFP fold-increase with $G\alpha_o$ and $G\alpha_oCA$ co-transfection. Lower panel: Total APP fold-increase with $G\alpha_o$ and $G\alpha_oCA$ co-transfection. **Go:Wt, SA or SE**: $G\alpha_o$ and Wt, SA or SE co-transfected cells; **GoCA:Wt, SA or SE**: cells co-transfected with $G\alpha_oCA$ and Wt, SA or SE. Data are expressed as mean±SEM, upon correction to Ponceau. *p<0.05, **p<0.01, ***p<0.001. n=4.

In synthesis, $G\alpha_o$ decreases APP levels, what may occur by directly or indirectly intervene in APP cleavage or in APP degradation. To analyse if $G\alpha_o$ decreases APP levels by increasing its cleavage to sAPP, the conditioned medium collected for each condition was analysed by Western blotting. The analysis of 6h (data not shown) and 24h medium Western blots (Fig. 27) revealed that sAPP levels do not increase with $G\alpha_o$ and $G\alpha_oCA$ overexpression. In fact, APP-GFPs/$G\alpha_oCA$ co-transfection seems to even decrease sAPP levels. Therefore, $G\alpha_o$ does not decrease APP levels by increasing APP cleavage but potentially by increasing APP degradation.

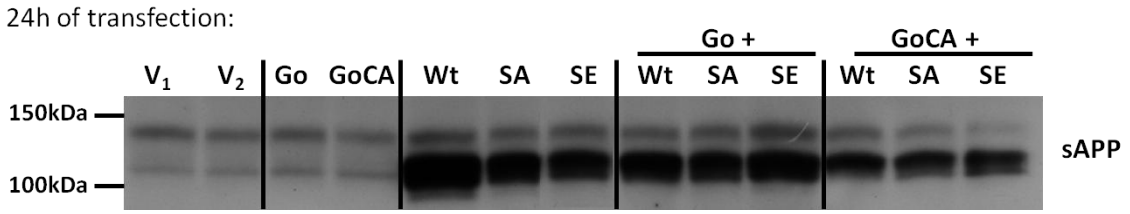

Fig. 27: Qualitative analysis of sAPP levels from the conditioned medium collected at 24h of transfection. Immunoblot analysis of medium from SH-SY5Y cells transfected with pcDNA3 (**V_1**) and N1-EGFP (**V_2**) vectors, $G\alpha_o$ and $G\alpha_oCA$ (**Go** and **GoCA**, respectively), wild-type and S655 phosphomutant APP-GFP (**Wt, SA, SE**) cDNAs, or co-transfected with APP-GFP fusion cDNAs and $G\alpha_o$ or $G\alpha_oCA$: **Go + Wt, SA or SE**: $G\alpha_o$ and Wt, S655A or S655E co-transfected cells; **GoCA + Wt, SA or SE**: cells co-transfected with $G\alpha_oCA$ and Wt, S655A or S655E. Evaluation of sAPP levels was performed using 22C11 antibody.

4.4. Visual analysis of cellular APP/$G\alpha_o$ levels

In order to visualize endogenous $G\alpha_o$ and APP levels in SH-SY5Y cells, and compare their cellular distribution, immunocytochemistry was performed in non-transfected cells fixed upon 6h and 24h of medium substitution. Fluorescence microscopy was further carried out using a Confocal microscope, and cells were randomly selected for analysis (Fig. 28). Very interestingly, both the 6h and 24h images demonstrate that cells with high APP content (mainly visible at the Golgi) have low $G\alpha_o$ levels and cells with high $G\alpha_o$ levels show medium APP levels. This result is completely consistent with the previous Western blot data. Of note, endogenous $G\alpha_o$ and APP appear to colocalize at the plasma membrane (when $G\alpha_o$ levels are higher) and at cytoplasmic vesicles, when $G\alpha_o$ levels are lower.

A.

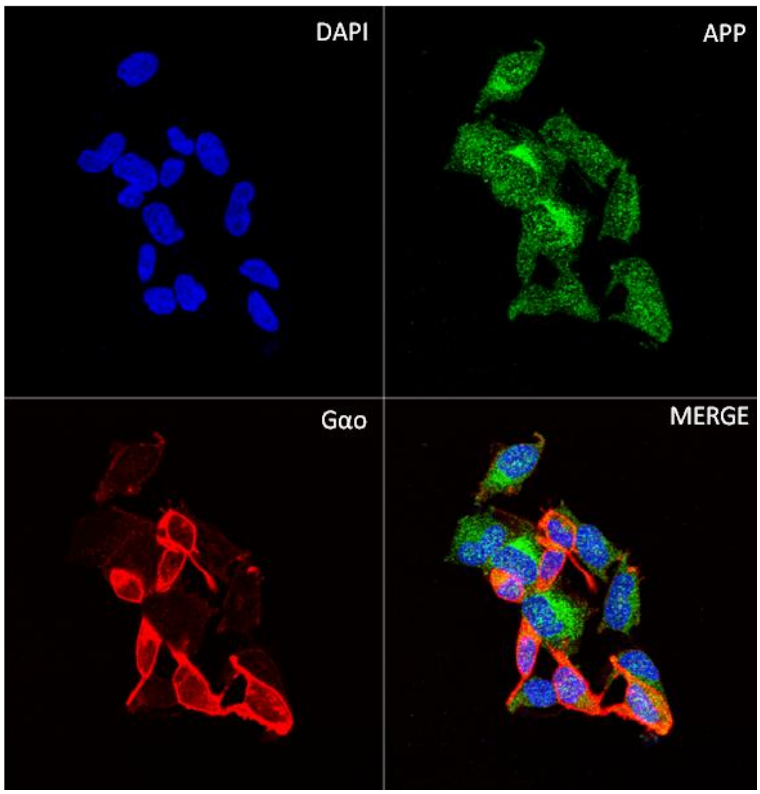

B.

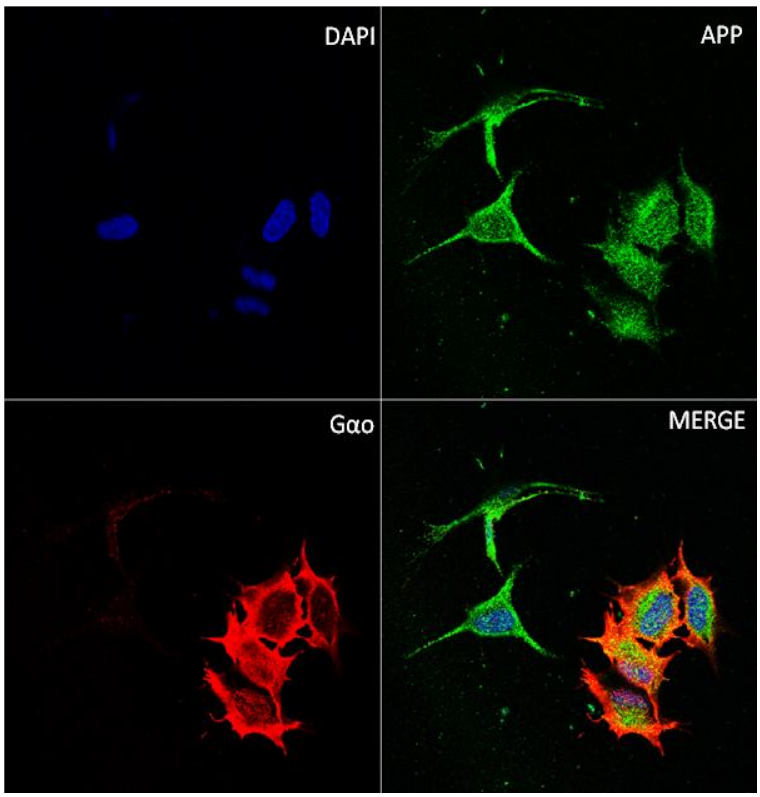

Fig. 28: Evaluation of endogenous APP and $G\alpha_o$ levels in SH-SY5Y non-transfected cells at 6h and 24h, by immunocytochemistry procedures. APP and $G\alpha_o$ cellular distribution was visualized using the 22C11 antibody and Alexa Fluor 488, and anti-$G\alpha_o$ antibody and Texas-Red, respectively. Coverslips was mounted on microscope glass slides with DAPI, to delimitate the nucleus of cells. Microphotographs represent non-transfected cells, plated in parallel with the transfected, and fixed at 6h (**A.**) and 24h (**B.**) since medium substitution.

4.5. Analysis of APP-Gα$_o$ binding

The effect of Gα$_o$ activation and APP S655 phosphorylation in APP-Gα$_o$ binding was analysed by using GFP-trap® to precipitate GFP fusion proteins. SH-SY5Y cells were plated at 70-80% confluence and, after 24h, co-transfected with: i) EGFP-N1 vector and Gα$_o$ cDNA (N1:G$_o$; control); ii) wild-type APP-GFP and Gα$_o$ cDNAs (G$_o$:Wt), to evaluate if Gα$_o$ binds to APP; iii) wild-type APP-GFP and Gα$_o$CA cDNAs (CA:Wt), to test if Gα$_o$ activation alters binding; iv) phosphorylated APP, SE, and Gα$_o$ cDNAs (G$_o$:SE), to analyse if the phosphorylated state of APP alters APP-Gα$_o$ binding.

After 6h of transfection, cells were collected to proceed with the pull-down assay. Afterwards, the precipitates, lysates and supernatants were separated by Western blot, and blots probed with the APP C-terminal antibody CT695, for APP and APP-GFP detection, and the polyclonal anti-Gα$_o$ antibody (Fig. 29).

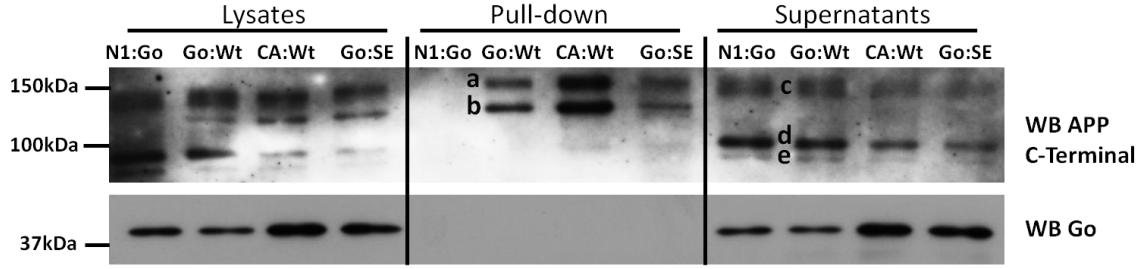

Fig. 29: Evaluation of APP-Gα$_o$ binding with Gα$_o$ activation and APP S655 phosphorylation. Western blot analysis of SH-SY5Y cells co-transfected and submitted to GFP pull-down assays. Confirmation of APP expression with antibody CT695 against APP C-terminal, which detected: **a)** APP-GFP 695 mature; **b)** APP-GFP 695 immature forms; **c)** endogenous APP 751/770 mature; **d)** and **e)** endogenous APP 751/770 and 695 immature forms, respectively. Analysis of Gα$_o$ and Gα$_o$CA cDNA transfection was performed using an anti-Gα$_o$ antibody. **N1:Go**: vector EGFP-N1 and G$_o$ cDNA co-transfected cells; **Go:Wt**: cells co-transfected with Gα$_o$ and wild-type APP-GFP cDNA; **CA:Wt**: cells co-transfected with Gα$_o$CA and wild-type APP-GFP cDNA; **Go:SE**: G$_o$ and SE APP-GFP (phosphorylated APP) cDNAs co-transfected cells.

APP-GFP (bands a, b) were detected in all G$_o$:Wt and G$_o$:SE lysates and precipitated samples, being excluded from the N1:G$_o$ co-transfection, as expected, and from supernatants, the later indicating that all APP-GFP were completely pulled-down and cleared from these samples. Of note, in lysates and supernatants we could detect endogenous APP in all conditions, but not in pulled-down samples, as expected. Unfortunately, Gα$_o$ expression was only verified in lysates and supernatants, while in the pulled-down samples no Gα$_o$ signal was detected.

5. Discussion

$G\alpha_o$ was described to induce neurite outgrowth via activation of two signaling cascades, the STAT3 and GRIN pathways (He, Gomes et al., 2005; Nakata and Kozasa, 2005). APP binds to $G\alpha_o$ but the role of APP in these pathways was never evaluated (Fig. 30). Nevertheless, APP and sAPP have been shown to modulate neuritogenesis in a complex and well-ordered manner, with APP phosphorylation at S655 enhancing its neuritogenic effect (Rocha, 2011). A potential functional co-interaction between APP and $G\alpha_o$ in neuritogenic signaling is therefore especially appealing and worth investigating.

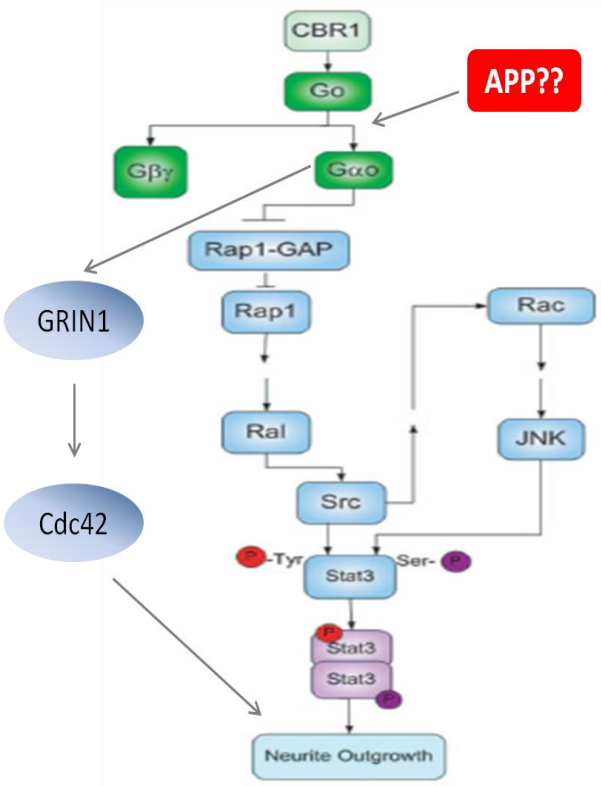

Fig. 30: $G\alpha_o$-induced neurite outgrowth through both GRIN1 and STAT3 signaling cascades. Overexpression of $G\alpha_o$ leads to GRIN1 and Rap1GAP activation, which in turn trigger cascades that promote neuritogenesis. Both of these proteins activate downstream signaling that activates Cdc42 and leads to STAT3 phosphorylation, respectively. The role of APP in $G\alpha_o$-induced neurite outgrowth by these two pathways is not yet known. Adapted from reference (He, Gomes et al., 2005)

Therefore, in the present work we addressed the role of APP and APP S655 phosphorylation in $G\alpha_o$-induced STAT3 signaling, and we have also evaluated the effects that APP and $G\alpha_o$ promote in each other metabolism.

From our first preliminary experiment we have concluded that the Turbofect™ reagent method was the more appropriate for $G\alpha_o$ and $G\alpha_o$CA cDNAs transfection in SH-

SY5Y cells, when compared to Polyplus and Turbofect™ plus CombiMag methods. The Polyplus rendered less transfection rates and, as expectedly, the combination of a magnetic particle, CombiMag, with the Turbofect™ transfection reagent enhanced the deliver efficiency for all $G\alpha_o$ cDNAs. However, due to the method in itself or to the higher amounts of $G\alpha_o$ expression, this combined method is associated with an increase in cell death, proving to be cytotoxic (Fig. 15).

Following, we tested the effect of $G\alpha_o$ and $G\alpha_o$CA overexpression in STAT3 signaling with time (2h, 4h, 6h, 8h and 24h). $G\alpha_o$ and $G\alpha_o$CA transfections could be observed mainly from 6h on, and alterations in STAT3 phosphorylation state were more significant at 6h and 24h, the time points chosen for the subsequent experiments (Fig. 16). At 6h, $G\alpha_o$ was able to induce STAT3 phosphorylation but, upon 24h of transfection, P-STAT3 levels decreased below pcDNA3 vector ones, evidencing a retro-inhibition mechanism of this pathway. This negative mechanism appeared to be strongly dependent on $G\alpha_o$ activation, since P-STAT3 was always found inhibited in $G\alpha_o$CA transfected cells, at all time points analysed. This is consistent with data on the literature evidencing not only a transiently STAT activation, but also suggesting the existence of an efficient negative feedback mechanism. Indeed, in normal cells, and under physiological conditions, STAT3 activation, mediated by phosphorylation at the Tyr705 residue, is a tightly controlled transient process. While some authors indicate that it lasts from 30 minutes to few hours (Debnath, Xu et al., 2012), other authors advocate cytokines-mediated STAT3 phosphorylation generally peaks 15 to 30 minutes following stimulation, further declining to baseline levels over one to two hours (Walker, Chaudhury et al., 2011). Either way, the residence time of the STAT3 active state is very quick, justifying the declining levels of P-STAT3 that we observed in our experimental conditions, especially for the activated $G\alpha_o$CA construct. This retro-inhibitory mechanism is believed to be partially due to a negative feedback from STAT3-target genes. Actually, in order to tightly control transcription of key STAT3-target genes, many STAT3 target genes are themselves negative regulators of STAT activation (Walker, Chaudhury et al., 2011).

Subsequently, we evaluated the effects of APP overexpression in $G\alpha_o$-induced STAT3 signaling and the role played by APP S655 phosphorylation in that regulation. For that, SH-SY5Y cells were transfected with the vectors pcDNA3 and N1-EGFP, Wt, SA and SE APP-GFPs, $G\alpha_o$ and $G\alpha_o$CA cDNAs, or co-transfected with the APP-GFP and $G\alpha_o$

cDNAs. As in pilot experiment, at 6h we could observe a stimulation of STAT3 phosphorylation, not only for $G\alpha_o$ but also for $G\alpha_oCA$ (Fig. 19), probably resulting from the lower $G\alpha_oCA$ transfection levels (compare Fig. 16 and Fig. 19). Activated $G\alpha_o$ was reported to enhance STAT3 levels (Ram, Horvath et al., 2000) and the lower increases in P-STAT3 levels that we observed for $G\alpha_oCA$ in our experimental conditions appears to result from the previously observed retro-inhibition mechanism.

Regarding the APP-GFPs proteins alone, these did not alter the phosphorylation of STAT3 except for the phosphomimicking S655E mutant, which slightly increases this signaling pathway relative to N1-EGFP values. This may potentially occur via secreted sAPP, since S655 phosphorylation increases sAPP production (Vieira, Rebelo et al., 2009) and sAPP was observed to potentially activate STAT3 (Kwak, Dantuma et al., 2010). S655E-induction of STAT3 may also occur via $G\alpha_o$. Indeed, as already mentioned, other major protein found in axonal growth cones is the $G\alpha_o$-binding protein GAP-43, whose expression is up-regulated by APP (Strittmatter, Valenzuela et al., 1990; Mucke, Masliah et al., 1994). The findings that GAP-43 acts as a GEF for $G\alpha_o$ protein suggests a potentially role for this protein in mediating phospho S655 APP-induced STAT3 activation.

Unexpectedly, all APP-GFPs/$G\alpha_o$ co-transfections decreased the $G\alpha_o$-induced STAT3 phosphorylation, and we were not able to observe an initial positive effect of APP on $G\alpha_o$-induced STAT3 activation. These negative effects could result from the enhancement of the previously observed retro-inhibition effect, which appears occur after $G\alpha_o$ and/or STAT3 activation, and may also involve $G\alpha_o$ downregulation. Apparently, this(ese) retro-inhibition effect(s) occurs after $G\alpha_o$ and/or STAT3 activation. Indeed, APP-GFPs/$G\alpha_oCA$ co-transfection led to a higher retro-inhibition effect, together with APP S655 dephosphorylation (mimicked by the SA APP mutant). Consistent results are shown at 24h (Fig. 20), where a general decrease in the P-STAT3/STAT3 ratio was detected for all $G\alpha_o$/$G\alpha_oCA$ and APP-GFP transfections and co-transfections, supporting that this retro-inhibition mechanism is also time dependent. Again, $G\alpha_oCA$ transfection and its co-transfection with APP-GFP cDNAs, especially with the S655A phosphomutant, resulted in negative effects on STAT3 phosphorylation levels.

In synthesis, at 6h and 24h, with different transfection conditions, we could observe a retro-inhibition mechanism in STAT3 signaling, that appears to be strongly $G\alpha_o$ activation-dependent (as seen in the 6h and 24h conditions), but also time-dependent (as

seen in the 24h condition, when compared to the 6h). In addition, mimicking S655 dephosphorylation through the use of the S655A mutant increases this effect, suggesting that APP S655 phosphorylation deviates APP from its negative role on $G\alpha_o$–induced STAT3 activation.

Further and somewhat expected, in all these transfection and co-transfection conditions tested, β-tubulin levels also showed alterations, which discarded its use as a loading control. The alterations of β-tubulin levels with APP-GFP and $G\alpha_o$ transfections are a response against the cellular morphological changes that are induced by these potentially neuritogenic proteins. In fact, our group had already reported differences on β-tubulin levels with cellular differentiation and Wt APP-GFP transfection, suggesting that β-tubulin can even be used as a differentiation cytoskeleton-related marker (Rocha, 2011). Ponceau S staining of proteins bands is widely used (Romero-Calvo, Ocon et al., 2010) and proved to be a good loading control to use in these transfection and co-transfection conditions.

We have further observed that increasing APP expression affected the intracellular levels of $G\alpha_o$, what could also partially relate APP with its previously observed $G\alpha_o$-related STAT3 retro-inhibition mechanism. APP-GFPs overexpression decreased endogenous $G\alpha_o$ levels to approximately half of their levels relative to control conditions, at 6h and 24h of transfection (Fig. 22). However, S655E APP-GFP only decreased $G\alpha_o$ levels upon 24h of transfection. Again, APP-induced $G\alpha_o$ downregulation is a time-, APP S655A dephosphorylated- and $G\alpha_o$–activated dependent effect, suggesting a partial correlation between this effect and the observed APP-induced STAT3 retro-inhibition (Fig. 19 and 20). APP-GFP could also decrease exogenous $G\alpha_o$ and $G\alpha_o$CA levels, upon their co-transfection (Fig. 23). These decreases were smaller than for the endogenous levels possibly due to the strong promoter of $G\alpha_o$ plasmids and their good transfection rates. Again, higher decreases could be observed upon 24h of transfection, when compared to the 6h period, and especially for the $G\alpha_o$ activated mutant, confirming its time- and activation-dependency. Moreover, this was especially true for the phosphomimicking S655E mutant, which a much more delayed effect on $G\alpha_o$ downregulation.

In conclusion, both endogenous and exogenous $G\alpha_o$ levels are diminished with APP overexpression. So, APP appears to participate in a $G\alpha_o$ inactivation mechanism, potentially by targeting $G\alpha_o$ for degradation. Since both APP-induced negative effects on

P-STAT3 and $G\alpha_o$ levels are time-, APP S655A dephosphorylated- and $G\alpha_o$–activated dependent, they are potentially interrelated, with APP decreasing $G\alpha_o$–induced STAT3 activation through $G\alpha_o$ downregulation.

In other hand, $G\alpha_o$ overexpression also had a similar effect on the APP levels, suggesting that both proteins are co-degraded to some extent. $G\alpha_o$ and $G\alpha_o$CA transfected cells were associated with slight decreases in endogenous APP levels, an effect also time-dependent, being more pronounced upon 24h of transfection (Fig. 25). The same results were obtained from APP-GFPs/$G\alpha_o$ and $G\alpha_o$CA co-transfection cells, which presented decreases in exogenous APP-GFP levels. Again, this effect is mainly time-dependent for the S655E phosphomimicking mutant, with its levels only significantly decreasing at 24h, for both the $G\alpha_o$ and $G\alpha_o$CA constructs. Nonetheless, $G\alpha_o$ and $G\alpha_o$CA co-transfections lead to similar decreases in APP-GFP and total APP levels, with APP downregulation being independent of a previous $G\alpha_o$ activation. This indicates that a previous APP-$G\alpha_o$ interaction and activation step is upstream APP-induction of a decrease in $G\alpha_o$ levels.

The later results indicate that $G\alpha_o$ decreases the APP half-life, with this decrease potentially occurring via interference on APP synthesis, cleavage or degradation. Since it has higher effects on exogenous APP proteins, $G\alpha_o$ appears to directly or indirectly intervene in APP cleavage or in APP degradation, rather than in its transcription rate. Our subsequent results strengthen the hypothesis of $G\alpha_o$-induced APP degradation, since the medium secreted sAPP data revealed that neither $G\alpha_o$ or $G\alpha_o$CA overexpression increase APP proteolysis to sAPP (Fig. 27). Moreover, APP-GFPs/$G\alpha_o$CA co-transfection seems to even decrease sAPP levels, in accordance with an APP/$G\alpha_o$ co-degradation hypothesis. The fact that $G\alpha_o$ is less able to decrease the levels of S655 phosphorylated APP (S655E) and vice-versa, together with the knowledge that the dephospho S655A mutant is preferentially targeted for lysosomal degradation (Vieira, Rebelo et al., 2010) suggests that the APP downregulation mechanism observed is APP/$G\alpha_o$ lysosomal co-degradation.

Remarkably, visualization of SH-SY5Y non-transfected cells fluorescence microphotographs (Fig. 28) revealed that cells with high APP levels express low $G\alpha_o$ levels, while cells with high $G\alpha_o$ levels show invariably medium or low APP levels. These results are completely consistent with our previous Western blot data and with unpublished data of our laboratory. Regarding cellular distribution, endogenous $G\alpha_o$ and APP appear to colocalize at the plasma membrane (when $G\alpha_o$ levels are higher) and at cytoplasmic

vesicles when $G\alpha_o$ levels are lower. Together with the fact that cells with high levels of APP have its localization mainly at its 'cellular reservoir' - the Golgi, make these locations a strongly support for APP/$G\alpha_o$ lysosomal co-degradation hypothesis.

Finally, we evaluated if APP-$G\alpha_o$ binding is affected by $G\alpha_o$ activation and APP S655 phosphorylation, by using GFP-trap® to precipitate the APP-GFP fusion proteins. Unfortunately, we cannot conclude anything regarding APP-$G\alpha_o$ binding, since no $G\alpha_o$ could be pulled-down with the APP-GFP proteins, under the conditions tested. These results raise a question of whether N-terminally fused GFP decreases the APP-$G\alpha_o$ binding strength, or if this binding is so fast that it is difficult to observe. Future experiments will involve e.g. immunoprecipitation of non GFP-fused Wt, S655A, and S655E cDNAs.

6. Conclusion

The experiments performed in this work indicate that APP-GFP and $G\alpha_o$/$G\alpha_o$CA co-transfected SH-SY5Y cells suffer a decrease in $G\alpha_o$-induced STAT3 signaling, possibly via a retro-inhibition effect on the STAT3 pathways, at the $G\alpha_o$ and STAT3 levels. This negative effect is enhanced by $G\alpha_o$ activation, APP S655 dephosphorylation, and by time of transfection (in particular for the phosphomimicking S655E mutant). From our data we proved that a downregulation of $G\alpha_o$ levels indeed occurs downstream APP (potentially after their interaction and subsequent $G\alpha_o$ activation) and, consistently, SH-SY5Y cells with high APP levels were observed to possess low $G\alpha_o$ levels. In fact, APP-GFP overexpression led to a decrease in endogenous and exogenous $G\alpha_o$ levels and, by its turn, $G\alpha_o$ overexpression decreased APP levels. These effects seem also to be time-dependent and $G\alpha_o$-activation dependent. Moreover, sAPP levels did not increase with APP/$G\alpha_o$ co-transfection, suggesting that $G\alpha_o$ enhances APP degradation, and that APP-$G\alpha_o$ co-degradation is part of the mechanism by which APP inhibits $G\alpha_o$-induced STAT3 activation. APP S655 phosphorylation delays this inactivation phase and/or the first activation phase, and this remains to be analysed. Figure 31 summarizes the pathways and the hypothesis that we take from these experiments.

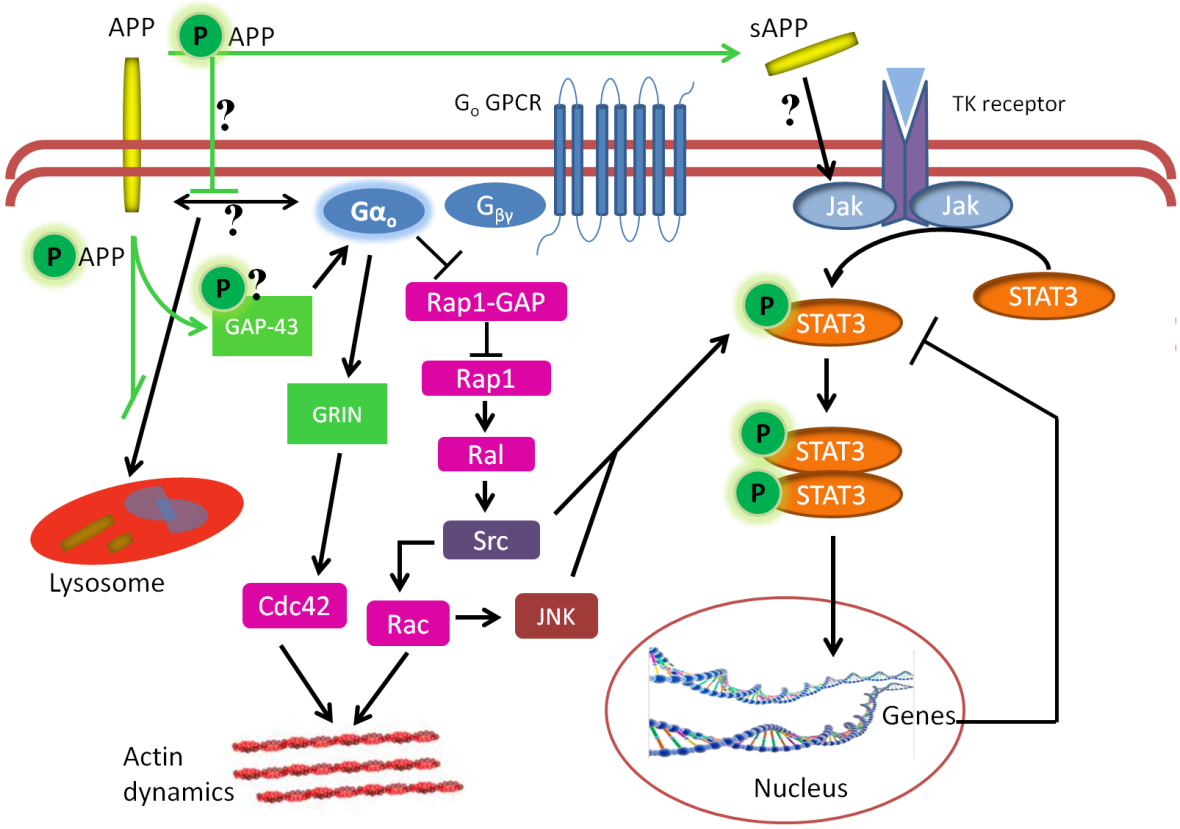

Fig. 31: Schematic model hypothesizing how APP regulates Gα$_o$/STAT3 signaling pathways. Right to left: JAKs bind to tyrosine kinase (TK), growth factor or cytokine receptors. The binding of the ligand to the receptor triggers activation of JAKs, increasing its kinase activity. They phosphorylate the receptor cytoplasmatic domain on tyrosine residues and create sites for STATs interaction. STAT3 recognize specific receptor phosphotyrosine residues and become tyrosine phosphorylated by JAKs. The phosphorylation of STAT3 at Tyr705 by receptor-associated Janus kinases allows homo- or heterodimerization of STAT3 transcription factors and subsequent translocation to the nucleus, activating transcription of their target genes. In order to tightly control transcription of key STAT3-target genes, many STAT3 target genes are themselves negative regulators of STAT activation. APP S655 phosphorylation increases Tyr705 phosphorylation of STAT3, potentially by increasing secreted sAPP levels, indirectly activating JAK/STAT signaling. G$_o$-coupled receptor, when stimulated by a ligand, activates G$_o$ subunits. The activated α-subunit reduces the stability of Rap1-GAP, which results in the activation of Rap1 and, subsequently Src and STAT3 activation that mediate gene expression. The Src activation also stimulates the small GTPase Rac1 and then c-Jun N-terminal kinase (JNK). Gα$_o$ overexpression also leads to GRIN1 activation and, consequently the activation of another small GTPase Cdc42; this, together with Rac1, regulates actin cytoskeleton remodelling that helps neuritogenesis. The role of APP in Gα$_o$-induced STAT3 activation is not yet known. GAP-43 has the ability to enhance Gα$_o$ activation, acting as a GEF. Indirectly, phospho S655 APP may potentially increase GAP-43 levels by increasing GAP-43 phosphorylation and thus decreasing its cleavage by calpain. Directly, APP-Gα$_o$ interaction leads first to Gα$_o$ activation (and subsequent signaling cascades activation), and second to APP-Gα$_o$ lysosomal co-degradation, in a mechanism that is overall enhanced by APP S655 dephosphorylation.

Future experiments will comprehend the detection of a first, fast, APP-Gα$_o$-induced STAT3 activation phase, the characterization of the inhibitory mechanism induced by APP on this pathway, and the recording and characterization of APP-Gα$_o$ binding by alternative methods.

7. References

Aberg, M. A., Ryttsen, F., Hellgren, G., Lindell, K., Rosengren, L. E., MacLennan, A. J., Carlsson, B., Orwar, O. and Eriksson, P. S. (2001). "Selective introduction of antisense oligonucleotides into single adult CNS progenitor cells using electroporation demonstrates the requirement of STAT3 activation for CNTF-induced gliogenesis." Mol Cell Neurosci **17**(3): 426-43.

Arakawa, T., Kita, Y. and Niikura, T. (2008). "A rescue factor for Alzheimer's diseases: discovery, activity, structure, and mechanism." Curr Med Chem **15**(21): 2086-98.

Arendt, T. (2001). "Alzheimer's disease as a disorder of mechanisms underlying structural brain self-organization." Neuroscience **102**(4): 723-65.

Bishop, G. M. and Robinson, S. R. (2002). "The amyloid hypothesis: let sleeping dogmas lie?" Neurobiol Aging **23**(6): 1101-5.

Blazer, L. L., Roman, D. L., Chung, A., Larsen, M. J., Greedy, B. M., Husbands, S. M. and Neubig, R. R. (2010). "Reversible, allosteric small-molecule inhibitors of regulator of G protein signaling proteins." Mol Pharmacol **78**(3): 524-33.

Bojarski, L., Herms, J. and Kuznicki, J. (2008). "Calcium dysregulation in Alzheimer's disease." Neurochem Int **52**(4-5): 621-33.

Bossy-Wetzel, E., Schwarzenbacher, R. and Lipton, S. A. (2004). "Molecular pathways to neurodegeneration." Nat Med **10 Suppl**: S2-9.

Bromberg, K. D., Lyengar, R. and He, J. C. (2011). "Regulation of neurite outgrowth by Gi/o signaling pathways." Front Biosci **13**: 4544-4557.

Brookmeyer, R., Johnson, E., Ziegler-Graham, K. and Arrighi, H. M. (2007). "Forecasting the global burden of Alzheimer's disease." Alzheimers Dement **3**(3): 186-91.

Chiba, T., Nishimoto, I., Aiso, S. and Matsuoka, M. (2007). "Neuroprotection against neurodegenerative diseases: development of a novel hybrid neuroprotective peptide Colivelin." Mol Neurobiol **35**(1): 55-84.

Chiba, T., Yamada, M. and Aiso, S. (2009). "Targeting the JAK2/STAT3 axis in Alzheimer's disease." Expert Opin Ther Targets **13**(10): 1155-67.

Chiba, T., Yamada, M., Sasabe, J., Terashita, K., Shimoda, M., Matsuoka, M. and Aiso, S. (2009). "Amyloid-beta causes memory impairment by disturbing the JAK2/STAT3 axis in hippocampal neurons." Mol Psychiatry **14**(2): 206-22.

Cole, S. L. and Vassar, R. (2007). "The Alzheimer's disease beta-secretase enzyme, BACE1." Mol Neurodegener **2**: 22.

Coleman, P., Federoff, H. and Kurlan, R. (2004). "A focus on the synapse for neuroprotection in Alzheimer disease and other dementias." Neurology **63**(7): 1155-62.

da Cruz e Silva, E. F. and da Cruz e Silva, O. A. (2003). "Protein phosphorylation and APP metabolism." Neurochem Res **28**(10): 1553-61.

da Cruz e Silva, O. A., Fardilha, M., Henriques, A. G., Rebelo, S., Vieira, S. and da Cruz e Silva, E. F. (2004). "Signal transduction therapeutics: relevance for Alzheimer's disease." J Mol Neurosci **23**(1-2): 123-42.

da Cruz e Silva, O. A., Iverfeldt, K., Oltersdorf, T., Sinha, S., Lieberburg, I., Ramabhadran, T. V., Suzuki, T., Sisodia, S. S., Gandy, S. and Greengard, P. (1993). "Regulated cleavage of Alzheimer beta-amyloid precursor protein in the absence of the cytoplasmic tail." Neuroscience **57**(4): 873-7.

da Cruz e Silva, O. A., Rebelo, S., Vieira, S. I., Gandy, S., da Cruz e Silva, E. F. and Greengard, P. (2009). "Enhanced generation of Alzheimer's amyloid-beta following chronic exposure to phorbol ester correlates with differential effects on alpha and epsilon isozymes of protein kinase C." J Neurochem **108**(2): 319-30.

De Strooper, B. and Annaert, W. (2000). "Proteolytic processing and cell biological functions of the amyloid precursor protein." J Cell Sci **113 (Pt 11)**: 1857-70.

Debnath, B., Xu, S. and Neamati, N. (2012). "Small Molecule Inhibitors of Signal Transducer and Activator of Transcription 3 (Stat3) Protein." J Med Chem.

Diverse-Pierluissi, M. A., Fischer, T., Jordan, J. D., Schiff, M., Ortiz, D. F., Farquhar, M. G. and De Vries, L. (1999). "Regulators of G protein signaling proteins as determinants of the rate of desensitization of presynaptic calcium channels." J Biol Chem **274**(20): 14490-4.

Duyckaerts, C., Delatour, B. and Potier, M. C. (2009). "Classification and basic pathology of Alzheimer disease." Acta Neuropathol **118**(1): 5-36.

Evin, G. and Weidemann, A. (2002). "Biogenesis and metabolism of Alzheimer's disease Abeta amyloid peptides." Peptides **23**(7): 1285-97.

American health assistance foundation (January 2012). from http://www.ahaf.org/alzheimers/about/understanding/brain-with-alzheimers.html.

Giambarella, U., Yamatsuji, T., Okamoto, T., Matsui, T., Ikezu, T., Murayama, Y., Levine, M. A., Katz, A., Gautam, N. and Nishimoto, I. (1997). "G protein betagamma complex-mediated apoptosis by familial Alzheimer's disease mutant of APP." EMBO J **16**(16): 4897-907.

Gomperts, B. D., Kramer, I. M. and Tatham, P. E. (2009). Signal Transduction.

Experimental genetics group (January 2012). from http://med.kuleuven.be/legtegg/AD.html.

Gudermann, T., Schoneberg, T. and Schultz, G. (1997). "Functional and structural complexity of signal transduction via G-protein-coupled receptors." Annu Rev Neurosci **20**: 399-427.

Hampel, H., Shen, Y., Walsh, D. M., Aisen, P., Shaw, L. M., Zetterberg, H., Trojanowski, J. Q. and Blennow, K. (2010). "Biological markers of amyloid beta-related mechanisms in Alzheimer's disease." Exp Neurol **223**(2): 334-46.

He, J. C., Gomes, I., Nguyen, T., Jayaram, G., Ram, P. T., Devi, L. A. and Iyengar, R. (2005). "The G alpha(o/i)-coupled cannabinoid receptor-mediated neurite outgrowth involves Rap regulation of Src and Stat3." J Biol Chem **280**(39): 33426-34.

Hewavitharana, T. and Wedegaertner, P. B. (2012). "Non-canonical signaling and localizations of heterotrimeric G proteins." Cell Signal **24**(1): 25-34.

Hooijmans, C. R. and Kiliaan, A. J. (2008). "Fatty acids, lipid metabolism and Alzheimer pathology." Eur J Pharmacol **585**(1): 176-96.

Horvath, C. M. (2000). "STAT proteins and transcriptional responses to extracellular signals." Trends Biochem Sci **25**(10): 496-502.

Hurowitz, E. H., Melnyk, J. M., Chen, Y. J., Kouros-Mehr, H., Simon, M. I. and Shizuya, H. (2000). "Genomic characterization of the human heterotrimeric G protein alpha, beta, and gamma subunit genes." DNA Res **7**(2): 111-20.

Isohara, T., Horiuchi, A., Watanabe, T., Ando, K., Czernik, A. J., Uno, I., Greengard, P., Nairn, A. C. and Suzuki, T. (1999). "Phosphorylation of the cytoplasmic domain of Alzheimer's beta-amyloid precursor protein at Ser655 by a novel protein kinase." Biochem Biophys Res Commun **258**(2): 300-5.

Jiang, M. and Bajpayee, N. S. (2009). "Molecular mechanisms of go signaling." Neurosignals **17**(1): 23-41.

King, G. D. and Scott Turner, R. (2004). "Adaptor protein interactions: modulators of amyloid precursor protein metabolism and Alzheimer's disease risk?" Exp Neurol **185**(2): 208-19.

Knust, E. (2001). "G protein signaling and asymmetric cell division." Cell **107**(2): 125-8.

Kong, G. K., Miles, L. A., Crespi, G. A., Morton, C. J., Ng, H. L., Barnham, K. J., McKinstry, W. J., Cappai, R. and Parker, M. W. (2008). "Copper binding to the Alzheimer's disease amyloid precursor protein." Eur Biophys J **37**(3): 269-79.

Kumar, S. and Walter, J. (2011). "Phosphorylation of amyloid beta (Abeta) peptides - a trigger for formation of toxic aggregates in Alzheimer's disease." Aging (Albany NY) **3**(8): 803-12.

Kwak, Y. D., Dantuma, E., Merchant, S., Bushnev, S. and Sugaya, K. (2010). "Amyloid-beta precursor protein induces glial differentiation of neural progenitor cells by activation of the IL-6/gp130 signaling pathway." Neurotox Res **18**(3-4): 328-38.

Lee, K. S., Park, J. H., Lee, S., Lim, H. J., Choi, H. E. and Park, H. Y. (2007). "HB-EGF induces delayed STAT3 activation via NF-kappaB mediated IL-6 secretion in vascular smooth muscle cell." Biochim Biophys Acta **1773**(11): 1637-44.

Lee, M. S., Kao, S. C., Lemere, C. A., Xia, W., Tseng, H. C., Zhou, Y., Neve, R., Ahlijanian, M. K. and Tsai, L. H. (2003). "APP processing is regulated by cytoplasmic phosphorylation." J Cell Biol **163**(1): 83-95.

Lemere, C. A. and Masliah, E. (2010). "Can Alzheimer disease be prevented by amyloid-beta immunotherapy?" Nat Rev Neurol **6**(2): 108-19.

Lin, L. F. and Luo, H. M. (2011). "Screening of treatment targets for Alzheimer's disease from the molecular mechanisms of impairment by beta-amyloid aggregation and tau hyperphosphorylation." Neurosci Bull **27**(1): 53-60.

Ling, Y., Morgan, K. and Kalsheker, N. (2003). "Amyloid precursor protein (APP) and the biology of proteolytic processing: relevance to Alzheimer's disease." Int J Biochem Cell Biol **35**(11): 1505-35.

Lukiw, W. J. and Bazan, N. G. (2000). "Neuroinflammatory signaling upregulation in Alzheimer's disease." Neurochem Res **25**(9-10): 1173-84.

Marotta, C. A., Majocha, R. E. and Tate, B. (1992). "Molecular and cellular biology of Alzheimer amyloid." J Mol Neurosci **3**(3): 111-25.

Merlo, S., Spampinato, S., Canonico, P. L., Copani, A. and Sortino, M. A. (2010). "Alzheimer's disease: brain expression of a metabolic disorder?" Trends Endocrinol Metab **21**(9): 537-44.

Mucke, L., Masliah, E., Johnson, W. B., Ruppe, M. D., Alford, M., Rockenstein, E. M., Forss-Petter, S., Pietropaolo, M., Mallory, M. and Abraham, C. R. (1994). "Synaptotrophic effects of human amyloid beta protein precursors in the cortex of transgenic mice." Brain Res **666**(2): 151-67.

Mucke, L., Masliah, E., Yu, G. Q., Mallory, M., Rockenstein, E. M., Tatsuno, G., Hu, K., Kholodenko, D., Johnson-Wood, K. and McConlogue, L. (2000). "High-level neuronal expression of abeta 1-42 in wild-type human amyloid protein precursor transgenic mice: synaptotoxicity without plaque formation." J Neurosci **20**(11): 4050-8.

Nakata, H. and Kozasa, T. (2005). "Functional characterization of Galphao signaling through G protein-regulated inducer of neurite outgrowth 1." Mol Pharmacol **67**(3): 695-702.

Neer, E. J. (1995). "Heterotrimeric G proteins: organizers of transmembrane signals." Cell **80**(2): 249-57.

Health news (January 2012). from http://www.healthinformer.net/alzheimer-disease-plaques-seen-with-conventional-mri-in-animal-model-for-the-first-time.html.

Ng, Y. P., Cheung, Z. H. and Ip, N. Y. (2006). "STAT3 as a downstream mediator of Trk signaling and functions." J Biol Chem **281**(23): 15636-44.

Nishimoto, I., Okamoto, T., Matsuura, Y., Takahashi, S., Murayama, Y. and Ogata, E. (1993). "Alzheimer amyloid protein precursor complexes with brain GTP-binding protein G(o)." Nature **362**(6415): 75-9.

O'Brien, R. J. and Wong, P. C. (2011). "Amyloid precursor protein processing and Alzheimer's disease." Annu Rev Neurosci **34**: 185-204.

Okamoto, T., Takeda, S., Murayama, Y., Ogata, E. and Nishimoto, I. (1995). "Ligand-dependent G protein coupling function of amyloid transmembrane precursor." J Biol Chem **270**(9): 4205-8.

Perez, R. G., Zheng, H., Van der Ploeg, L. H. and Koo, E. H. (1997). "The beta-amyloid precursor protein of Alzheimer's disease enhances neuron viability and modulates neuronal polarity." J Neurosci **17**(24): 9407-14.

Ram, P. T., Horvath, C. M. and Iyengar, R. (2000). "Stat3-mediated transformation of NIH-3T3 cells by the constitutively active Q205L Galphao protein." Science **287**(5450): 142-4.

Ram, P. T. and Iyengar, R. (2001). "G protein coupled receptor signaling through the Src and Stat3 pathway: role in proliferation and transformation." Oncogene **20**(13): 1601-6.

Rebelo, S., Vieira, S. I., Esselmann, H., Wiltfang, J., da Cruz e Silva, E. F. and da Cruz e Silva, O. A. (2007). "Tyr687 dependent APP endocytosis and Abeta production." J Mol Neurosci **32**(1): 1-8.

Rocha, J. F. (2011). Understanding APP-dependent neuronal differentiation. Health Science Department, Universidade de Aveiro. **Master Molecular Biomedicine:** http://hdl.handle.net/10773/7389.

Romero-Calvo, I., Ocon, B., Martinez-Moya, P., Suarez, M. D., Zarzuelo, A., Martinez-Augustin, O. and de Medina, F. S. (2010). "Reversible Ponceau staining as a loading control alternative to actin in Western blots." Anal Biochem **401**(2): 318-20.

Russo, C., Venezia, V., Repetto, E., Nizzari, M., Violani, E., Carlo, P. and Schettini, G. (2005). "The amyloid precursor protein and its network of interacting proteins: physiological and pathological implications." Brain Res Brain Res Rev **48**(2): 257-64.

Schettini, G., Govoni, S., Racchi, M. and Rodriguez, G. (2010). "Phosphorylation of APP-CTF-AICD domains and interaction with adaptor proteins: signal transduction and/or transcriptional role--relevance for Alzheimer pathology." J Neurochem **115**(6): 1299-308.

Selkoe, D. J. (1999). "Translating cell biology into therapeutic advances in Alzheimer's disease." Nature **399**(6738 Suppl): A23-31.

Selkoe, D. J. (2001). "Alzheimer's disease: genes, proteins, and therapy." Physiol Rev **81**(2): 741-66.

Selkoe, D. J. (2004). "Alzheimer disease: mechanistic understanding predicts novel therapies." Ann Intern Med **140**(8): 627-38.

Shaked, G. M., Chauv, S., Ubhi, K., Hansen, L. A. and Masliah, E. (2009). "Interactions between the amyloid precursor protein C-terminal domain and G proteins mediate calcium dysregulation and amyloid beta toxicity in Alzheimer's disease." FEBS J **276**(10): 2736-51.

Shan, D., Chen, L., Wang, D., Tan, Y. C., Gu, J. L. and Huang, X. Y. (2006). "The G protein G alpha(13) is required for growth factor-induced cell migration." Dev Cell **10**(6): 707-18.

Siderovski, D. P., Diverse-Pierluissi, M. and De Vries, L. (1999). "The GoLoco motif: a Galphai/o binding motif and potential guanine-nucleotide exchange factor." Trends Biochem Sci **24**(9): 340-1.

Small, S. A. and Gandy, S. (2006). "Sorting through the cell biology of Alzheimer's disease: intracellular pathways to pathogenesis." Neuron **52**(1): 15-31.

Sola Vigo, F., Kedikian, G., Heredia, L., Heredia, F., Anel, A. D., Rosa, A. L. and Lorenzo, A. (2009). "Amyloid-beta precursor protein mediates neuronal toxicity of amyloid beta through Go protein activation." Neurobiol Aging **30**(9): 1379-92.

Strittmatter, S. M., Fishman, M. C. and Zhu, X. P. (1994). "Activated mutants of the alpha subunit of G(o) promote an increased number of neurites per cell." J Neurosci **14**(4): 2327-38.

Strittmatter, S. M., Valenzuela, D., Kennedy, T. E., Neer, E. J. and Fishman, M. C. (1990). "G0 is a major growth cone protein subject to regulation by GAP-43." Nature **344**(6269): 836-41.

Takahashi, K., Niidome, T., Akaike, A., Kihara, T. and Sugimoto, H. (2008). "Phosphorylation of amyloid precursor protein (APP) at Tyr687 regulates APP processing by alpha- and gamma-secretase." Biochem Biophys Res Commun **377**(2): 544-9.

Thinakaran, G. and Koo, E. H. (2008). "Amyloid precursor protein trafficking, processing, and function." J Biol Chem **283**(44): 29615-9.

Vieira, S. I., Rebelo, S., Domingues, S. C., da Cruz e Silva, E. F. and da Cruz e Silva, O. A. (2009). "S655 phosphorylation enhances APP secretory traffic." Mol Cell Biochem **328**(1-2): 145-54.

Vieira, S. I., Rebelo, S., Esselmann, H., Wiltfang, J., Lah, J., Lane, R., Small, S. A., Gandy, S., da Cruz, E. S. E. F. and da Cruz, E. S. O. A. (2010). "Retrieval of the Alzheimer's amyloid precursor protein from the endosome to the TGN is S655 phosphorylation state-dependent and retromer-mediated." Mol Neurodegener **5**: 40.

Vrotsos, E. G., Kolattukudy, P. E. and Sugaya, K. (2009). "MCP-1 involvement in glial differentiation of neuroprogenitor cells through APP signaling." Brain Res Bull **79**(2): 97-103.

Walker, S. R., Chaudhury, M. and Frank, D. A. (2011). "STAT3 Inhibition by Microtubule-Targeted Drugs: Dual Molecular Effects of Chemotherapeutic Agents." Mol Cell Pharmacol **3**(1): 13-19.

Wan, J., Fu, A. K., Ip, F. C., Ng, H. K., Hugon, J., Page, G., Wang, J. H., Lai, K. O., Wu, Z. and Ip, N. Y. (2010). "Tyk2/STAT3 signaling mediates beta-amyloid-induced neuronal cell death: implications in Alzheimer's disease." J Neurosci **30**(20): 6873-81.

Wettschureck, N. and Offermanns, S. (2005). "Mammalian G proteins and their cell type specific functions." Physiol Rev **85**(4): 1159-204.

Wu, E. H., Lo, R. K. and Wong, Y. H. (2003). "Regulation of STAT3 activity by G16-coupled receptors." Biochem Biophys Res Commun **303**(3): 920-5.

Xu, J. J., Chen, E. Y., Lu, C. L. and He, C. (2009). "Recombinant ciliary neurotrophic factor promotes nerve regeneration and induces gene expression in silicon tube-bridged transected sciatic nerves in adult rats." J Clin Neurosci **16**(6): 812-7.

Appendix

Cell culture Solutions and Immunocytochemistry

- **PBS (1x)**

For a final volume of 500 ml, dissolve one pack of BupH Modified Dulbecco's Phosphate Buffered Saline Pack (Pierce) in deionised H2O. Final composition:

- 8 mM Sodium Phosphate
- 2 mM Potassium Phosphate
- 140 mM Sodium Chloride
- 10 mM Potassim Chloride

Sterilize by filtering through a 0.2 μm filter and store at 4ºC.

- **10% FBS MEM:F12 (1:1)**

- MEM (Gibco, Invitrogen)	4,805 g
- F12 (Gibco, Invitrogen)	5,315 g
- $NaHCO_3$ (Sigma)	1,5 g
- Sodium pyruvate (Sigma)	0,055 g
- Streptomycin/Penicillin/Amphotericin solution (Gibco, Invitrogen)	10 mL
- 10% FBS (Gibco, Invitrogen)	100 mL
- L-glutamine (200 mM stock solution)	2,5 mL

→ Dissolve in distilled (d) H_2O;

→ Adjust the pH to 7.2/ 7.3;

→ Adjust the volume to 1000 mL with dH_2O.

- **4% Paraformaldehyde**

For a final volume of 100 mL, add 4g of paraformaldehyde to 25 mL deionised H_2O. Dissolve by heating the mixture at 58ºC while stirring. Add 1-2 drops of 1 M NaOH to clarify the solution and filter (0.2 μm filter). Add 50 mL of 2X PBS and ajust the volume to 100 mL with deionised H_2O.

SDS-PAGE and Immunoblotting Solutions

- **LGB (Lower gel buffer) (4x)**

To 900 ml of deionised H2O add:

- Tris	181.65 g
- SDS	4 g

Mix until the solutes have dissolved. Adjust the pH to 8.9 and adjust the volume to 1L with deionised H_2O.

- **UGB (Upper gel buffer) (5x)**

To 900 ml of deionised H2O add:

- Tris	75.69 g

Mix until the solute has dissolved. Adjust the pH to 6.8 and adjust the volume to 1 L with deionised H_2O.

- **30% Acrylamide/0.8% Bisacrylamide**

To 70 ml of deionised H2O add:

- Acrylamide	29.2 g
- Bisacrylamide	0.8 g

Mix until the solute has dissolved. Adjust the volume to 100 ml with deionised water. Filter through a 0.2 μm filter and store at 4ºC.

- **10% APS (ammonium persulfate)**

In 10 ml of deionised H2O dissolve 1 g of APS. Note: prepare fresh before use.

- **10% SDS (sodium dodecilsulfate)**

In 10 ml of deionised H2O dissolve 1 g of SDS.

- **Loading Gel Buffer (4x)**

- 1 M Tris solution (pH 6.8)	2.5 mL (250 mM)
- SDS	0.8 g (8%)
- Glicerol	4 ml (40%)
- β-Mercaptoetanol	2 ml (2%)
- Bromofenol blue	1 mg (0.01%)

Adjust the volume to 10 ml with deionised H_2O. Store in darkness at room temperature.

- **1 M Tris (pH 6.8) solution**

To 150 ml of deionised H2O add:
- Tris base 30.3 g

Adjust the pH to 6.8 and adjust the final volume to 250 ml.

- **10x Running Buffer**

- Tris	30.3 g (250 mM)
- Glycine	144.2 g (2.5 M)
- SDS	10 g (1%)

Dissolve in deionised H_2O, adjust the pH to 8.3 and adjust the volume to 1 L.

- **Resolving (lower) gel solution** (60 ml)

	7.5%	or	**10%**
- H_2O	29,25 ml		25,2 ml
- 30% Acryl/0.8% Bisacryl solution	15 ml		19,8 ml
- LGB (4x)	15 ml		15 ml
- 10% APS	300 µL		300 µL
- TEMED	30 µL		30 µL

- **Resolving (lower) gel solution for gradient gels** (60 ml)

	5%	and	**20%**
- H_2O	17.4 ml		2.2 ml
- 30% Acryl/0.8% Bisacryl solution	5 ml		20 ml
- LGB (4x)	7.5 ml		7.5 ml
- 10% APS	150 µL		150 µL
- TEMED	15 µL		15 µL

- **Stacking (upper) gel solution** (20 ml)

	3.5%
- H_2O	13.2 ml
- 30% Acryl/0.8% Bisacryl solution	2.4 ml
- UGB (5x)	4.0 ml
- 10% APS	200 µL
- 10% SDS	200 µL
- TEMED	20 µL

- **1x Transfer Buffer**

- Tris 3.03 g (25 mM)
- Glycine 14.41 g (192 mM)

Mix until solutes dissolution. Adjust the pH to 8.3 with HCl and adjust the volume to 800 ml with deionised H_2O. Just prior to use add 200 ml of methanol (20%).

- **10x TBS (Tris buffered saline)**

- Tris 12.11 g (10 mM)
- NaCl 87.66 g (150 mM)

Adjust the pH to 8.0 with HCl and adjust the volume to 1L with deionised H_2O.

- **10x TBST (TBS+Tween)**

- Tris 12.11 g (10 mM)
- NaCl 87.66 g (150 mM)
- Tween 20 5 ml (0.05%)

Adjust the pH to 8.0 with HCl and adjust the volume to 1L with deionised H_2O.

- **Membranes Stripping Solution** (500 ml)

- Tris-HCl (pH 6.7) 3.76 g (62.5 mM)
- SDS 10 g (2%)
- β-mercaptoetanol 3.5 ml (100 mM)

Dissolve Tris and SDS in deionised H_2O and adjust with HCl to pH 6.7. Add the mercaptoethanol and adjust volume to 500 ml.

- **ECL home-made** (250 ml)

Solution A - ECL luminol solution (Stock solution):

- 20 mM luminol (in DMSO) * 1.25 ml (100µM)
- 100 mM 4-iodophenol (in DMSO) * 5 ml (2mM)
- 0.1 M Tris (pH 9.35) 125 ml (50 mM)

Adjust volume to 250 ml with deionised H_2O.
* Protect from the light; conserve at -20ºC

Solution B – Hydrogen peroxide

Pull-down solutions

- **Lysis buffer** (5 ml)

- 50 mM Tris (pH 8)	250 µl of 1M Tris (pH 8)
- 25% glycerol	1250 µl 100% glycerol
- 0.5% Gepac-ca-630 (NP40)	250 µl 10% NP40
- 200 mM NaCl	200 µl 5M NaCl
- β-mercaptoethanol	0,35 µl β-mercaptoethanol
- 1 mM PMSF	50 µl 100 mM PMSF
- protease inhibitor cocktail	5 µl of protease inhibitor cocktail

Keep all on ice.

- **Wash buffer** (20 ml)

- 10 mM Tris (pH 8)	200 µl of 1M Tris (pH 8)
- 0.1% Gepac-ca-630 (NP40)	200 µl 10% NP40
- 150 mM NaCl	600 µl 5M NaCl
- 0.25 mM EDTA	40 µl 0.25M EDTA
- 1 mM PMSF	200 µl 100 mM PMSF
- protease inhibitor cocktail	20 µl of protease inhibitor cocktail

Keep all on ice.